Records of Oceanog. Works in Japan

Volume 5, No. 1
New Series

Feb. 1959

TBV7 P.68

RECORDS OF OCEANOGRAPHIC WORKS IN JAPAN

Published by
Science Council of Japan

BOARD OF EDITORS

Editor-in-Chief
Shinkishi HATAI

Editors
Yoshio HIYAMA — Kōji HIDAKA
Yasuo MIYAKE — Hiroshi NIINO

With
the Co-operation of

Physical Oceanography
Kōji FUKUTOMI — Shōichirō HAYAMI
Mashito NAKANO — Tadayoshi SASAKI
Kanji SUDA — Ryūtarō TAKAHASHI
Michitaka UDA

Chemical Oceanography
Masayoshi ISHIBASHI — Yasuo MATSUDAIRA
Ken SUGAWARA

Geological Oceanography
Shōzaburō HANZAWA

Biological Oceanography
Denzaburō MIYADI — Yō K. OKADA
Isao TAKI — Yukio YAMADA

Fisheries
Hiroaki AIKAWA — Motosaku FUJINAGA
Takeo IMAI

Secretary
Buei ARAYA

SUGGESTION TO AUTHORS OF PAPERS FOR THE RECORDS OF OCEANOGRAPHIC WORKS IN JAPAN

An author wishing to contribute a paper to the RECORDS OF OCEANOGRAPHIC WORKS IN JAPAN should submit in compliance with the following suggestions:

1. Manuscripts will be accepted within the scope of
   Physical Oceanography — Geological Oceanography
   Chemical Oceanography — Biological Oceanography and
   Fisheries
2. An original and a copy of his manuscript should be type-written double-spaced in 21×29.5 cm paper, within 12 sheets, making 6 printed pages including plates and tables.
3. The manuscript should be addressed to the competent editor and mailed to the official in charge of the Science Council of Japan, Ueno Park, Tokyo, Japan.
4. The author is asked to follow this publication for forms of headings and references, etc.
5. The editors reserve the right to accept the manuscripts and to make minor editorial changes in them, so that all paper may conform to overall style of this publication.

CONTENTS

A Note on the Ice and Ocean Conditions in the Sea near Syowa Base in Antarctica ..... Jiro Fukuoka .. 1
Experiments on Evaporation from Wavy Water Surface ..... Setsuo Okuda and Shōitirō Hayami .. 6
A Hypothesis on Transmission of Energy of Tsunami Waves .... Kozo Yoshida .. 14
A Practical Method for a Determination of Reflection of Long Gravitational Waves ..... Kiheiji Ogawa and Kozo Yoshida .. 38
An Estimation of the Average Compensation Depth by a Study of the Vertical Distribution of Dissolved Oxygen ..... Akira Okubo .. 51
Preliminary Report on the Shelf Sediments off Kamo Yamagata, Japan ..... Hideo Kagami .. 60
Morphometric Comparison of the Albacore from the Indian and the Pacific Ocean ..... Kenji Kurogane and Yoshio Hiyama .. 68
A Measure of Role of Utilization of Plankton-feeders by Carnivorous Fishes in a Certain Area ..... Fujio Yasuda and Yoshio Hiyama .. 85
Measurements of Submarine Light Polarization .. Tadayoshi Sasaki, Noboru Okami Seiichi Watanabe and Gohachiro Oshiba .. 91

Records of Oceanographic Works
in Japan Vol. 5, No. 1,
February 1959

A Note on the Ice and Ocean Conditions in the Sea near Syowa Base in Antarctica

By
Jiro Fukuoka
(Meteorological Research Institute, Tokyo)

1. Introduction

The Japanese Antarctic Research Expedition was unavoidable to abandon the plan of the all around year observation in Antarctica on 24th February 1958 because of the violence of nature. It is very regrettable. But it is difficult and important to make clear why the failure to observe for all around year in Antarctica occurred. In order to assure the cause of this failure I have used the data taken on

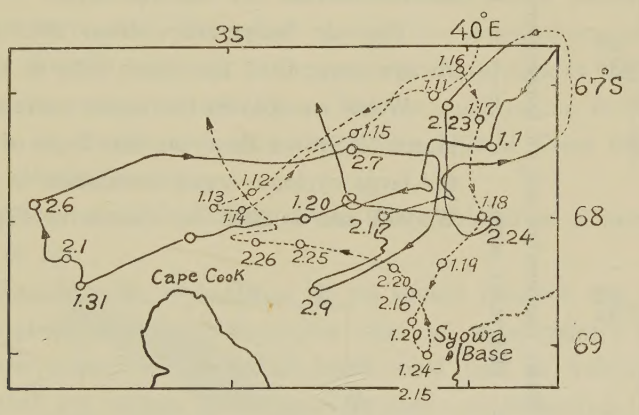

Fig. 1. Route of Soya.
----○---- 1957, ——○—— 1958 legend: 1.20→20th Jan.

board the Research Vessel Soya from 1956 to 1957 (1st Research Expedition) and from 1957 to 1958 (2nd Research Expedition) and the data of foreign countries and have analyzed the state of sea ice and hydrography near Syowa Base. The routes of Soya in both expeditions are shown in Fig. 1.

2. Water temperature

In this study it is assumed that the water temperature difference due to change of space is not shown, that is, observation is carried out in alike location in 1957 and 1958. Of course the assumption is not enough to analyze the data. But in order to utilize a few data this assumption is inevitable.

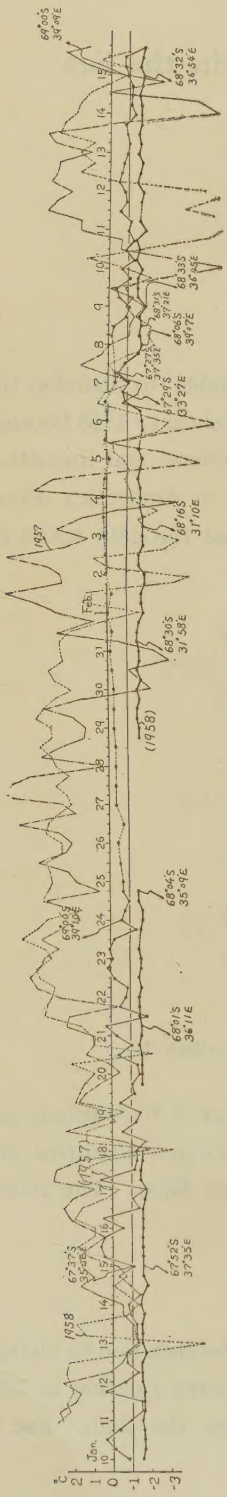

Fig. 2. Water temperature and air temperature on board Soya. ---- 1958 air temp. —●— 1958 water temp., —·—·— 1957 air temp. —●— 1957 water temp.

Water temperature observed from 1957 to 1958 is lower about 1°C than that from 1956 to 1957 (Fig. 2). It is impossible to decide whether water temperature lowering occurs everywhere in the Antarctic circumpolar ocean or is seen locally in the sea near Syowa Base because available data are very scanty. As at the northern part of the pack ice zone, water temperature from 1957 to 1958 also was lower by 0.5°C than water temperature from 1956 to 1957, it may be reasonable to consider that the water temperature lowering is not very local, but is seen in the rather wide area.

But the clear decision about water temperature distribution should be obtained on the analysis of the plentiful data observed on board Research Vesseles of other countries and whaling ships.

The air temperature from 1957 to 1958 is not always lower than that from 1956 to 1957 (Fig. 2).

When we studied the ocean current in the sea adjacent to Syowa Base on the basis of the past data, the large cyclonic ocean ciroulation is seen from the Weddell sea to 20°E as shown in Fig. 3. Through

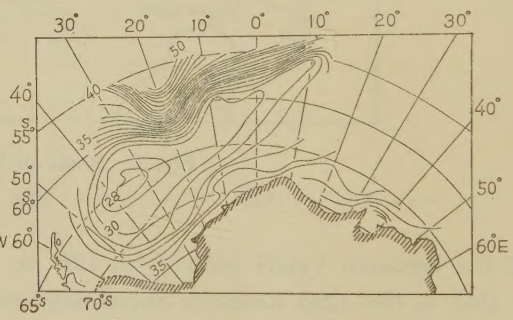

Fig. 3. Dynamical topography (0–1000 db) after H. Mosby.

the ocean current formed cyclonic circulation the very cold sea water moved toward north along the Palmer Peninsula (Graham Land) and then moved eastward along 62°S.

Though in the sea near the Prince Harald Coast the westward current is seen, it is not clear whether

this westward current forms a part of the above large cyclonic circulation or not. But the westward ocean current seems to transport ice near Syowa Base.

To refer the salinity distribution, the cold water may be connected to the water of the Weddell Sea. HERDMAN stated that the Weddell Sea is the weighty origination area of ice-berg and many ice-bergs are transported eastward by the cold sea water.

We must study the relation between ice volume and cold sea water from the Weddell Sea and also the westward ocean current which transports ice-berg and sea ice in the near future.

3. Wind distribution and sea ice

Ice-berg and sea ice distributions observed in 1st and 2nd Research Expeditions could not be compared with each other on the basis of observational data because available data are very scanty.

It is said that the failure of the whole year observation plan in Antactica is mainly due to ice increasing. So I shall consider the states of ice in the following.

(1) whether there is much ice in the sea near Antarctica or not in 1958.
(2) whether ice generated near Syowa Base is much or not in 1958.
(3) whether ice transported near the Prince Harald Coast from the remote area is plentiful or not.
(4) whether ice volume is determined by the combination of above three conditions or not.

Under the consideration of condition (1) we should research the data in observational base in other country. Though the data of other country have not been accepted, all observational parties except Japan could land at Antarctica. So it is not considered that ice volume is much everywhere in Antarctica than the mean state.

As regard the condition (2), we can not obtain the clear data. About ice conditions in all around year observation it is said that the significant difference between 1957 and 1958 is not seen.

Condition (3) is the most important.

Generally speaking, ice is used to transport by the ocean current, but the surface ocean current around Antarctica is dependent upon wind distribution. So I studied the wind distribution in 1956–1957 and 1957–1958 on the basis of the data of Soya. From Fig. 4 it is seen that south or west wind often blows from 8th to 31st January 1957, but east wind is possibly dominant in the same interval of 1958. The wind-roses of February 1–15 1957 and 1958 are not seen significant differences each other.

According to EKMAN drift current theory, surface current occurs to the direc-

tion of deflecting 45° to left against the wind direction in the South Hemisphere. That is, when east wind dominates, surface ocean current generated by the wind has south-west direction. Ocean current toward SW acts on the ice as the pressing movement to the land of Antarctica.

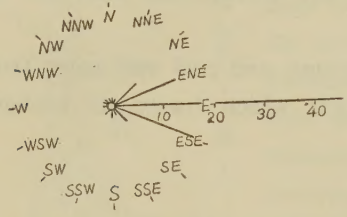

Wind-rose 1958 Jan. 8~31.

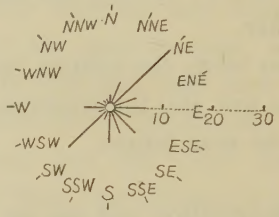

Wind-rose 1957 Jan. 8~31.

Fig. 4 (a). Wind-rose on board Soya.

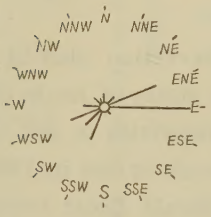

Wind-rose 1958 Feb. 1~15.

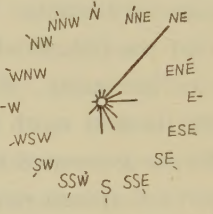

Wind-rose 1957 Feb. 1~15.

Fig. 4 (b). Wind-rose on board Soya.

Next, we can obtain the ocean current velocity generated by the wind drift on the basis of FUKUTOMI's idea. The mean wind velocity of 1958 is 8.0 m/s. After FUKUTOMI the ocean current corresponding to 8.0 m/s (wind velocity) is about 20 cm/s.

When ocean current of 20 cm/s continues for 15 days, the distance of drift current is 259 km. In order to avoid the damage generated by drift ice it is necessary to patrol the ice condition in the range of 260 km from the present position in the north-east quadrant.

From the above explanations it is important to forecast the wind direction and velocity for the prevention from the drifting ice damage. The ice patrol by the airplane is important to accomplish the landing at Antarctica, but otherwise the distribution of water temperature for wide area also should be utilized for the indirect inference of the ice conditions. As east wind of 1958 continues in longer interval than of 1957, the drift current toward the land of Antarctica of 1958 seems to predominate than of 1957. So ice seems to have become hard and nonshatterable in 1958 by the pressing movement toward the land of Antarctica. But this explanation stated above is merely a speculation.

4. Problem in future

The relation between the ice hardening and duration of east wind will be observed and studied, and the drifting of ice berg and sea ice by east wind will be observed in the rather wide area.

References

Discovery Report, Station List 1937–39 Vol. 24.

T. FUKUTOMI: Study of ice (the 14th report) On the Steady Drift-Current and Steady Drift of Sea-Ice due to Wind in the Frozen Sea. (in Japanese with English summary) Low Temp. Sci. 7 1951.

H. F. P. HERDMAN: The Antarctic Pack Ice. Trident Vol. 17 Feb. 1955.

Report of transportation of 1st Japanese Antarctic Research Expedition. (mimeograph in Japanese) Marinetime Safty Agency.

H. MOSBY: The waters of the Atlantic Antarctic Ocean. Scientific Results of the Norwegian Antarctic Expeditions 1927–1928.

Records of Oceanographic Works
in Japan Vol. 5, No. 1,
February 1959

Experiments on Evaporation from Wavy Water Surface

By
Setsuo Okuda
(Okayama Univ., Fac. of Science, Physical Institute)
and
Shōitirō Hayami
(Kyoto Univ., Fac. of Science, Geophysical Institute)

Abstract

A series of experiments is carried out to investigate an evaporation rate of water from wavy surface generated by wind and the effects of swell on the evaporation rate.

Numerical values of evaporation coefficient Γ and evaporation factor K are computed from experimental results. In strong wind, splashing of sprays makes the evaporation rate increase promptly and the effect of sprays is more significant on evaporation than that of generation of waves. It seems that mere existence of swell does not affect the evaporation rate.

1. Introduction

Various formulas to estimate the evaporation rate from meteorological elements have been offered by many authors, but at present, as pointed out by Sverdrup (1951) the available empirical evidence is too scanty and too inconsistent to decide what assumption may be acceptable. In order to get more reliable data, it is necessary to carry out laboratory experiments as well as a large number of observations over lakes or seas.

So far, many experimental studies of evaporation in laboratories under uniform meteorological conditions have been carried out, but in these experiments evaporating surfaces have been so small and so stable that the results of these experiments have been of little use in estimating the evaporation rate from large and wavy water surface.

In order to fill up this gap, we carried out the experiments on the evaporation from wavy water surface in a long wind flume of about 20 m long at Ujigawa Hydraulics Laboratory, Kyoto University.

2. Experimental Methods

The dimensions of the flume and the positions of measuring instruments used in our experiments are shown in Fig. 1. The methods of measuring various meteorological and hydrodynamical elements are described in the following respectively.

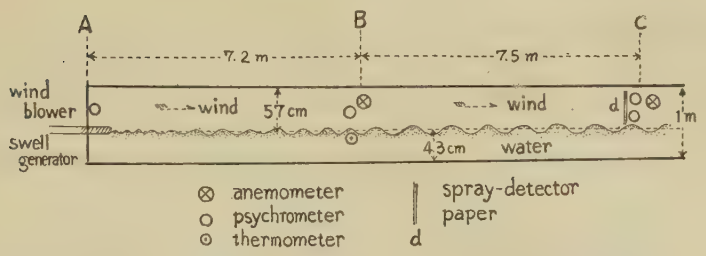

Fig. 1. Wind Flume and Measuring Instruments.

(i) Wind Velocity

The mean wind velocity was measured by small anemometers of Robinson type (arm length 4 cm, cup diameter 1.5 cm) with relayrecorder at the sections B and C.

(ii) Air Temperature and Humidity

Air temperature and humidity were measured by small psychrometer with dry and wet bulb thermometers (0–50°C 1/10°C) and the water vapour pressure was calculated according to Sprung's formula.

When strong wind splashed the sprays from wavy water surface, in order to keep off sticking of sprays on dry bulbs, we covered the bulbs with caps through which only air flow could pass.

(iii) Water Temperature

Surface water temperature was measured by inserting a thermometer under the water surface. The water vapour pressure at the surface was nearly equal to the saturation vapour pressure at the water temperature.

(iv) Water Drops—Sprays

When the wind velocity exceeded a definite value (about 11–14 m/sec at the section B) water drops began to splash from water surface. The sprayed water drops, were observed by the use of the filter paper (No. 1511 made by Tōyō Rosi Co. size 5×50 cm) containing uniformly the minute powder of "water-blue" according to the method of Maruyama and Hama (1954). We exposed the spray-detector paper to the sprays for about 5 or 10 sec, holding it vertical and normal to the wind direction.

(v) Surface Current Velocity

In order to determine the surface velocity of drift current, we dropped a board of veneer (3×3×0.3 cm size) saturated beforehand with water on the water surface at section B and measured the travel time from the starting point B to the points of finite distance (1.8, 3.6, 5.4 m).

(vi) Wave Form

We measured only wave height and wave length of representative waves at the constant wind with the naked eye and by a scale on the side wall.

3. Experimental Results

In this section we shall illustrate graphically only representative results of our experiments.

Fig. 2 shows the vertical distributions of wind velocity and humidity at the

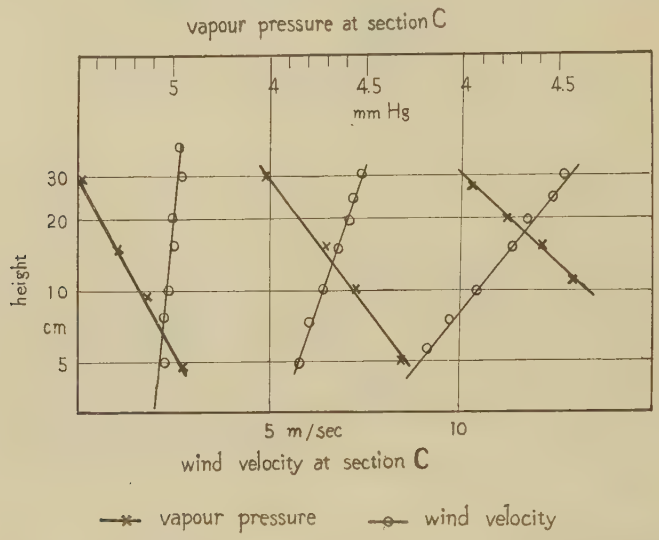

Fig. 2. Vertical Distribution of Wind Velocity and Humidity.

section C for the cases of low, medium and strong wind. They are nearly distributed according to logarithmic law.

Fig. 3 shows the vertical distribution of horizontal mass transport by sprayed

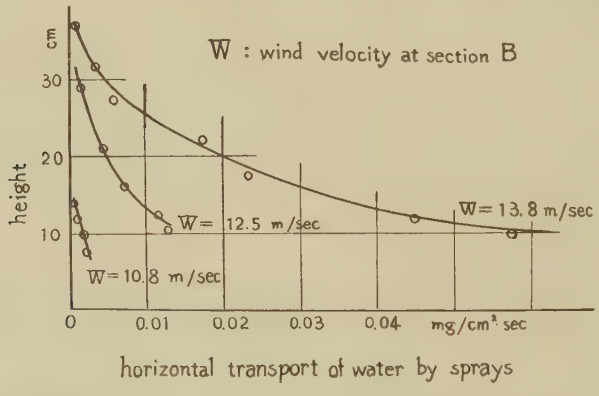

Fig. 3. Vertical Distribution of Horizontal Transport of Water by Sprays.

water drops through section C. It seems that the mass transport increases rapidly as soon as the wind velocity exceeds a critical value. This critical velocity depends on the wave form, especially on the wave steepness. The diameters of sprayed

drops are less than 1.5 mm but lower limit of drop diameter can not be determined by our spray-detector paper.

Fig. 4 shows the increases of drift current velocity, wave height and wave

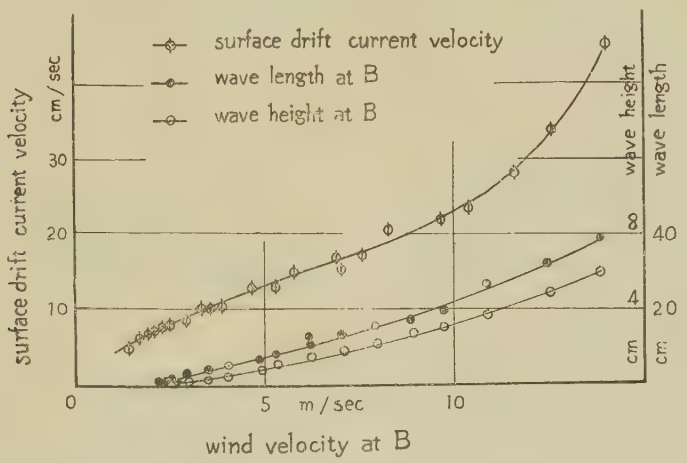

Fig. 4. Wave Height, Wave Length and Drift Current Velocity related to Wind Velocity.

length in relation to the wind velocity. Wave height and wave length were measured at section B, and drift current velocity was measured between section B and C. As the wind velocity increases, the drift current velocity, wave height and wave length increase almost linearly.

4. Analysis of Evaporation Rate

(i) Theoretical Consideration

When the changes of wind velocity and humidity along wind direction are negligibly small and the stationary state is approximately reached, evaporation rate E is given by

$$E=-\rho k_0^2\left(\frac{dq}{d\ln z}\right)\left(\frac{dw}{d\ln z}\right), \qquad (1)$$

where, ρ represents the density of air, k_0 Karman's constant (about 0.40), q specific humidity, w wind velocity and z-axis is taken vertically upward. Equation (1) corresponds to Thornthwaite-Holzmann's formula for evaporation rate.

Montgomery (1940) introduced an evaporation coefficient, defined by

$$\Gamma\equiv-\frac{1}{q_s-q}\frac{dq}{d\ln z}, \qquad (2)$$

where q_s represents the specific humidity at water surface.

Making use of Γ, a new expression of E is given by

$$E=k_0\rho w_*\Gamma(q_s-q), \qquad (3)$$

where w_* is so-called friction velocity and in neutral stability approximately given by

$$w_*=k_0\frac{dw}{d\ln z}\,. \qquad (4)$$

SVERDRUP (1951) used vapour pressure "e" instead of specific humidity "q" and wrote eq. (3)

$$E\equiv K(e_s-e)w\,, \qquad (5)$$

and called K evaporation factor.

We shall put the suffix a under Γ or K, to specify the height (z=a) at which we compute the numerical value of Γ or K, and use, after SVERDRUP, units such that pressure in (mb) and wind velocity in (m/sec) and evaporation rate in (mm/day) for practical purposes.

(ii) Discussion of Experimental Results

Previous to the computation of evaporation rate, we must examine applicability of assumptions in the above theory to our experiments, that is, we must check whether the measurements are really carried out in stationary state and the changes of various elements along wind direction are negligibly small. The results of the measurements carried out every fifth minute show that after the wind blows for 10–15 minutes, all elements reach nearly stationary values, and between sections B and C, especially in front of C, horizontal changes of various elements are negligibly small except in the very strong wind. Even in the strongest wind the error of computed value on account of horizontal change does not exceed 10%.

Now, numerical values of $dw/d\ln z$ and $dq/d\ln z$ are calculated graphically from slopes of lines in Fig. 2. Introducing these values into eq. (1) we obtain values of evaporation rate.

They ranged from 0.1 mm/day in low wind to 35 mm/day in strong wind. In order to compare our results with those of others we must compute Γ and K. SVERDRUP showed many theoretical and empirical values of Γ_{800} and K_{800}, in graphical forms. But we have no data of wind velocity and humidity above 40 cm high, so we have to obtain probable values of these elements by the extraporation of the relation in Fig. 2.

The extraporated values of wind velocity at 800 cm high do not differ so much from the values estimated on the basis of Van Dorn's data (1953) which were obtained from many observations on a yacht pond.

In Fig. 5A we showed the relation between Γ_{800} and W_{800} obtained from our experiments, comparing it with the result collected by SVERDRUP. In this figure Γ_{800} ranges from 0.08 to 0.11 nearly independently of wind velocity except in strong wind which makes the value of Γ_{800} increase promptly on account of splashing of sprays. In Fig. 5B we showed the relation between K_{800} and W_{800} obtained from

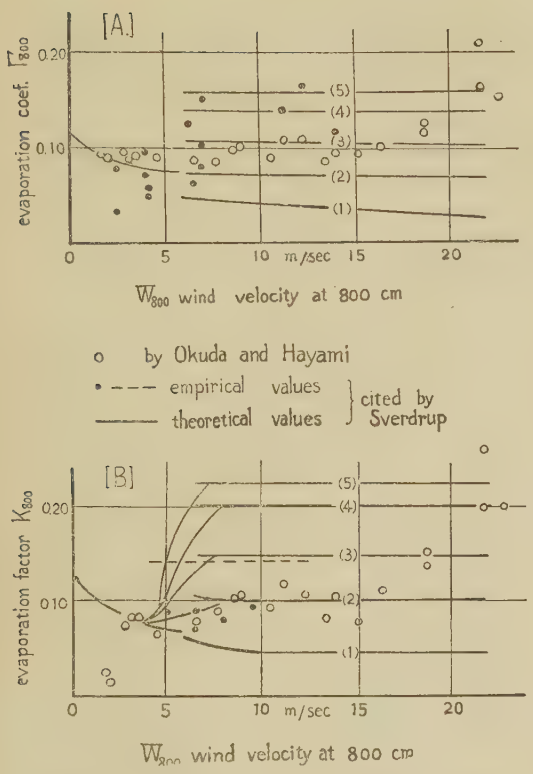

Fig. 5. Γ and K related to Wind Velocity.

our experiments, comparing it with the result collected by Sverdrup. In this figure, below the wind velocity of 3 m/sec, K_{800} increases abruptly from very low value to 0.08, and holds nearly constant value between 0.08–0.12 until W_{800} exceeds about 17 m/sec, and above this wind velocity it increases promptly on account of splashing of sprays.

It is interesting that our values of K and Γ do not differ so much from those obtained from observations over seas, but it must be noticed that a critical velocity at which the sprays begin to splash depends on the wave form and the fetch and that the critical wind velocity in the wind flume will be different from the one over seas. From our experiments, it seems that there are two transitional regions of wind velocity at which the evaporation rate changes abruptly. Firstly, the generation of waves changes the state of water surface and rapidly increases the evaporation rate. Secondly, above a critical wind velocity the splash of sprays increases the evaporation rate more promptly.

It is rather the splash of sprays than the generation of waves that governs strongly the general situation of evaporation phenomenon.

5. Effects of Swell on Evaporation Rate

In order to investigate the effect of swell on evaporation rate if any, we generated swell by a special swell-generating apparatus (Pneumatic Wave Generator) connected with the wind flume. We observed vertical distributions of wind velocity and humidity at various combinations of swell size and wind velocity and computed Γ_{800} and K_{800} from the observed values. Some results of the investigations are shown in Tables 1 and 2.

Though the observation error may bring an uncertainty of 0.01 into the computed values of Γ and K, we can not find in Table 1 any appreciable change of evaporation rate caused by the swell. Table 2 shows that the steeper is the form of swell, the lower is the critical wind velocity at which sprays begin to splash.

Table 1. Effects of Swell on Γ and K

Wind Velocity W_{800}	Swell			Γ_{800}	K_{800}
	Wave Length	Wave Height	Period		
23 m/sec.	7.2 m	9 cm	4.8 sec.	0.20	0.24
		No Swell		0.20	0.24
17	6.3	9	3.3	0.18	0.16
		No Swell		0.17	0.18
10.5	6.3	10	3.3	0.13	0.11
		No Swell		0.11	0.11
	3.6	10	2.1	0.115	0.095
		No Swell		0.11	0.10
	1.8	9.5	1.3	0.14	0.11
		No Swell		0.12	0.12

Table 2. Effects of Swell on Critical Wind Volecity (measured at Section B)

Wave Length	Wave Height	Period	Critical Wind Velocity
1.8 m	9.5 cm	1.3 sec.	10.8 m/sec.
3.6	10	2.1	11.0
7.2	10	4.8	11.5
	No Swell		13.2

Acknowledgement

The authors wish to thank Dr. T. KAWAHARA (Miye Univ.) and Mr. S. MATSUBARA (Okayama Univ.) for their valuable criticism and kind discussions. The authors also wish to express their cordial thanks to Mr. S. ADACHI, Mr. H. KUNISHI and Mr. H. HIGUCHI (Kyoto Univ.) for their generous help in carrying out experiments.

References

FRANCIS, J. R. D. (1954): "Wind Stress over a Water Surface", Quart. Jour. of Roy. Met. Soc., Vol. 80, No. 345, p. 438.

MARUYAMA, H. and HAMA, K. (1954): "Continuous Observation of Rain Drops and Snow Flakes" Tenki (Weather) Vol. 1, No. 2, p. 18. (in Japanese)

MONTGOMERY, R. B. (1940): "Observations of Vertical Humidity Distribution above the Oceans Surface and Their Relation to Evaporation" Pap. phys. Ocean Meteor. M. I. T. Woods Hole ocean Inst. Vol. 7 No. 4 30 pp. cited by SVERDRUP (1951).

SVERDRUP, H. U. (1951): "Evaporation from the Oceans" p. 1071–1081 marine meteorology, Compendium of Meteorology.

Van DORN, W. G. (1953): "Windstress on an artificial pond", Jour. of Mar. Res., Vol. 12 No. 3 p. 249–276.

Records of Oceanographic Works
in Japan Vol. 5, No. 1,
February 1959

A Hypothesis on Transmission of Energy of Tsunami Waves

By
Kozo Yoshida
(Geophysical Institute, Tokyo University, Tokyo)

1. Introduction

Most of the observations of tsumami waves have ever been made at coastal stations and none in deep oceans free enough from coastal effects. This unfortunate situation makes it difficult to understand what the tsunami waves look like in the deep ocean. Wave records at coasts in cases of tsunamis do revel a large number of oscillations in sea level. However, one could hardly interpret some of those oscillations as representing tsunami waves when and where they were generated at the distant source region. Essentially at the origin, they might not contain more than one or two crests and troughs. Or, they might do several or more of them. There are so large modifications of the wave characteristics due essentially to the high irregularities in the topographic conditions of the ocean, that very little could be known about the tsunami waves in the open ocean from the information obtained at coastal stations.

Of course, one of the most desirable things to do is to make direct measurements of tsunami waves in the open ocean. Another way of approach to this problem might be given by some statistical studies based on the analysis of a large number of records at coastal stations provided that the data were available from the stations distributed over ocean-wide scales and from various cases of past tsunamis. On the other hand, in this case, the information to be obtained should be interpreted only in a statistical sense. The present study belongs to the latter type of approach.

It has been confirmed to a certain extent that the frontal part of energy of tsunami waves does travel over large distances from the source region to the coastal station with a speed of long gravity waves. However, the distributions of wave energy in space and time after the time of arrival of the first wave appear to be somewhat complicated. This does not seem to permit any simple assumption on energy propagation of tsunami waves. It is most likely that such a complexity of energy transmission will principally be due to the complexity in the topographic conditions in the ocean. Obviously one should consider the actual irregularities in the ocean floor which prevent the long waves like tsunamis to travel without appreciable reflection, diffraction and dissipation of energy.

It has long been recognized that the occurrence of the highest waves is appreciably delayed for the cases when the waves come to coasts at greater distances from the source region. For instance, the first wave may be highest and succeeding waves will be lower in the case when the epi-center is relatively close to the stations. For the stations, at larger distances, the second or the third waves may be highest; for the stations, say many thousands kilometers from the source region, the fifth, tenth, or even much later part of waves may contain largest energies. In other words, the characteristic form of the energy envelope of the tsunami records depends essentially upon the travel distance of the waves. The portion containing the maximum energy will occur earlier for the smaller travel distance and later for the larger travel distance (Figs. 1a and b). However, this phenomenon of some statistical nature has only been recognized qualitatively, and no quantitative study has yet been attempted on a basis of analysis of past tsunami records.

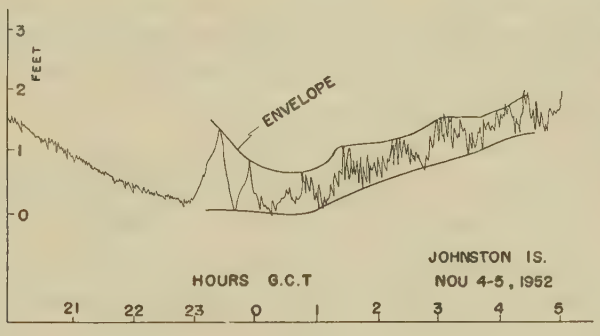

EXAMPLES OF TSUNAMI RECORDS (1)

Fig. 1a.

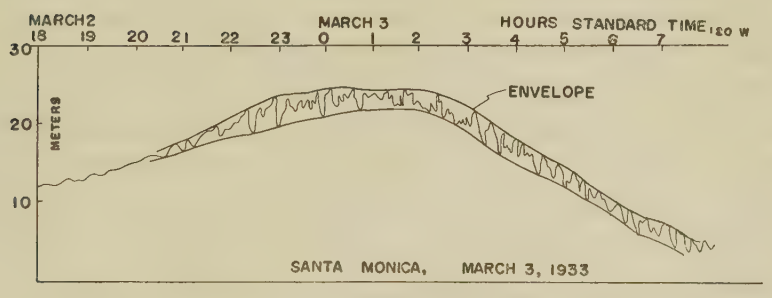

EXAMPLES OF TSUNAMI RECORDS (b)

Fig. 1b.

The first thing to do in the present work is to establish the quantitative relationship empirically between the delay in the time arrival of the envelope peak and the travel distance (or travel time). If this were done to some satisfactory extent,

the second thing would be to account for this on a theoretical basis. The former part of the work has just lately been done by Dr. R. TAKAHASI (1958) and the result does indicate certain remarkable relationship between the mentioned factors. Factual evidences are not enough to require any detailed theoretical explanation, so that it may only be worth while to deal with a theoretical model which is as simple as possible. Since the relationship indicates that the delay time is a function of travel time only, only the general statistical conditions of the transmission of energy on the course of the propagation, that is, the variations with travel distances, need to be considered. Individual cases of topographic conditions need not be considered. **If the ocean floor is completely flat** and no coastal boundary exists, the tsunami wave generated more or less impulsively at the origin would travel at a rate nearly equal to the long wave velocity with a slight degree of ordinary dispersion. In such a case, the envelope peak velocity would be nearly equal to the phase velocity (or front velocity) with a former about 95% of the latter, and the observed features do reveal apparent discrepancies from this. Statistically speaking, the greater the distance over which waves travel, the greater the amounts of such irregularities in the ocean floor, say such obstacles, would be. If the energy once reflected or diffracted should never come back to arrive at the coastal stations and should finally dissipate in the open oceans, the actual facts should not be accounted for. Some of the energies once reflected or diffracted would be lost to contribute nothing to any coastal stations, but some of the energies, after reflection or diffraction, would go to coasts in different directions and some other part of them may come back to coasts in the same direction after some complicated processes (such as multiple reflection).

The observed delay characteristics could be explained by the **envelope peak velocity** of which the ratio to the average phase velocity depends essentially upon a factor related to irregularities in topographic conditions. The envelope peak velocity decreases with increasing degree of irregularities. Or, one would say that this factor depends upon average degree of reflection and various other processes which prevent the wave energy to travelling over such complicated topographies can hardly be traced on their detailed dynamics of reflection, diffraction, refraction and scattering. Instead, the present approach is to view the process on somewhat statistical points and the discussion will not go into any detail of dynamical mechanism of reflection, diffraction and so on. With such approach, one cannot see much about how energy will be reflected in invidual cases, for instance. The effect of actually known distribution of the bottom configuration cannot be considered. The present author feels it rather important, however, to obtain somethings of the transmission of energy from such statistical view.

In fact, Takahasi's analysis of wave records revealed somewhat more complicate

features of the relations than we had ever had in mind on a vague empirical basis.

Owing to a lack in observational data as well as in our knowledge of the processes, a proposed theory is quite hypothetical. In fact, a simplest model which the author and Mr. Ogawa (1957) had discussed has turned out not to be valid for explaining some outstanding features revealed in Takahasi's analysis. It is desired that with much more and better sets of data in future the hypothetical nature of the theory should later removed.

As a result, the process is described as a diffusion from wave source travelling with a peak velocity which depends upon the degree of irregularity in bottom configurations. Due to the presence of the much higher irregularities in shallower parts of the oceans adjacent to continents, somewhat modified model will be considered for the stations at continental edges. In 1952, Takahasi (unpublished) made an analysis of records of 1933 Sanriku Tsunami with a special interest of coda part of tsunami waves. He estimated the rate of decay with time for amplitudes of tsunamis which is found nearly constant for differet stations. To account for the rate of decay obtained by Takahasi, somewhat modified model is proposed at such later stages which takes account of reflection back and forth at various boundaries corresponding to the process of energy transmission more like diffusion than waves.

2. A Simple Model for Oceanic Stations

(i) a description of the model.

Suppose that a single wave containing energy E is generated at the source region. (Assume that the source region is of the dimension comparable to a wave length of the generated wave). No further generation of energy is assumed. Frictional dissipation being neglected, the total energy will be E in total at all of the subsequent time. The first wave advances with a velocity C and carries an energy kE after it advances over one wave length, L. This first wave has left an energy $(1-k)E$ at the source region, so that it is assumed that the second wave is generated by gaining this amount of energy. The first wave, or the front wave, would contain energy k^2E when it advances over another wave length. Then, in

Table 1

$n=t/T$ \ $r=x/L$	0	1	2	3	4	....
0	E	0	0	0	0	
1	$(1-k)E$	kE	0	0	0	
2	$(1-k)^2E$	$2k(1-k)E$	k^2E	0	0	
3	$(1-k)^3E$	$3k(1-k)^2E$	$3k^2(1-k)E$	k^3E	0	
4	$(1-k)^3E$	$4k(1-k)^3E$	$6k^2(1-k)^2E$	$4k^3(1-k)E$	k^4E	

a similar way, the second wave has an energy $2k(1-k)E$ and the third $(1-k)^2E$ at the same time. The schematical representation of this process is given in Table 1. In this table, n refers to the total number of waves present expressed in wave period, T, to which the travel time of the first wave corresponds, so that n may stand for time $(=t/T)$. The number r refers to the number of wavelength to which the travel distance of the first wave corresponds, so that r must stand for distance $(=x/L)$.

For instance, the line for $n=3$ should represent the spatial distribution of waves at a time $3T$, energy for $r=3$ in this case representing that of the first (front) wave. The column for $r=3$, on the other hand, should represent the time distribution of waves at a distance $3L$. This represents more or less the time curve on a tsunami wave record installed at a fixed station. Energy for $n=3$ in this case represents that for the front wave.

It is readily seen that the amount of energy at any point of the above diagram is obtained by well-known binomial coefficient. Let the energy for any set of n and r be denoted by $E(n, r)$ and let $R(n, r)=E(n, r)/E$. Then

$$R(n, r)=\binom{n}{r} k^r (1-k)^{n-r} \tag{1}$$

For large values of n and r, this is well approximated by the normal frequency distribution:

$$R(n, r)\simeq \frac{1}{\sqrt{2\pi nk(1-k)}} \mathrm{Exp}\left[-(r-kn)^2/2nk(1-k)\right] \tag{2}$$

This is a solution of the differential equation

$$\frac{\partial R}{\partial n}=-k\frac{\partial R}{\partial r}+\frac{k(1-k)}{2}\frac{\partial^2 R}{\partial r^2} \tag{3}$$

which comes, for $n\gg 1$ are $r\gg 1$, from a difference equation,

$$R(r, n+1)=kR(r-1, n)+(1-k)R(r, n) \tag{4}$$

The difference equation (4) is evidently a general representation of the process under consideration.

Hence the process is considered to be a sort of diffusion of energy from the the travelling energy source. **The peak of this energy envelope which contains the maximum energy travels with a speed of kc approximately, where c is the phase velocity of the individual long wave.** Immediately from (1), the time of the arrival of the highest energy is given by

$$n_m=\frac{r}{k}-1 \tag{5}$$

or putting $n_m=r+S_m$

$$S_m = r\frac{1-k}{k} - 1 \qquad (6)$$

For $S \gg r \gg 1$

$$\varepsilon \simeq -\frac{1}{T}\ln(1-k) \qquad (7)$$

where

$$\frac{\partial \ln E}{\partial t} = -\varepsilon$$

These equation can directly be compared with tsunami wave records. The numerical value of the constant parameter, k, is really unknown to us. It is attempted in the later section to determine the numerical value of k and to give an interpretation for this constant. Before doing it, of course we must look into the observed results and see whether or not the actual tendency from statistical analysis of tsunami records is consistent with that given by this hypothetical theory.

(ii) Physical interpretation

(a) It is known that a single wave which travels over the ocean of more or less irregular bottom may undergo some what irregular multiple reflections and may become longer train of waves as it travels over larger distances. The constant k could be interpreted as an average transmission coefficient and $1-k$ as an average reflection coefficient for wave passing through a bottom irregularity of a dimension of one wave length. The reflected energy is assumed to be trapped. The trapped energy will decrease, after some multiple reflections, due to escape into either direction. Under the present consideration, however, the energy which is reflected back in the direction opposite to the peak advance is neglected.

As the topographic distribution in the real ocean is quite irregular the quantities like k must be taken as average values. Furthermore, such waves will not only undergo reflection but also diffraction, refraction and scattering. Hence k may be taken as a ratio of free penetration and $1-k$ as that of trapped or stored.

(b) The bottom topography is quite irregular and consequently the behaviors of wave energy must be quite complex. Moreover, individual cases of tsunami waves arriving at various stations may differ largely from case to case, depending upon local topographic conditions of the coasts. Hence, it may be better that the whole process should be described in term of statistics and it might possibly be expressed in term of probability.

The energy at the source is supplied instantaneously. Apart from the smaller effects of ordinary dispersion, the energy at time after the arrival of the first wave as recorded at coastal stations must be the portion of energy which travelled over some larger distances than the first wave did. The idea is simple and is given by

that the greatest energy will be contained in the part which travelled over certain additional distances or paths.

The probability that the total energy E arrives at a station, located at a distance r, without any stop on the course is

$$\binom{r}{r}k^r(1-k)^0=k^r$$

The probability that E arrives there with one-time stop at any one of divisions is

$$\binom{r+1}{1}k(1-k)$$

Thus, the equation (1)

$$R(n,\ r)=\binom{n}{r}k^r(1-k)^{n-r}$$

gives the probability that the whole energy E arrives at a station of a distance r after s time stops, where

$$n=r+s$$

As the energy E is introduced instantaneously at $r=0$, the probability for s-time stops may give the probability that E is observed, at a distance r and a time $n=r+s$. Under such irregular distributions of bottom topographies, $E(n,\ r)$ can be interpreted to give the square of the amplitude to be observed on a wave record at n and r.

In the above, k is interpreted as the probability that the whole energy is carried by the wave at a single passage of the wave with the phase velocity without any portion of energy left behind. Hence, $1-k$ is the probability that the whole energy is left uncarried at this passage.

The probability can be that which a whole energy arrives at a station r after $(r+s)$ travelling. For each step, the probability for going one step forward is k and that for stopping during one step time is $1-k$. We seek for a probability that the energy E will be observed at a station r, for a time n, that is, the probability that $n=r+s$ steps would make a resultant path of r, $r+s$ corresponding to the energy trapped s times.

This is a random walk problem, of which the solution is well known. Two-dimensional cases can also be dealt with readily.

If the ocean floor is completely flat, there is nothing such as reflection and we have $k\equiv 1$. If the source region is completely enclosed and no energy goes out of this region but the whole energy is trapped, we must have $k\equiv 0$. The probability that E goes out of a point is k and that E is trapped is $1-k$. This means that the probability which the ocean floor **at any point** is compleletely flat is k and the probability which the ocean region is completely enclosed is $1-k$. $1-k$ might therefore be interpreted as a probability reflection coefficient or a probability bottom distribution giving reflection coefficient $1-k$. It can easily be seen that total

energy at a fixed time n is

$$\sum_{r=0}^{r=n} E(n, r)=E$$

and that total energy integrated with time at a fixed station r is

$$\sum_{n=r}^{n=\infty} E(n, r)=E/k$$

(iii) Comparison with Observations

If the simple model described above be valid, a single constant parameter k should be sufficient to give most essential observed feature of the envelope form as a function of r and n on statistical basis. (Fig. 2.).

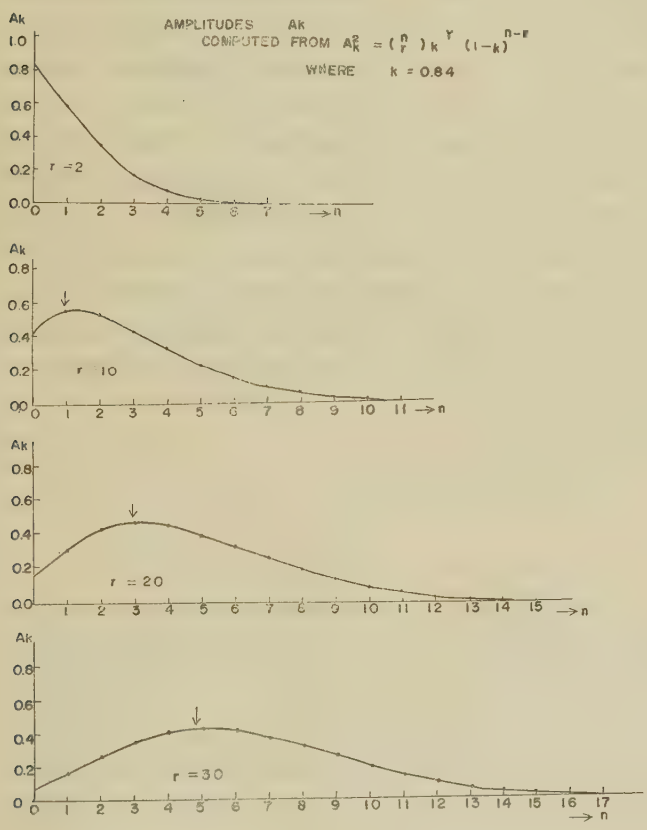

Fig. 2.

In fact, very rough idea which we have so far had on some empirical basis does not seem to be inconsistent with the model. The difference in time of arrival between the first wave and the highest wave is known to increase with travel distance. However, no quantitative relationship between them had been so far examined. One of the first things to be examined in the present work has been to dermine the numerical value of k from a comparison with data if it should at all be possible.

Observed data to be useful would desirably be selected from tsunamis which were recorded on ocean wide stations. Only few are available for this purpose, and we chose two of tsunamis, one is the Kamchatka Tsunami, Nov. 4, 1952, and the other is the Aleutian Tsunami, Mar. 9, 1957. From these tsunami records, an extensive analysis has just been made by Prof. R. Takahasi (1958). The present

discussion is therefore essentially based on those results obtained by TAKAHASI.

Time interval from the arrival of the first wave to the largest maximum wave is plotted against the travel time, that is the time from the occurrence of earthquake to the arrival of the first wave. In both cases of two tsunamis, revealed is a remarkable fact that oceanic stations (or island stations) and continental stations (along the continental edge of the ocean) appear to show distinctly separate pictures*1. Each of these two groups of plot shows nearly a straight line on the diagram of which slope and the origin differs from each other group.

In both of these two different tsunamis, nearly the same features are found: (1) The slope of the straight line is about 1/3 for continental stations and (2) about 1/10 for oceanic stations. (3) For the straight-line for the continental stations, the time interval from the first to the maximum wave does not approach to zero but to about 3 hours as the travel time comes close to zero. The features revealed indicate that, when the travel distance is small, the first wave is highest for the oceanic stations, whereas the maximum wave will come about 3 hours later for the continental stations. (corresponding to the 4th to 8th wave heighest, say). The rate of increase in the time interval between the first and the heighest wave with travel distances is greater for the continental stations than for the oceanic stations.

If one could definite the speed of travel of the portion containing maximum energy (let us call, the energy peak velocity, C_p) the slope may correspond to something like

$$\frac{(\text{travel distance}/\overline{C}_p)-\text{travel time}}{\text{travel time}}$$

or

$$\frac{C}{C_p}-1$$

where C is the phase velocity of the the wave or the speed of travel of the first wave.

Then the average peak velocity (or effective peak velocity) must be smaller for the continental stations than for the oceanic stations. If the average peak velocity approaches to the phase velocity, the slope tend to zero and the first wave would always be the highest.

Such difference in (peak velocity—phase velocity) or the streching of the distance between the front and the peak could be explained by putting different numerical

*1 All island stations in the mid-Pacific areas appear to belong to the group of oceanic (islands) stations under the present classification. Most of the stations along the Pacific coasts of Japan and along the west coast of the North and South American Continents indicate the type of records belonging to the continental station group. Only a few exceptions are found as far as the two tsunamis are concerned. Detailed descriptions should refer to Takahasi's paper (1958).

values of k for each of different groups. It can be seen that the value of k close to 0.9 for oceanic stations and that close to 3/4 for continental stations would account for the difference in the slope for both group. However, another fact, the third fact, that the arrival of the peak is delayed by about 3 hours even for small travel distance cannot be explained by such a simple model as described above.

Here are, at least, three quantitative conditions which should be explained. It is a way then that a more realistic model should be considered which may include two or three parameters. It may readily be imagined that the effects of continental slope, shelf and bays would account for the observed tendency. The occurrence of considerably stronger degree of trapping of the energy in the continental slope, shelf and bays and of much lower rate of escaping of energy would lead to the delayed occurrence of the peak.

Consider a pulse passing through an irregular transition. After the passage the pulse becomes a long train of waves. This transition puts an effect of making some of frontal energy left behind. The longer train will be produced if degree of reflection is effectively larger. The continental slope, shelf and bays must have such strong effects. With sufficiently strong effect of this coastal trapping, it may turn out that the front wave should hardly be the highest at the continental stations. With adequate magnitude of this effect, the delay will be close to 3 hours.

At the same time, we should explain why the slope of the time distance curve at the continental stations should be nearly three times as large as that at the oceanic stations.

3. Model for Continental Stations

(i) a description of the model

Among various possibilities which might be able to account for the observed features, a model modified from the previous simple one with the inclusion of the continental effects will be taken up. A large portion of the energy coming from the open ocean may be trapped in the regions of continental slopes, continental shelf and bays. This gives an effect brought by placing a marginal region where the constant k in the previous model is considerably small. With this marginal region, the rate of entering the zone from deep oceans as well as that of escaping the zone is much slower than that encountered in the open ocean.

The marginal zone is assumed to have a width of r_α L.

Put $r=r_k+r_\alpha$, and the energy distribution at the continental stations is given by

$$R(r+s,\ r)=\sum_{s_k=0}^{s}\left[\binom{r_k+s_k}{r_k}k^{r_k}(1-k)^{s_k}\right]\left[\binom{r_\alpha+s-s_k}{r_\alpha}\alpha^{r_k}(1-\alpha)^{s-s_k}\right]$$

$$=\sum_{s_k=0}^{s}\binom{r_k+s_k}{r_k}\binom{r+s-r_k-s_k}{r-r_k}k^{r_k}\alpha^{r-r_k}(1-k)^{s_k}(1-\alpha)^{s-s_k}$$

For simplicity, if we put $r_\alpha=1$,

$$R=\alpha k^{r-1}(1-\alpha)^s\sum_{s_k=0}^{s}(1+s-s_k)\binom{r-2+s_k}{r-2}\sigma^{s_k} \tag{9}$$

where

$$\sigma=\frac{1-k}{1-\alpha}$$

Put

$$M=\sum_{s_k=0}^{s}\binom{r-2+s_k}{r-2}\sigma^{s_k}$$

and (9) become

$$R=\alpha k^{r-1}(1-\alpha)^s\left[(1+s)M-\sigma\frac{d}{d\sigma}M\right]$$

For sufficiently large values of s,

$$M\simeq(1-\sigma)^{-(r-1)},$$

and hence

$$R\simeq\frac{\alpha k^{r-1}}{(1-\sigma)^r}(1-\alpha)^s[(1+s)(1-\sigma)-(r-1)\sigma] \tag{10}$$

This gives

$$\frac{\partial\ln R}{\partial s}=\ln(1-\alpha)+\frac{1-\sigma}{(1+s)(1-\sigma)-(r-1)\sigma} \tag{11}$$

and $\dfrac{\partial\ln R}{\partial s}=0$ occurs S_m such as

$$S_m+1=(r-1)\frac{\sigma}{1-\sigma}-\frac{1}{\ln(1-\alpha)} \tag{12}$$

since $S_m\gg 1$

$$S_m\simeq(r-1)\frac{1-k}{k-\alpha}-\frac{1}{\ln(1-\alpha)} \tag{13}$$

or

$$\frac{S_m}{r}\simeq\frac{1-k}{k-\alpha}-\frac{1}{r}\left[\frac{1}{\ln(1-\alpha)}+\frac{1-k}{k-\alpha}\right] \tag{14}$$

For $s\gg r$

$$\frac{\partial\ln R}{\partial s}\simeq\ln(1-\alpha)$$

and hence

$$\varepsilon \simeq -\frac{1}{T}\ln(1-\alpha) \tag{15}$$

For the oceanic stations, (6) can be written

$$\frac{S_m}{r} = \frac{1-k}{k} - \frac{1}{r} \tag{16}$$

Now we may be able to determine the range of values which κ and α would take to satisfy the three necessary conditions. Since the factual relations are not quantitatively very accurate, we may give certain range of allowance for observed quantities.

The slope of the straight-line for oceanic station is about 1/10 for average but we take the values 0 to 1/5. That for continental stations is about 1/3 for average but we may take 1/4 to 1/3. The time of delay of the highest wave arrival at nearest distances for continental stations is about 3 hrs for average but we take 4 to 8 as a number of wave corresponding to 2.5 hrs to 5.5 hrs approximately. (see Takahasi, 1958). In our terms,

$$0 \leq \frac{1-k}{k} \leq \frac{1}{5}$$

$$\frac{1}{4} \leq \frac{1-k}{k-\alpha} \leq \frac{1}{3}$$

$$4 \leq -\frac{1}{\ln(1-\alpha)} \leq 8$$

It is seen from those conditions that very narrow range of values for k and α are allowed to be taken. The values are approximately

$$k = 0.84 \tag{17}$$

and

$$\alpha = 0.20 \tag{18}$$

With these values,

$$\frac{1-k}{k} = 0.19$$

$$\frac{1-k}{k-\alpha} = 0.25$$

$$-\frac{1}{\ln(1-\alpha)} = 4.6$$

which may very roughly fit the observed features. (Fig. 3). For three conditions

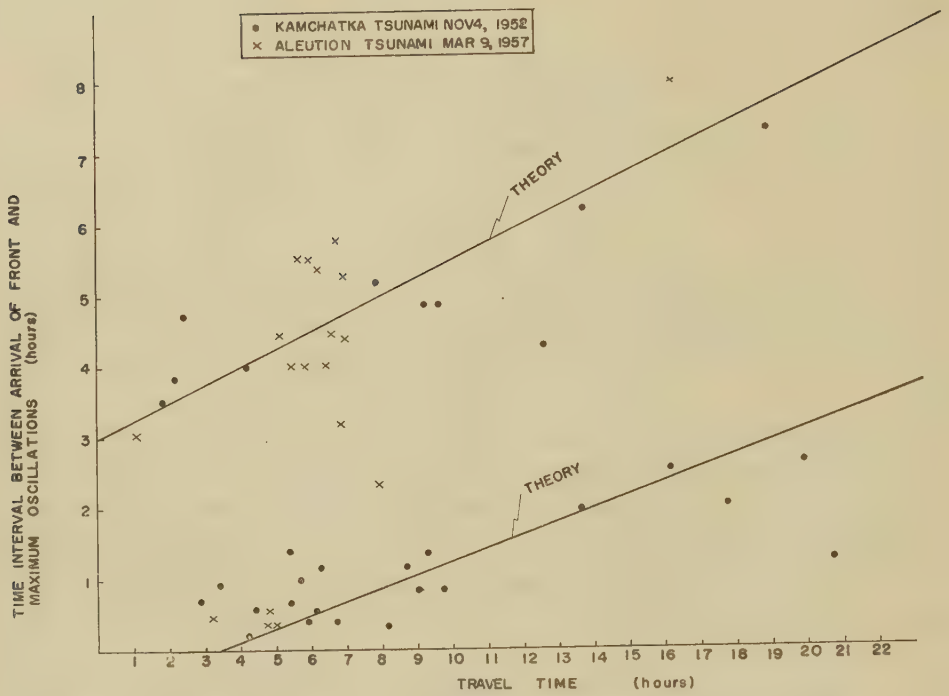
• KAMCHATKA TSUNAMI NOV4, 1952
× ALEUTION TSUNAMI MAR 9, 1957
THEORY
THEORY
TIME INTERVAL BETWEEN ARRIVAL OF FRONT AND MAXIMUM OSCILLATIONS (hours)
TRAVEL TIME (hours)

Fig. 3. Relation between arrival time of the heighest wave and travel time

to be fulfilled, we have assumed only two adjustable constants. The rough success obtained with those two parameters suggests that another parameter not included here may not be more essential as far as the present problem is concerned, although its inclusion may slightly improve our fitness. This may mean that the observed features can be explained roughly by k and α as given by (17) (18), and that the two conditions for the continental stations are not independent of each other. In order to obtain more complete fit, we may have the third parameter. There may be various possible parameters of course, but it may be likely that the width of the continental region R or r_α in number of wavelength, which was assumed as unity in the above, may be the one. This could in actuality be the case considering that some energy of tsunamis may be trasmitted in a form of edge waves over some appreciable distances.

More important point is, however, to examine whether or not the numerical values for k and α thus determined are considered reasonable, or, in other words, whether or not we could interpret the constants of k and α on some reasonable basis of independent considerations. This point will be remarked in the later section.

(ii) An interpretation for the model

In the following, E_0, E_1 and E_2 will refer to the energy contained at a time t

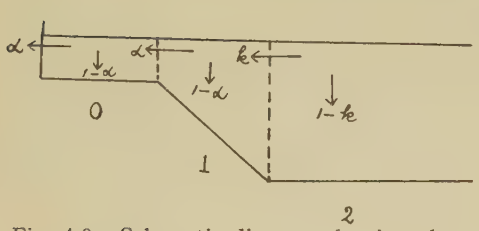

Fig. 4.0. Schematic diagram showing three regions 0, 1 and 2.

in the continental shelf or bay, continental slope and the deep ocean part adjacent to the slope. Regions 1 and 0 are those in which more energy may be trapped as that we may assume the transmission coefficient smaller. The difference equations governing the energy budget are as follows.

$$E_0(t+T)=\alpha E_1(t)+(1-\alpha)E_0(t) \tag{19}$$

$$E_1(t+T)=kE_2(t)+(1-\alpha)E_1(t) \tag{20}$$

Evidently $E_2(x,\ t)$ is governed by (4), and if we consider only the case when n and r are large,

$$E_2(r,\ n)\simeq\frac{E}{\sqrt{2\pi nk(1-k)}}\mathrm{Exp}\left[-\frac{(r-kn)^2}{2nk(1-k)}\right] \tag{21}$$

For $t\gg T$ (or $n\gg 1$ in previous notation), (19) and (20) can be approximated by

$$\frac{\partial E_0}{\partial t}+\frac{\alpha}{T}E_0=\frac{\alpha}{T}E_1$$

and

$$\frac{\partial E_1}{\partial t}+\frac{\alpha}{T}E_1=\frac{k}{T}E_2$$

respectively. Using n instead of t as before,

$$\frac{\partial E_0}{\partial n}+\alpha E_0=\alpha E_1 \tag{22}$$

$$\frac{\partial E_1}{\partial n}+\alpha E_1=\alpha E_2 \tag{23}$$

From these,

$$\frac{\partial^2 E_0}{\partial n^2}+2\alpha\frac{\partial E_0}{\partial n}+\alpha^2 E_0=\alpha kE_2 \tag{24}$$

The solution of (24) with E_2 as given by (21) and with the condition $E_0\to 0$ for $n\to r$ is

$$E_0(n,\ r)=\alpha kE\int_r^n\frac{(n-m)e^{-(n-m)\alpha-(r-km)^2/2mk(1-k)}}{\sqrt{2\pi mk(1-k)}}dm \tag{25}$$

This corresponds to the expression for E given by (9). In the similar way,

$$E_1(n,\ r)=kE\int_r^n\frac{e^{-(n-m)\alpha-(r-km)^2/2mk(1-k)}}{\sqrt{2\pi mk(1-k)}}dm \tag{26}$$

From (22) one can see that the maximum of E_0 occurs when $E_0=E_1$, and that at this time $(\partial E_1)/(\partial n)<0$. Hence the maximum of E_0 occurs when E_1 is decreasing or at some time after the maximum of E_1 occurs. Thus, the maximum of E_0 occurs in some delay from that of E_1. From (23), it is seen that the maximum of

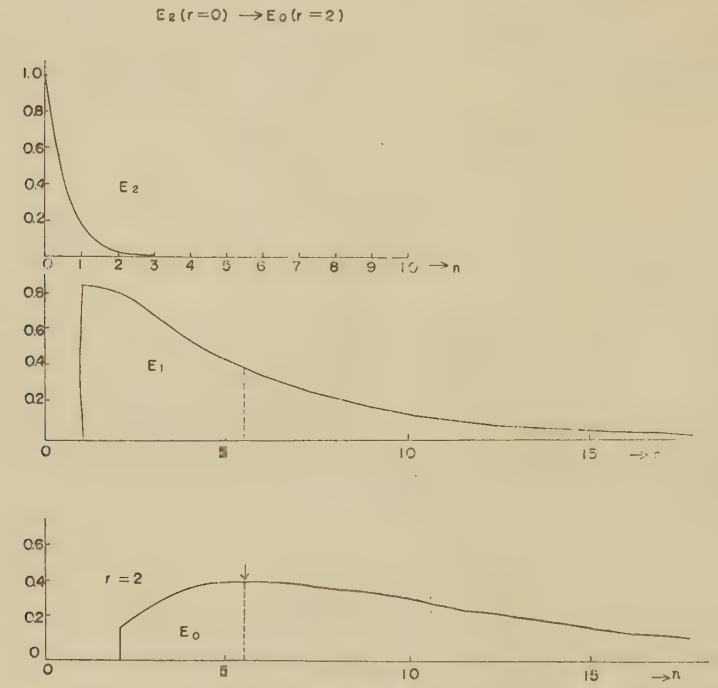

Fig. 4a.

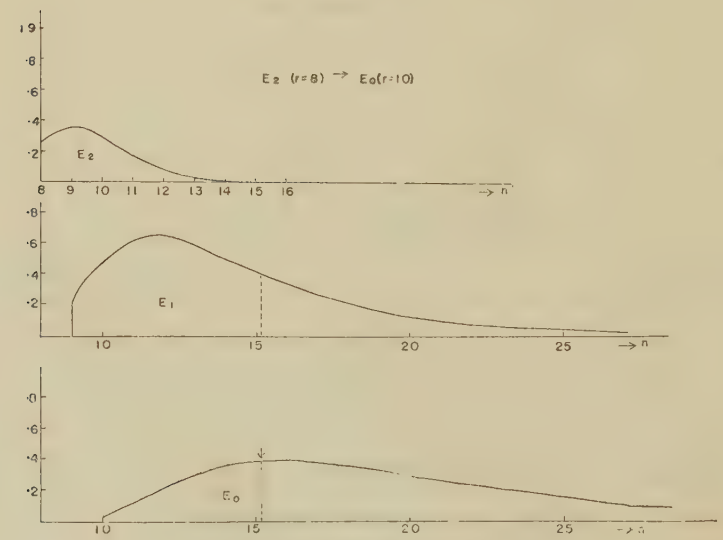

Fig. 4a.

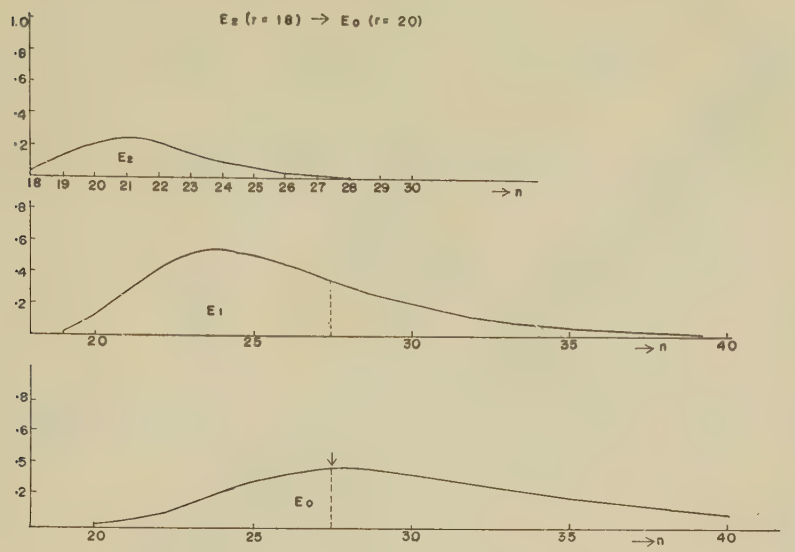

Fig. 4c.

Fig. 4 (a, b, c). Theoretical energy envelope in regions near continental edges. Numerical values for E_2, E_1 and E_0 are expressed in ratios to E.

E_1 occurs when $E_1=(k/\alpha)E_2$. In the same way, the maximum of E_1 occurs in some delay from that of E_2. For the same values of r the maximum of E_0 is delayed from that of E_2. This can also be interpreted by that the speed of the peak travel in the coastal region is reduced as r increases. The peak velocity is given by $\alpha c/(1+\beta\alpha r)$ where β is $(1-k/k)\alpha/k$. Eq. (22) tells that in the coastal region, energy is accumulated or decays according to the difference between E_1 and E_0. E_0 increase during the period $E_1 > E_0$, and it decrease at latter stages when $E_1 > E_0$. (Figs. 4 a, b, c and Fig. 5).

4. Remarks on the Parameters k and α.

The establishment of a physical significance of the parameters k and α should be most essential to the validity of the present hypothetical theory. It is therefore necessary to give a physical interpretation for what k and α should represent in such a statistical model and to examine whether or not the numerical magnitudes of k and α determined above should be reasonable. In spite of the critical importance of making this sort of check, the critical test would rather be difficult to be done because the parameters may represent quantities too much involved and partially because the theory may be based on too much simplified model.

So far only energy envelope as a function of time at a fixed station has been checked with observations. Of course, the theoretical model also gives spatial distributions of energy at a fixed instance or at successive instances which should be

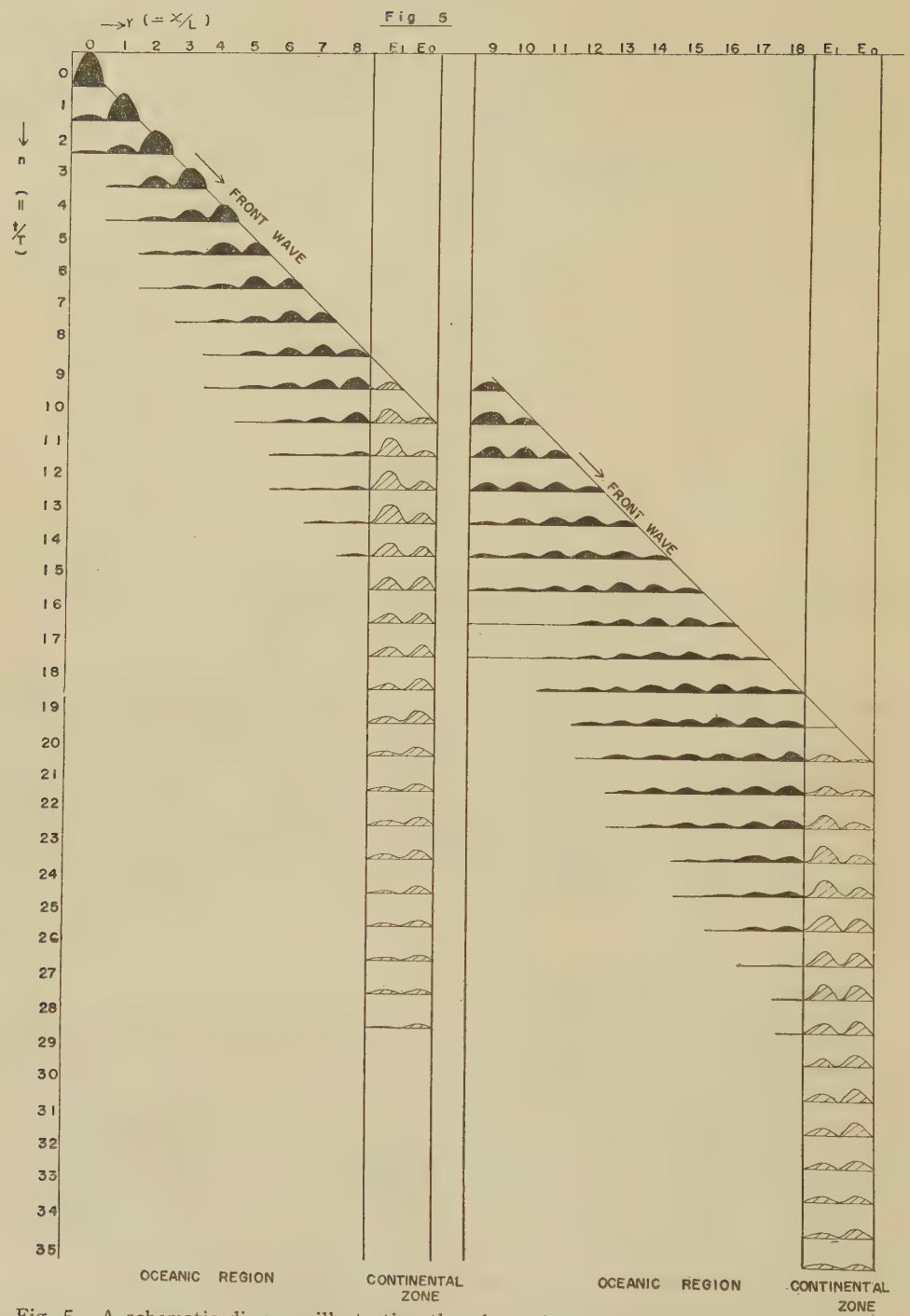

Fig. 5. A schematic diagram illustrating the theoretical energy distributions of waves generated at a source region ($r=0$, $n=0$). Each of continental zones is assumed to be located at a travel distance $x=8L$ and $x=18L$ respectively. In the latter case, diagram for $r \geq 9$ should be continued from that for $r \leq 8$ without insertion of the other continental zone.

tested by the observed distributions. This test seems to be more difficult since local effects of individual coasts are dominant and the difference in these local effects may be greater than that in travel distance.

According to our theory, energy of the first wave in the open ocean or for the oceanic stations decreases with travel distance as given by

$$E_k(n=r,\ r)/E=k^r=e^{r\ln k} \tag{27}$$

The energy of the first wave at continental stations decreases according to

$$E_\alpha(n=r,\ r)/E=\left(\frac{\alpha}{k}\right)k^r=\frac{\alpha}{k}e^{r\ln k} \tag{28}$$

With the numerical values $k=0.84$ and $\alpha=0.20$, the **amplitude** of the first wave in each case is given by

$$A_k/\sqrt{E}\simeq e^{-0.087(x/L)} \tag{29}$$

$$A_\alpha/\sqrt{E}\simeq 0.49e^{-0.087(x/L)} \tag{30}$$

respectively, where L is a mean wavelength of the tsunami wave. The energy of the highest wave in the open ocean or for the oceanic stations is

$$E_k/E\sim\frac{1}{\sqrt{2\pi(1-k)r}} \tag{31}$$

and that for the continental station is

$$E_\alpha/E\sim-\frac{\alpha}{k}\,\frac{k-\alpha}{1-\alpha}\,\frac{1}{\ln(1-\alpha)}\,\mathrm{Exp}\left[-\left\{1+\frac{1-\alpha}{k-\alpha}\ln(1-\alpha)\right\}\right]$$
$$\cdot\mathrm{Exp}\left[r\left\{\ln k-\ln(k-\alpha)+\frac{1-\alpha}{k-\alpha}\ln(1-\alpha)\right\}\right] \tag{32}$$

with $k=0.84$ and $\alpha=0.20$, one obtains $\ln(1-\alpha)\simeq-0.223$, $\ln k\simeq-0.174$, $\ln(k-\alpha)\simeq-0.445$, $(1-\alpha)/(k-\alpha)\simeq1.25$, and then

$$E_k/E\sim\frac{1}{\sqrt{r}} \tag{33}$$

$$E_\alpha/E\sim0.42e^{-0.008(x/L)} \tag{34}$$

For an example, putting a wavelength $L=400$ km and a travel distance $x=3000$ km, we obtain

(A_k) first$/\sqrt{E}\simeq0.52$

(A_α) first$/\sqrt{E}\simeq0.25$

(A_k) max$/\sqrt{E}\simeq0.61$

(A_α) max$/\sqrt{E}\simeq0.63$

Considering that the coastal and shoaling effects will greatly amplify the wave height, the rate of amplitude decrease as obtained above is not considered to be unacceptable.

Table 2

	Amplitude of first wave		Amplitude of highest wave		
r	$A_k/\sqrt{E}$	$A_\alpha/\sqrt{E}$	$A_k/\sqrt{E}$	$A_\alpha/\sqrt{E}$	travel distances (in km.) for $L=400$ km
0	1.00	0.49	1.00	0.64	0
2	0.84	0.42	0.84	0.63	800
4	0.70	0.35	0.71	0.63	1,600
6	0.59	0.30	0.64	0.63	2,400
8	0.50	0.25	0.60	0.62	3,200
10	0.42	0.21	0.59	0.61	4,000
20	0.18	0.09	0.47	0.59	8,000
30	0.07	0.04	0.43	0.57	12,000

The theoretical amplitude of the first wave and the highest wave for various values of travel distance r are given in the following table 2. The numerical values are the ratio of the values to the amplitude at the source ($r=0$). In Figs. 6a and 6b, those recorded amplitudes for the two cases of tsunamis are plotted against the travel distances. The plotted points scatter so much that one could hardly draw any definite curve to fit them. For the amplitudes of first wave in both cases of these tsunamis, a theoretical curve is drawn in order to show that the order of magnitude of a slope of this straight line, related to k and α, on these graphs is not unacceptable. On the other hand the plots for the highest waves show so much scatter that the validity of the theory can

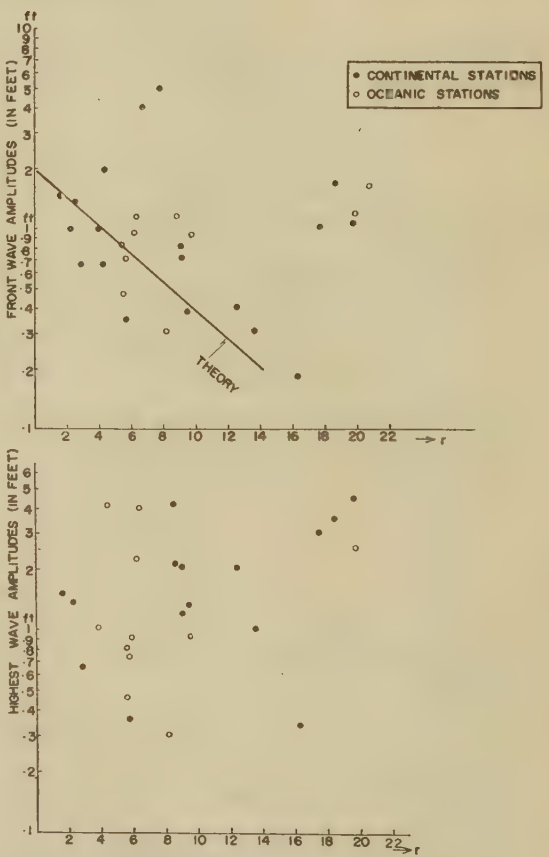

Fig. 6a. Plot of "front wave amplitudes" and of "highest wave amplitudes" against travel distances" for Kamchatka Tsunami of Nov. 4, 1952.

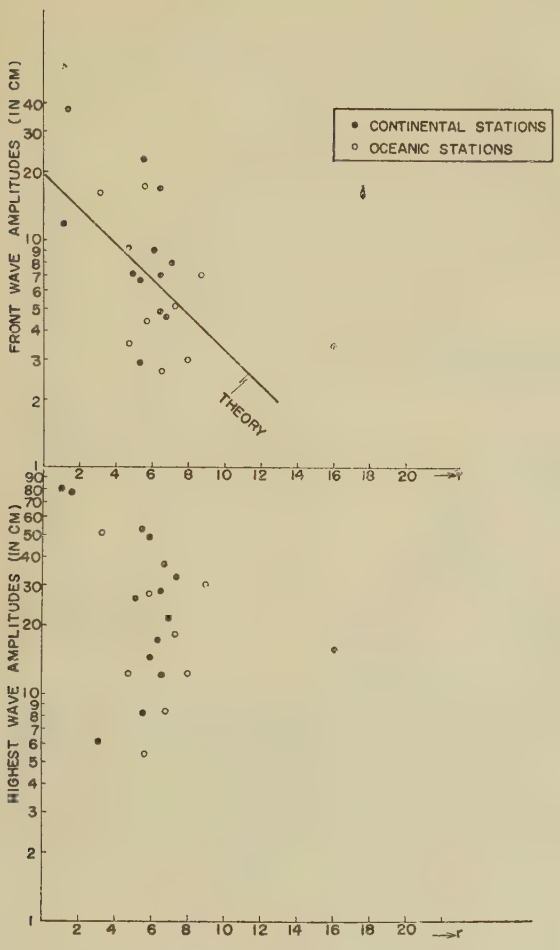

Fig. 6b. Plot of "front wave amplitudes" and of "highest wave amplitudes" against travel distance" for Aleutian Tsunami for Mar. 9, 1957.

hardly be tested from these pictures.

Evidently k as well as α should be determined by the statistical distributions of bottom and coastal topographies and somewhat be affected by periods of tsunami waves. The present study will not go, however, to such discussions as determination of the values of k and α in that way.

5. Decay Process

As mentioned in the introduction, TAKAHASI found from the analysis of records of 1933 Sanriku Tsunamis that the amplitudes of the coda part of the waves at most of the stations can be expressed in a form

$$A \sim t^{-1/2} e^{-\varepsilon t}$$

where ε is found to be about $1 \times 10^{-5} \mathrm{sec}^{-1}$ for all the stations examined. This observational result reveals an apparent inconsistence with the theoretical result from the model considered above. The rate of decay during the later stages of the process would be given by the equations (7) and (15) if the above model is assumed to be applicable to the later stages. With the numerical values for k and α as determined above, the decay constant is

$$\varepsilon_k = -\frac{\partial \ln E_k}{\partial t} \simeq \frac{1.8}{T}$$

and

$$\varepsilon_\alpha = -\frac{\partial \ln E_\alpha}{\partial t} \simeq \frac{0.22}{T},$$

where T is a period of tsunami.

Putting $T=30\,\text{min.}\simeq 1.8\times 10^{3}\,\text{sec.}$,

$$\varepsilon_k \simeq 1\times 10^{-3}\,\text{sec}^{-1} \tag{35}$$

and

$$\varepsilon_\alpha \simeq 1.2\times 10^{-4}\,\text{sec}^{-1} \tag{36}$$

Takahasi's result gives the energy decay

$$E\sim t^{-1}e^{-2\varepsilon t}$$

and hence

$$-\frac{\partial \ln E}{\partial t}\sim \frac{1}{t}+2\varepsilon \tag{37}$$

As the concerned time t is nearly 10 to 30 hours in his analysis, the decay constant needs to be of the order of magnitude

$$(3\sim 5)\times 10^{-5}\,\text{sec}^{-1} \tag{38}$$

It appears therefore that the theoretical rates of decay given by (35) and (36) are **too large** to account for the observed rate given by (38). Furthermore, the observed rate appears to vary slightly with t according to t^{-1}.

This apparent discrepancy in the decay rate between theory and observation is not unexpected. The model employed for the earlier stages of the process will not be valid for the later stages. It is obvious that our calculation based on the assumption that energy reflected far back in the direction opposite to the peak advance is neglected in consideration. The time required to the wave travel across the ocean width is nearly

$$t\simeq \frac{10^{9}}{2\times 10^{4}}\,\text{sec.} = \frac{1}{2}\times 10^{5}\,\text{sec.}\simeq 14\,\text{hrs.}$$

Hence, for some later stages, those part of energy which comes from the other boundary of the ocean would not be negligible. Not only the energy reflected at the opposite boundary of the ocean but also those at a number of places acting as a sort of strong reflectors in the ocean regions will contribute to the process. In contrast to the earlier stages at which the portion of energy envelope containing the maximum concentration of energy occurs, the process at this stage is more alike to the **diffusion** than to the wave-like propagation of peak (see Appendix). Under this situation at later stages, the energy goes from place in more confused ways and the resulted diffusion may take place rather two-dimensionally. Then it follows that energy will decay according to t^{-1}. The factor of $e^{-2\varepsilon t}$ as observed will remain still unexplained. This might possibly be accounted for by frictional dissipation which has been ignored to consider the earlier stage processes. Unfortunately it is not known how much the rate of decay of energy due to frictional dissipation

could be. The observed rate of decay mentioned above seems to require that the decay time due to friction is

$$\frac{1}{1\times10^{-5}}\text{sec.}=1\times10^{5}\text{ sec.}\simeq28\text{ hrs.}$$

Appendix to § 5

(i) At later stages, the energy budget will be described by

$$E(x,\ t+T)=k[E(x-L,\ t)+E(x+L,\ t)]+(1-2k)E(x,\ t)$$

For $x\gg L$ and $t\gg T$, this can be reduced to

$$T\frac{\partial E}{\partial t}+\frac{T^2}{2}\frac{\partial^2 E}{\partial t^2}\simeq kL^2\frac{\partial^2 E}{\partial x^2}$$

with $t/T=n$ and $x/L=r$,

$$\frac{\partial E}{\partial n}+\frac{1}{2}\frac{\partial^2 E}{\partial n^2}=k\frac{\partial^2 E}{\partial r^2}$$

For sufficiently large values of n, this becomes the ordinary diffusion equation

$$\frac{\partial E}{\partial n}\simeq k\frac{\partial^2 E}{\partial r^2}$$

of which solution is

$$E\simeq\frac{1}{2\sqrt{\pi kn}}e^{-r^2/4kn}\simeq\frac{1}{2\sqrt{\pi kn}}$$

It can easily be seen that, at earlier stages not much later than the time when the envelope peak reaches coasts, this part of energy is much smaller than the part of energy given by the previous model of wave-diffusion-type.

The wave-diffusion-type energy will decay rapidly and at the later stages, purely diffusion-type energy will be dominant. Hence it will be more adequate for the description of the later stages of decay that the diffusion-type energy is applied. It appears, furthermore, that the two-dimensional diffusion may better be applied, so that the energy will decay according to t^{-1}.

(ii) Later decay stages at coastal stations:

Difference equations are

$$E_0(n)=\alpha E_1(n-1)+(1-\alpha)E_0(n-1)$$
$$E_1(n)=kE_2(n-1)+\alpha E_0(n-1)+(1-\alpha-k)E_1(n-1)$$

leading to

$$\frac{\partial E_0}{\partial n}=\alpha(E_1-E_0)$$
$$\frac{\partial E_1}{\partial n}=k(E_2-E_1)+\alpha(E_0-E_1)$$

Hence, eliminating E_1,

$$\frac{\partial^2 E_0}{\partial n^2}+(2\alpha+k)\frac{\partial E_0}{\partial n}+\alpha kE_0=\alpha kE_2$$

Free modes are $e^{\omega_1 n}$ and $e^{\omega_2 n}$ where

$$\omega_1\simeq\frac{1}{2}[-(2\alpha+k)-\sqrt{k^2+4\alpha^2}]$$

$$\omega_2\simeq\frac{1}{2}[-(2\alpha+k)+\sqrt{k^2+4\alpha^2}]$$

or

$$\omega_1 \simeq -k \quad \text{and} \quad \omega_2 \simeq -\alpha$$

Thus

$$E_0 = \frac{\alpha k}{k-\alpha}\left[e^{-\alpha n}\int_{\tau}^{n} e^{\alpha\xi}E_2(\xi)d\xi - e^{-kn}\int_{\tau}^{n} e^{k\xi}E_2(\xi)d\xi\right]$$

If we put

$$E_2|_{n\to\infty} \simeq \frac{E}{2\sqrt{\pi k n}}$$

we have

$$E_0/E \simeq \frac{\alpha k}{k-\alpha}\,\frac{1}{\sqrt{\pi k}}\left[e^{-\alpha n}\int_{\sqrt{\tau}}^{\sqrt{n}} e^{\alpha\eta^2}d\eta - e^{-kn}\int_{\sqrt{\tau}}^{\sqrt{n}} e^{k\eta^2}d\eta\right]$$

However, it can be seen from (32) that
for $\alpha n \gg 1$

$$E_0(n) \simeq E_2(n)$$

Then

$$E_0(n) \simeq \frac{E}{2\sqrt{\pi k}\sqrt{n}}$$

For two-dimensional diffusion

$$E_0(n) \propto n^{-1}$$

At somewhat earlier stage when $\alpha n \simeq 1$, (32) is

$$\frac{\partial E_0}{\partial n} = \alpha(E_2 - E_0)$$

This gives a process of radiation of energy.

(iii) Fluctuation in the envelope at decay stages:

The decay curves of the amplitude envelope reveal some fluctuaions which look quite irregular but appear to show some periodic variations. (See Takahasi's figure).

The wave train has the portion where the heighest wave are contained, this being simply called the peak, and one would expect the occurrence of the reflection of the peak back and forth at various boundaries such as the ends of bays, continental shelf, continental slope and those at the edge on the other side on ocean. Data are not available enough to make us go further into further quantitative study on this rough speculation.

6. Summary

Tsunami wave records usually reveal characteristic shape of envelope which, in a statistical sense, appears to depend only upon the travel distance of the tsunami at the station. Somewhat more detailed analysis of the records has revealed another important feature that such envelope characteristic differ materially between the records at oceanic stations (in midocean areas) and at continental stations (along the coasts of continents). The time interval between the arrival of the first wave and that of the highest wave (or the mean arrival time of the portion containing the maximum energy) is found to increase linearly with the travel distances. This relationship is examined for a few cases of recent tsunamis, and the obtained results seem to show certain simple features could be accounted for by a simple theoretical model as presented in this article. This theory would only be applicable to statis-

tical conditions and not to individual cases. Even for the statistical cases, the theory may probably be too crude, although most of the general features from observations seem to be in rough consistence with the theoretical results. Many problems, however, remain unsolved: (1) physical interpretation of numerical constants k and α; (2) decay processes during the later stages; (3) rate of decrease of amplitudes (or energy) with travel distance, and so on. With more observations, especially with measurements in the open ocean, the whole problem might have to be reconsidered from entirely different views.

However, it might be of some interest to see that certain outstanding features revealed on tsunami records at coastal stations can be interpreted fairly well by such statistical considerations of processes concerning the transmission of energy as discussed above. Perhaps, similar ideas would also be applicable to certain other geophysical phenomena such as energy transmission of seismic waves.*

Acknowledgement

This work was supported by the funds provided by the Scripps Institution of Oceanography, University of California, under contract with the Japanese Organization for Tsunami Investigation.

References

TAKAHASI, Ryutaro (1952): Coda of tsunami waves. (unpublished. read at the annual meeting of the Seismological Society of Japan, 1952)

TAKAHASI, Ryutaro (1958): On the type of tsunami records. (unpublished)

YOSHIDA, Kozo and Kiheiji OGAWA (1957): A hypothesis on transmission of energy by tsunamis. (a preliminary report for 1957 JOTI Project)

* In 1944, Prof. C. Tsuboi of the Geophysical Institute, Tokyo University, suggested to the author an idea concerning an energy transmission of seismic waves which is essentially similar to that described in this article.

Records of Oceanographic Works
in Japan Vol. 5, No. 1
February, 1959

A Practical Method for a Determination of Reflection of Long Gravitational Waves

By
Kiheiji Ogawa[1] and Kozo Yoshida
(Geophysical Institute, Tokyo University, Tokyo)

1. Introduction

Long gravitational waves with wavelengths as large as those of tsunamis are known to be subjected to an appreciable reflection of energy when they travel in the ocean. The unevenness of the ocean bottom is so considerable within a wavelength of the wave, that one can hardly expect that tsunami waves travel from the deep water to the coast without significant amount of reflection. Of course, the tsunami waves are greatly enlarged as they enter the shallow water, and reflection occurs at the coast, at the mouth of bay, at the edge of the continental shelf and so on, causing various types of oscillations. In fact, some of the apparent periods appearing on tsumani wave records are nothing but those corresponding to the secondary generated waves due to those types of marked reflection. It is thus of importance to study such "strong reflection" occurring at conspicuous topographic discontinuities.

On the other hand, partial reflection of waves due to irregularities in the bottom configuration can be appreciable and cannot by any means be disregarded. This is the case when the waves travel in the ocean of which depth varies from place to place continuously and more or less irregularly. An estimate of such kind of reflection, as we might call it "weak reflection" tentatively, involves certain difficult problems which, to our present knowledge, have not yet been solved. The ordinary way taken in such cases has been that the reflection coefficient is computed by assuming one or several regions of which each has a constant bottom slope, or by assuming several of regions of which each has a different constant depth and is connected with an abrupt transition at each boundary. However, this should not be considered very useful in many cases of practical application. The actual condition of depth distribution is as complex as one can see on ordinary bathymetric charts.

For the time being, let us confine ourselves to the simplified case of one-dimensional propagation. That is to say, diffraction and refraction of energy are disregarded, by assuming that the wave has sufficiently long crestline so that the

[1] Now at Japanese Hydrographic Office.

effects of curvatures of crestlines are negligible even over a long distance of propagation. It is assumed that the bottom varies only in the direction of wave travel, and that the isobaths are nearly given by parallel straightlines so that the curvatures of the isobaths as seen on charts do not affect the propagation.

This simplification of one-dimensional propagation should of course be an oversimplification, and we must consider the problem on a realistic two-dimensional basis. Yet, the one-dimensional case is still useful, because the two-dimensional problem may be accomplished by some additional modification applied to the result of one-dimensional case.

The two-dimensional problems will be considered in another paper. It should be noted at this point that the existing technique is only that of the ordinary refraction diagram which was initially employed for swell in shallow water and which is based on the assumption of no reflection nor diffraction of wave energy.

Returning to the topics of one-dimensional case, obtained is a solution which makes it possible to evaluate the approximate reflection as an integral or sum of certain characteristic quantities measurable from the actual depth distributions on charts. It is supposed that very small-scale irregularities of bottom and sufficiently gradual change in depth may not make any appreciable contribution to reflection of tsunamis. Those irregularities which may have something to do with reflection of tsunamis are supposed to be, very roughly speaking, of certain scale comparable with that of waves or of appreciable change in depth over a shorter distance. Of course, one must always encounter an extreme difficulty from physical point of view in deriving reflection of waves travelling in the water of continuously variable depth. This point is related to a dynamical mechanism of reflection of waves which is not known to us. Although this point is indeed important, the problem is far out of our scope of the present practical study.

From the point of view as stated above, it is attempted in this paper to find a rough estimate of reflection on the basis of the hydrodynamical equations which may provide a method as useful as possible in its practical application. The most part of the paper is concerned with an approximate solution which is valid only when the reflection is relatively weak. The accuracy of this solution under the conditions, as encountered in case of tsunamis, is examined somewhat in detail. Very rigorous discussions of the errors may not be meaningful, for the model of one-dimensional propagation is not at all accurate enough in itself. The reflection coefficient is obtained in a form of an integral which can easily be computed from somewhat smoothed distribution of depth. The present authors noticed recently, when the present study was nearly completed, that the similar results* had already

* Very recently, Dr. C. S. Cox has kindly shown us an unpublished paper by F. URSELL (1947) dealing with a similar problem of long gravity waves.

been obtained independently by WALKER and WAX (1946), BREMMER (1949, 1951) and SCHELKUNOFF (1951) in the papers dealing with the electromagnetic waves. Therefore, the details of the mathematical derivations will not be presented here. However, the idea and the method which those papers contained may perhaps be new to oceanographers and perhaps to most of seismologists who are particularly interested in tsunamis.

It may perhaps be worth noting that tsunami wave is not likely to be a long train of waves but is more likely to be of a type of a solitary wave in the deep water, that one should deal with reflection of such type of wave instead of that of an infinite train of waves. The energy contained in the first or second apparent wave crest is usually of more practical interest than that contained in the later portion of the apparent train of waves. The amount of energy which is reflected away from the frontal portion of tsunami waves may probably differ considerably from that of waves of infinite train.

2. Theory of Reflection

The discussions in the present work are entirely based on a simple one-dimensional model of long gravitational wave which propagates in water of variable depth, as expressed by the dynamical equations.

$$\frac{\partial u}{\partial t}=-g\frac{\partial \zeta}{\partial x} \tag{1}$$

$$\frac{\partial \zeta}{\partial t}=-\frac{\partial}{\partial x}(uh) \tag{2}$$

where u is horizontal velocity, ζ the surface elevation, h the depth of water, and g is gravity.

Assuming that u and ζ vary with time as $e^{i\sigma t}$, and denoting $M=uh$ where M is volume transport of water, (2) and (1) can be written

$$\frac{dM}{dx}=-i\sigma\zeta \tag{3}$$

$$\frac{d\zeta}{dx}=-\frac{i\sigma}{gh}M \tag{4}$$

The wave equations for M and ζ are given by

$$\frac{d^2M}{dx^2}+\frac{\sigma^2}{gh}M=0 \tag{5}$$

and

$$\frac{d^2\zeta}{dx^2}+\frac{1}{h}\frac{dh}{dx}\frac{d\zeta}{dx}+\frac{\sigma^2}{gh}\zeta=0 \tag{6}$$

respectively.

In this paper, the approximation is essentially based on an assumption that the whole region is divided into a large number of sub-regions of which each region is considered to have a constant depth. Of course, errors introduced by this approximation increases as the number of divisions decreases. If each region were assumed to be of a linear bottom slope instead of a constant depth, the accuracy would be higher. However, such model leads to make the analytical expressions too complicated to be used in practice. It is seen from (5) and (6) that errors due to the assumption will be less if we use the equation for M than that for ζ. Therefore, we use at first the volume transport M for the consideration of reflection coefficient.

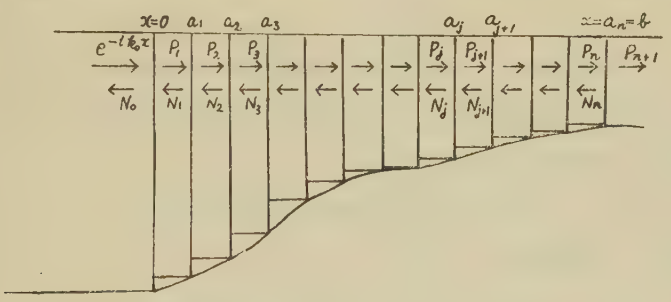

Fig. 1.

The reflection coefficient q_M for the volume transport M can be derived by considering transmissions and reflections at each discontinuity of the water depth on the incident wave. First, we divide the region of inhomogeneous water depth $0<x<b$ into the subintervals $0<x<x_1$, $x_1<x<x_2$, $x_2<x<x_3$, $\cdots$, $x_{n-1}<x<x_n=b$ (Fig. 1).

Now, we assume that the incident wave progresses from the negative x direction, being represented by $e^{i(\sigma t-k_0x)}$ for the region $x<0$ which contains uniform depth of water. In the course of propagation, reflection and transmission will occur at these discontinuities $x=0$, $x=a_1$, $x=a_2$, $\cdots\cdots$, $x=a_n=b$. First, at the point $x=0$, there can be two kinds of waves by the process of decomposition of the incident wave. Dropping time factors, they are (1) transmitted wave P_1 penetrating the layer $0<x<a_1$, and represented by $A_1\exp\{-ik_1x\}$, and (2) a reflected wave N_0 returing to the region $x<0$ and represented by $B_0\exp\{ik_0x\}$. With the physical consideration that the volume transport and its first derivative, M and dM/dx, must be continuous at each discontinuity, reflection and transmission coefficient at $x=a_j$ can be represented in case when the wave progresses from the negative x-direction by

$$r_j=\frac{k_j-k_{j+1}}{k_j+k_{j+1}} \quad \text{and} \quad t_j=\frac{2k_j}{k_j+k_{j+1}} \tag{7}$$

and

$$r_j'=\frac{k_{j+1}-k_j}{k_j+k_{j+1}} \quad \text{and} \quad t_j'=\frac{2k_{j+1}}{k_j+k_{j+1}} \tag{8}$$

in case where the wave progresses from the positive x-direction. Denoting the primary transmitted waves and the primary reflected waves at each sub-interval by $P_1, P_2, \cdots, P_n$ and $N_0, N_1, \cdots, N_n$ respectively, the following relations will be obtained:

$$\frac{P_{j+1}(x_j)}{P_j(x_j)}=\frac{2k_j}{k_j+k_{j+1}},$$

and

$$\frac{N_j(x_j)}{P_j(x_j)}=\frac{k_j-k_{j+1}}{k_j+k_{j+1}}.$$

Now the reflected wave in the region $x\leq 0$ which is generated at $x=0$ would be r_0 at $x=0$, and that at $x=a_1$ would be

$$P_1r_1t_0'e^{-2ik_1a_1}=t_0r_1t_0'e^{-2ik_1a_1} \qquad \text{at } x=0,$$

and that at $x=a_2$, would be

$$P_2r_2t_1't_0'e^{-2ik_2(a_2-a_1)-2ik_1(a_1-0)}=t_0t_1r_2t_1't_0'e^{-2ik_2(a_2-a_1)-2ik_1a_1} \qquad \text{at } x=0,$$

and that at $x=a_j$, would be likewise

$$t_0t_1t_2\cdots t_{j-1}r_jt_{j-1}'t_{j-2}'\cdots t_1't_0'e^{-\sum_{j=1}^{j}2ik_j(a_j-a_{j-1})}. \qquad \text{at } x=0.$$

Therefore, the primary reflected wave which is generated by one time reflection at the discontinuities would be at $x=0$

$$\sum_{j=0}^{n} t_0t_1t_2\cdots t_{j-1}r_jt_{j-1}'t_{j-2}'\cdots t_0'e^{-\sum_{l=1}^{j}2ik_l(a_l-a_{l-1})}.$$

Letting the sub-interval infinitely small, the above expression may be reduced to

$$q_M=\frac{1}{4}\int_0^b\frac{1}{h}\frac{dh}{dz}\exp\left\{-2i\sigma\int_0^z\frac{dz}{\sqrt{gh}}\right\}dz \tag{9}$$

It is easy to see that this expression would represent the first order approximation to the reflection coefficient. Likewise, for the surface elevation, we obtain the similar expression for the first-order reflection coefficient

$$q_\zeta=-\frac{1}{4}\int_0^b\frac{1}{h}\frac{dh}{dz}\exp\left\{-2i\sigma\int_0^z\frac{dz}{\sqrt{gh}}\right\}dz \tag{10}$$

Thus, reflection coefficients for ζ and M can be derived which result from the one-

time reflection at each discontinuity and letting the subinterval infinitely small. Likewise, higher-order reflection coefficients may be derived easily by considering the reflections of more times at the discontinuities.

But now it still remains to find the conditions under which the expressions for the reflection coefficient (9) and (10) are sufficiently accurate for the practical use, and at least two ways to this aim can be considered. One way is to construct the solution M which consists of infinite series, each terms originating from finite number of reflections, and to test whether the series can be a solution of the given wave equation (5). The study in this direction was already accomplished by H. Bremmer in 1949 and 1951. He shows that the well-known W.K.B. approximation for the wave equation can be interpreted physically as the first term of the infinite series of which each term represents a term originating from a certain particular number of reflections in the media. It is seen that u_1 in his notation which represents backward-going once-reflected wave coincides exactly with our expression for q_M.

Another way to the investigation, which is more preferable to the former in this case, is to stand on a higher level in the field of reflection problems. This can be achieved for some part by deriving the differential equation for the reflection coefficient.

In the above-mentioned step-wise approximation of the actual water depth, volume transport M_i at each sub-interval has the expression of

$$M_i = A_i e^{-ik_i x} + B_i e^{ik_i x} + O[(x-a_i)^3] \,. \tag{11}$$

Now, using the continuity conditions for the mass transport M and its first derivative dM/dx at each discontinuity point $x=a_i$ and letting a_{i+1} approach to a_i use being made of the relation (11), we have the following system of differential equations for A and B

$$\begin{aligned} &\left(\frac{dA}{dx} - ik'xA\right) + (B' + ik'xB)e^{2ikx} = 0 \,, \\ &-\{ikA' + (kk'x + ik')A\} + (ikB' - kk'xB - ik'B)e^{2ikx} = 0 \,. \end{aligned} \tag{12}$$

Now, from the substitution of (13) into the left-hand side of the equation (5), it can be shown easily that the volume transport M represented by

$$M = A(x)e^{-ikx} + B(x)e^{ikx} \tag{13}$$

with the relations (12) holding for A and B is a solution of the wave equation (5).

Another derivation of the same conclusion may be obtained by the way described below. We assume here that the solutions for the volume transport M and surface elevation ζ are of the form

$$M(x)=A(x)e^{-ikx}+B(x)e^{ikx}$$
$$\zeta(x)=\frac{k(x)}{\sigma}\{A(x)e^{-ikx}-B(x)e^{ikx}\} \tag{14}$$

Then from the condition that eqs. (14) must satisfy the equations (3) and (4) we obtain the desired relation (12).

Now the above being established, it is straight forward to derive the differential equation for the reflection coefficient. Put

$$q_M=\left(\frac{B(x)}{A(x)}\right)e^{2ikx}\,, \tag{15}[1]$$

we obtain the equation for q_M as

$$\frac{dq_M}{dx}=\frac{2i\sigma}{\sqrt{gh}}q_M-\frac{1}{4}\frac{1}{h}\frac{dh}{dx}(1-q_M^2) \tag{16}$$

Likewise, we obtain the equation for q_ζ as

$$\frac{dq_\zeta}{dx}=\frac{2i\sigma}{\sqrt{gh}}q_\zeta+\frac{1}{4}\frac{1}{h}\frac{dh}{dx}(1-q_\zeta^2) \tag{17}$$

It will be evident from the method of derivation that the relations (16) and (17) for q_M and q_ζ are valid in general case when the water depth varies in arbitrary fashion.

It is now obvious that our previously obtained results (9) and (10) are the approximate solutions of (16) and (17) in cases where $|q_M|$, $|q_\zeta|\ll 1$.

These nonlinear differential equations of Ricatti Type can be integrated by numerical methods in the general case.

Thus, it became evident that the step-wise approximation of the arbitrarily-shaped water depth is valid so long as the limiting procedure in the interval being made even in the case of surface elevation ζ. When the slope of the water depth is gentle, one-time reflection is more effective than the higher-times reflection and W.K.B. approximation can be applied. On the contrary, when the slope of the water depth is sufficiently steep, the higher-times reflections are more effective and the approximation in the former becomes failing.

3. Discussion and applications of the results in Sec. 2

In Sec. 2, we investigated in some detail the physical and analytical aspects of reflection in one-dimensional case. An infinitesimal increment of reflection coefficient was determined by the local characteristics of wave length, first derivative of

[1] It is evident that the relation (15) represents the reflection coefficient in the usual case, since Ae^{-ikx} and Be^{ikx} represent progressive waves in the positive and negative x-direction respectively in homogeneous water depth.

logarithmic water depth and reflection coefficient there. But it has too complicated a relation to derive analytically exact solution, and it seems only to permit us two approximate ways of solution analytically, the one corresponding to the weak reflection, the other to the strong reflection its first main term corresponding to the case of constant water depth with finite discontinuity at one point.

In the former case, as described in Sec. 2, it has physically some definite meaning and it is also easy to see the characteristics of reflection, since it has rather simple integral forms as its first few terms.

Between these two extreme approximations, there lies the region of strong reflection where it fails, of course, to use the above approximations, and we shall have the need to use numerical analysis method there. But here, it becomes perplexing to inquire the characteristics of reflection. It has been frequent to estimate reflection coefficient by approximating an actual water depth with a linear zig-zag line, but it will be necessary to have some information as to the errors introduced by that procedure. To this point, numerical analysis of the equation (16) or (17) will have a little some advantage of the latter.

Now, it will be one of the most important problems in propagation of long water waves to investigate the aspects of reflection in case of a solitary wave or an arbitrary form of wave as the incident wave, from a practical point of view, since many long waves in the ocean like tsunamis have such characteristics.

Some of these problems being still under investigation, they will be described below briefly.

(i) *Numerical Analysis*

The method due to Runge-Kutta, or mixed one of Runge-Kutta and Levy will be convenient in this case.

It will be efficient to make use of the method such that the first four point is determined by Runge-Kuttas' method, after then Levy's method being used. As to the details on these methods, one could refer to the text-books on numerical analysis.

At this point, it might be necessary to mention some way to calculate $d(\log h)/dx$ from the known values of water depth $h(x)$, and it will be sufficient in this case to replace first derivative of logarithmic water depth by two-point finite difference such as

$$\left(\frac{1}{h}\frac{dh}{dx}\right)_x = \frac{1}{h(x)}\frac{h(x+\Delta x)-h(x-\Delta x)}{2\Delta x} - \frac{1}{3!}\frac{1}{h(x)}\left(\frac{d^3h}{dx^3}\right)_x (\Delta x)^2 + \cdots ,$$

the error being of the order $1/3! \cdot 1/h \cdot d^3h/dx^3 \cdot (\Delta x)^2$. Then its final error accumulated in the course of integration will be of the order

$$\frac{1}{24}\int_a^b \frac{1}{h}\frac{\partial^3 h}{\partial x^3}(\Delta x)^2(1-q^2)dx\,, \tag{3.1}$$

and estimation can be made by calculating approximately the integral (3.1), or qualitatively the errors will be very small if we take Δx as

$$\mathrm{Max}\left[\frac{d}{L}\left(\frac{\Delta x}{L}\right)^2\right] \ll \frac{h}{10|a-b|}$$

where L and d represent local characteristic wave length and amplitude of water depth respectively.

(ii) *Examples of Weak Reflection and its Simple Characteristics*

First, we note that the sequential solution for weak reflection with the boundary condition that $q=0$ at $x=c$ can be represented by

$$q=q_1+q_3+q_5+\cdots\,, \tag{1}$$

where

$$q_1=-\int_c^x be^{-\int_x^z a dx}dz\,, \quad q_3=\int_c^x bq_1^2 e^{-\int_x^z a dx}dz, \cdots$$

and

$$a(x)=\frac{2i\sigma}{\sqrt{gh}}$$

and

$$b(x)=\frac{\pm 1}{4h}\frac{dh}{dx}\,,$$

the upper sign referring to volume transport and the lower to surface elevation.

Now, it will be a convenient way of approximation to replace the actual water depth with successive straight lines. Hence, we consider first the case of water depth with constant slope and then that by the approximation with straight line.

1) A case of the water depth with constant slope. In this case where the water depth in the interval $0<x<a$ is expressed by $h=h_1-kx$ (Fig. 2), the first order reflection coefficient $q_{1\zeta}$ for the surface elevation ζ can be expressed by

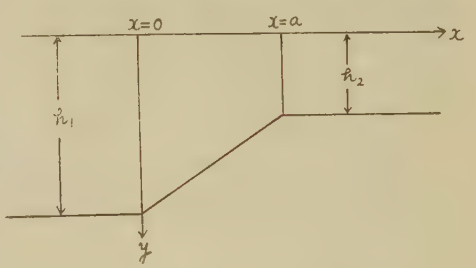

Fig. 2.

$$q_{1\zeta}=\frac{1}{2}\exp\left\{-\frac{4i\sigma}{k}\sqrt{\frac{h_1}{g}}\right\}\int_{4\sigma/k\cdot\sqrt{h_2/g}}^{4\sigma/k\cdot\sqrt{h_1/g}}\frac{1}{t}\exp(it)dt \tag{2}$$

If the condition $4\sigma/k\cdot\sqrt{g/h}\gg 1$ is satisfied, the expression (2) can be expanded into

power series of $k/4\sigma\cdot\sqrt{g/h}$ such as

$$q_{1\zeta}\simeq\frac{1}{2}\exp\left\{-\frac{4\sigma i}{k}\sqrt{\frac{h_1}{g}}\right\}\cdot\left\{\frac{k\sqrt{g}}{4\sigma}i\left(\frac{e^{i\cdot 4\sigma/k\cdot\sqrt{h_2/g}}}{\sqrt{h_2}}-\frac{e^{i\cdot 4\sigma/k\cdot\sqrt{h_1/g}}}{\sqrt{h_1}}\right)\right.$$
$$\left.+\left(\frac{k\sqrt{k}}{4\sigma}\right)^2\left(\frac{e^{i\cdot 4\sigma/k\cdot\sqrt{h_2/g}}}{h_2}-\frac{e^{i\cdot 4\sigma/k\cdot\sqrt{h_1/g}}}{h_1}\right)+\cdots\right\} \quad (3)$$

Likewise, at the same condition that $4\sigma/k\cdot\sqrt{h/g}\gg 1$, the third order reflection coefficient $q_{3\zeta}$ for the surface elevation can be represented by using equations (3) and (1) as

$$q_{3\zeta}=\frac{1}{2}\exp\left\{-\frac{4i\sigma}{k}\sqrt{\frac{h_1}{g}}\right\}\int_{\sqrt{h_1}}^{\sqrt{h_2}}\frac{q_1^2(u)}{u}e^{4i\sigma/k\sqrt{g}\cdot u}\,du=\text{order of }\left(\frac{k}{4\sigma}\sqrt{\frac{g}{h}}\right)^3.$$

Hence, convergency of the series (1) will be very satisfactory in this case. This series is, of course, exactly the same as that derived from the usual reflection coefficient formula by using asymptotic expansions of Bessel Functions.

2) A method for the simple estimation of weak reflection. Here the method is described with the straight line approximation. The water depth h can be expressed in this case as $h=h_1(x)+m(x)$ where $h_1(x)$ is a linear function of x. Then, the first order reflection coefficient $q_1^{(1)}$ and the first order errors $\delta q_1^{(1)}$ are represented by

$$q_1^{(1)}=\pm\frac{1}{4}\int_a^b\frac{k}{h_1}e^{-2i\int_a^x\sigma/\sqrt{gh_1}\cdot dx}\,dx\,,$$

$$\delta q_1^{(1)}=\pm\frac{1}{4}\int_a^b\left[\left\{-\frac{k}{h_1}\frac{m}{h_1}+\frac{1}{h_1}\frac{dm}{dx}+\frac{k}{h_1}i\int_a^x\frac{\sigma}{\sqrt{gh_1}}\frac{m(x)}{h_1}dx\right\}\times e^{-2i\int_a^x\sigma/\sqrt{gh_1}\cdot dx}\right]dx$$

where k represents the slope of linear depth dh_1/dx and the positive and negative signs correspond to the case for the volume transport M and for the surface elevation ζ respectively.

Then, $q_1^{(1)}$ is readily integrable according to the equation (3), and it will also be evident that one had better select $m(x)$ such that its value may be distributed about zero equally.

iii) *Case of a solitary wave or waves of a given spectrum.*

In this case, the aspects of reflection will considerably differ from those in case of sine waves of infinite train, since wave components have strong non-uniformity in the effect of reflection and the reflected wave is to be much distorted from the original.

Now, let the form of a solitary wave be

$$\zeta=F\left(t-\frac{x}{v_0}\right)$$

for constant water depth, where ζ denotes surface elevation, v_0 wave velocity $\sqrt{gh_0}$. Then, the reflected wave at the initial discontinuity point $x=a$ will be given by

$$G(t)=\frac{1}{\pi}\Re\int_0^\infty q(\sigma)\int_{-\infty}^{\infty}\zeta(u)e^{-i\sigma u}du\,e^{i\sigma(t-a/v_0)}d\sigma$$

where $q(\sigma)$ represents reflection coefficient of an infinite sine wave train of frequency σ. If we put $A(\sigma)$ as

$$A(\sigma)=\frac{1}{\pi}\int_{-\infty}^{\infty}\zeta(u)e^{-i\sigma u}\,du$$

then $G(t)$ can be expressed by

$$G(t)=\Re\int_0^\infty q(\sigma)A(\sigma)e^{i\sigma(t-a/v_0)}\,d\sigma\ ,$$

where $A(\sigma)$ may be called the spectral distribution of wave height.

Now, it is evident that, in the long water wave region, reflection has the tendency to become weaker or stronger as frequency of an infinite sine-wave train becomes higher or lower correspondingly, and it will be reasonable to assume that in the surface gravity wave region where frequency is much higher, reflection will be very small.

Then, calculation of the reflected wave $G(t)$ when incident wave $F(t-x/v_0)$ is given will be made by the following approximation: the effect of surface gravity wave component will be neglected, and the region of long wave components will mainly contribute to the reflection. This approximation will be reasonable at least so long as the part of surface gragity wave components in the spectral decomposition of surface elevation is not much greater than the remainder part. But it is still troublesome in this approximation, when main contribution to the reflection is due to the wave components of strong reflection, and it will be simple only in case when wave components of weak reflection are mainly responsible.

If we introduce here characteristic frequencies σ_* and σ^* as the separation frequency of weak reflection from strong one and of long water wave from surface gravity wave respectively, an criterion for the simplest case to hold in which component ranges of strong reflection as well as of surface gravity wave character are negligibly responsible for the reflected wave will be given by

$$\left|\Re\int_0^{\sigma_*}q(\sigma)A(\sigma)e^{i\sigma(t-a/v_0)}\,d\sigma\right|\ll\operatorname*{Max}_t\left|\Re\int_{\sigma_*}^{\sigma^*}q(\sigma)A(\sigma)e^{i\sigma(t-x/v_0)}\,d\sigma\right|\ .$$

Now, from physical point of view that energy must conserve, reflection coefficient $q(\sigma)$ at the initial discontinuity $x=a$ must be smaller than or equal to unity in its

absolute value. Hence, above inequality may be transformed into

$$\int_0^{\sigma_*} |A(\sigma)| d\sigma \ll \operatorname*{Max}_t \left| \Re \int_{\sigma_*}^{\sigma^*} q(\sigma) A(\sigma) e^{i\sigma(t-a/v_0)} d\sigma \right| ,$$

which may be used in practice as a criterion for that case.

4. Concluding Remarks

It can be concluded from the preceding analysis that the differential equation for the reflection coefficient can be used for practical purposes and the simple approximations are valid in the cases of both very large variations of logarithmic water depth and weak reflection. In the latter case, we are ready for the calculation by use of the successive straightlines approximation of the water depth.

Thus, in case of compound configuration of the bottom, the first, we divide the region of variable depth into three kinds of subregions where two ways of extreme approximation are valid respectively or neither of them are valid. Second, we construct the solution for the reflection coefficient based on the differential equation. For the case of solitary wave, it may be worth attempting to integrate the original wave equation numerically from the standpoint of the Cauchy's "Anfangswertprobleme".

Neither of any quantitative discussion nor any example for actual numerical computation of reflection coefficient is included in the present article. We regret that the result obtained within the scope of present work may not give more than a discussion of mathematical basis for the actual application. Methods described above might not be most practical as yet, but better ways might be desired. However, the differential equations for the reflection coefficient should be useful by any means. From the solution of the equations, one could obtain the reflection coefficient defined at any desired places and not only for the region $x \leq 0$. It should also be useful for practical application that reflection in case of solitary type waves can be found which will be of special interest for tsunami problems. On the other hand, the problem should be attacked for two-dimensional variations in ocean depths which should be taken into account to make the application more practicable. If we might disregard the details of individual occurrence of reflection and be interested in some average situations of the energy transmission, we might be able to stand on a different point of view, that is, on some statistical means dealing with irregular depth distributions.

An attempt in such direction has been made by one of the present author recently (Yoshida, 1958).

Acknowledgement:

The study was supported by the funds provided by the Scripps Institution of

Oceanography, University of California, under contract with the Japanese Organization for Tsunami Investigation, Tokyo.

References

BREMMER, H.: Physica, **15**, p. 593 (1949).

BREMMER, H.: "The W.K.B. approximation as the first term of a geometric optical series." Commun. Pure and Appl. Math. **4** (1951)

SCHELKUNOFF, S. A.: "Remarks concerning wave propagation in stratified media." Commun. Pure and Appl. Math. **4** (1951).

WALKER, L. R. and N. WAX: "Non-uniform transmission lines and reflection coefficients." J. Appl. Phys. **17** (1946) pp. 263–265.

YOSHIDA, Kozo: A hypothesis on transmission of energy of tsunami waves (1958, in Press).

Records of Oceanographic Works
in Japan Vol. 5, No. 1,
February, 1959

An Estimation of the Average Compensation Depth by a Study of the Vertical Distribution of Dissolved Oxygen

By
Akira Okubo
(Oceanographical Section, Japan Meteorological Agency)

Abstract

By a study of the vertical distribution of dissolved oxygen on the basis of the diffusion equation in which an annual variation of the vertical eddy diffusivity is taken into consideration, the author estimates the average annual depth of compensation at the ocean weather stations "*T*" and "*X*". The computed results are found to be reasonable in comparison with other experimental and empirical informations. In addition to this, the relationship between the depth of compensation and that of being just saturated with oxygen is discussed.

1. Preface

The depth at which oxygen production by the activities of plants and oxygen consumption due to the respiration and oxidation are equal is called the *compensation depth*. This depth evidently varies with the season of the year, the time of day, locality, the biological character of the water, etc. For a given locality one can introduce such terms as daily compensation depth with various conditions of the cloudiness average monthly compensation depth, average annual compensation depth, and so on.

The concept of the compensation depth plays an important role in the studies of not only the productivity in connection with the photosynthesis but also the vertical distribution of oxygen in the upper layer.

Nevertheless, the depth of compensation has scarecely been examined by means of actual observations such as an assimilation experiment over a period long enough to determine the average values at a given locality in the open sea.

In this paper the author will attempt to estimate the average annual depth of compensation by a study of the vertical distribution of dissolved oxygen.

2. Principle of the present method of estimation

We shall confine ourselves to the discussion in the sea area where can be disregarded the effects of advection and horizontal mixing. Then, the basic equation governing the diffusion of oxygen is given by

$$\frac{\partial O_2}{\partial t}=\frac{\partial}{\partial z}\left(K_z\frac{\partial O_2}{\partial z}\right)+R(t,\ z)\ , \tag{1}$$

where K_z is the vertical eddy diffusivity and $R(t,\ z)$ represents the local time change of oxygen concentration due to biological processes.

It may be easily understood that the depth of compensation corresponds to the layer at which the term $R(t,\ z)$ or its mean values over a certain length of time is equal to nought.

Let it be assumed that the expansion of O_2 into a series of harmonic terms should be permitted. Then,

$$\begin{aligned}O_2(t,\ z)=\overline{O_2(z)}+O'(z)\cos(\alpha t-\mu_1(z))+O''(z)\cos(2\alpha t-\mu_2(z))\\ +O'''(z)\cos(3\alpha t-\mu_3(z))+\cdots,\end{aligned} \tag{2}$$

where the bar denotes an average annual value and $\alpha=2\pi/\tau$ and τ is the period length of the 1st harmonic term that corresponds to an annual component of O_2.

As to the vertical eddy diffusivity it may be put

$$K_z=K\{1+\gamma\cos(\alpha t-\phi)\}\ , \tag{3}$$

together with $|\gamma|<1$, from the consideration of an annual variation of the upper (homogenous) mixing layer on which the vertical eddy diffusivity primarily depends (Okubo, 1959).

After substituting the expressions (2) and (3) into the basic equation, each term is averaged over a year. Then,

$$\frac{\partial\overline{O_2}}{\partial t}=K\frac{\partial^2}{\partial z^2}\overline{[\{1+\gamma\cos(\alpha t-\phi)\}\{\overline{O_2}+O'\cos(\alpha t-\mu_1)+O''\cos(2\alpha t-\mu_2)+\cdots\}]}+\overline{R}\ . \tag{4}$$

Since the annual mean value of dissolved oxygen is expected to remains unaltered year after year, one may put

$$\frac{\partial\overline{O_2}}{\partial t}=0\ , \tag{5}$$

Consequently, the following condition must be satisfied at the average annual compensation depth ($R=0$):

$$\frac{d^2}{dz^2}\overline{[\{1+\gamma\cos(\alpha t-\phi)\}\{O_2+O'\cos(\alpha t-\mu_1)+O''\cos(2\alpha t-\mu_2)+\cdots\}]}=0\ . \tag{6}$$

In other words the curvature of the expression in the bracket must be zero at the compensation depth when plotted against z. By performing the calculation the equation (6) is reduced to

$$\frac{d^2}{dz^2}\left[\overline{O}_2+\frac{\gamma O'}{2}\cos(\mu_1-\phi)\right]=0\,, \tag{7}$$

where the terms containing an integral such as

$$\int_0^\tau \cos(n\alpha t-\mu_n)\,dt \quad \text{and} \quad \int_0^\tau \cos(\alpha t-\phi)\cos(n\alpha t-\mu_n)dt \quad (n\neq 1)$$

have vanished as it might be expected.

In order to get an additional criterion it may be convenient to integrate the equation (4), of cource, subject to the condition (5), over the depth from the sea surface to z. Then

$$K\frac{d}{dz}\left[\overline{O}_2+\frac{\gamma O'}{2}\cos(\mu_1-\phi)\right]=-\int_0^z \overline{R}(\eta)d\eta+\text{constant}\,. \tag{8}$$

Since the biological effects that influence the oxygen content always lead to the net production of oxygen above the depth of compensation and to the net consumption of oxygen below that depth, the first integral in the right-hand side of the equation (8) must have the largest negative value at the depth of compensation. Consequently, the following criterion must be also fulfilled at the average annual compensation depth.

$$\frac{d}{dz}\left[\overline{O}_2+\frac{\gamma O'}{2}\cos(\mu_1-\phi)\right]=\text{largest negative value.}$$

On the basis of the condition (7), together with the above criterion, the average annual depth of compensation is to be estimated later on.

3. Examples of estimation of the average compensation depth

In order to apply the above method to actual cases it is necessary first of all to select the observations that are carried out not only more than 10 times or so a month but also over a long period such as at least a few years, in a limited sea area. Fortunately, the data suitable for this purpose are available from the observations at the ocean weather stations "X" (39°N, 153°E) and "T" (29°N, 135°E), where oceanographical observations were carried out more than 10 times a month, on the average, during the periods from March 1948 to November 1953 at St. "X" and from September 1948 to November 1953 at St. "T", respectively. On the basis of the data of observation at both ocean weather stations, monthly mean values of dissolved oxygen for the standard levels are computed and the *normal* values of them for each month of the year are determined from these monthly means during the year under investigation, which are shown in Table 1. Moreover, harmonic constants of the annual variation of the normal oxygen distribution

Table 1. "Normal" value of dissolved oxygen (ml/L) at Sts. "T" and "X".

(a) St. "T" (29°N, 135°E).

Depth (m)	Jan.	Feb.	Mar.	Apr.	May	June	July	Aug.	Sept.	Oct.	Nov.	Dec.
0	5.36	5.48	5.63	5.43	5.22	5.14	4.94	4.70	4.79	4.87	5.08	5.30
10	5.33	5.51	5.62	5.48	5.19	5.16	4.99	4.73	4.74	4.87	4.99	5.25
25	5.36	5.54	5.64	5.43	5.20	5.20	5.06	4.84	4.78	4.87	4.94	5.26
50	5.33	5.43	5.56	5.43	5.19	5.27	5.34	5.26	5.06	5.02	5.02	5.32
75	5.29	5.45	5.50	5.36	5.17	5.25	5.34	5.21	5.21	5.10	5.12	5.22
100	5.30	5.45	5.44	5.43	5.09	5.17	5.19	5.05	5.13	4.99	5.06	5.13
150	5.05	5.22	5.32	5.18	5.00	5.12	5.00	4.89	4.94	4.89	4.90	4.91
200	4.83	5.04	5.04	5.09	4.95	5.04	4.97	4.84	4.87	4.88	4.90	4.89

(b) St. "X" (39°N, 153°E).

Depth (m)	Jan.	Feb.	Mar.	Apr.	May	June	July	Aug.	Sept.	Oct.	Nov.	Dec.
0	6.00	6.10	6.38	6.38	6.25	5.86	5.45	5.12	5.25	5.68	5.67	5.93
10	5.90	6.03	6.51	6.36	6.25	5.84	5.52	5.16	5.24	5.72	5.68	5.89
25	5.91	6.03	6.38	6.32	6.22	5.99	5.70	5.46	5.34	5.74	5.66	5.81
50	5.90	6.00	6.27	6.23	6.11	5.86	5.58	5.78	5.76	5.27	5.64	5.91
75	5.98	6.02	6.25	6.19	6.00	5.58	5.13	5.12	5.22	5.27	5.32	5.78
100	5.96	6.02	6.21	6.12	5.96	5.48	5.07	4.94	4.92	5.17	4.95	5.51
150	5.73	6.11	6.19	5.84	5.83	5.57	5.15	5.10	5.14	5.20	4.92	4.98
200	5.14	5.50	5.87	5.67	5.74	5.52	5.19	5.10	5.25	5.24	4.99	4.84

Table 2. Harmonic constants of the annual variation of dissolved oxygen at Sts. "T" and "X".

(a) St. "T" (29°N, 135°E)

Depth (m)	$\overline{O_2}$ (ml/L)	O' (ml/L)	μ_1 (°)
0	5.16	0.39	47
10	5.16	0.40	53
25	5.18	0.37	55
50	5.27	0.19	72
75	5.27	0.13	72
100	5.20	0.18	60
150	5.04	0.17	73
200	4.94	0.10	94

(b) St. "X" (39°N, 153°E)

Depth (m)	$\overline{O_2}$ (ml/L)	O' (ml/L)	μ_1 (°)
0	5.84	0.52	58
10	5.84	0.51	59
25	5.88	0.42	72
50	5.86	0.33	73
75	5.69	0.56	54
100	5.54	0.67	60
150	5.48	0.56	72
200	5.34	0.37	91

are tabulated only for the annual means and annual components (Table 2). Then, if we take γ and ϕ as 0.9 and 60° (for St. "T") and 75° (for St. "X"), respectively (OKUBO, loc. cit.), the expression in the bracket of the equation (7) can be evaluated for the standard depths, the results of which are indicated in Fig. 1 by plotting against z as well as tabulated in Table 3 in order to make convenient for

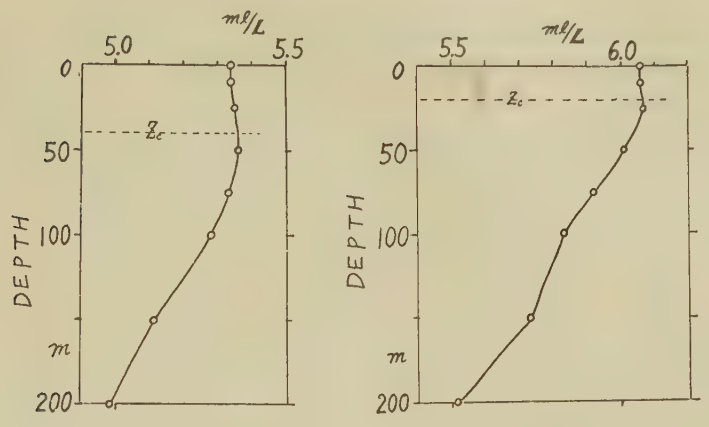

(a) St. "T" (b) St. "X"

Fig. 1. The vertical variations of the expression $\overline{O_2}+\frac{\gamma O'}{2}\cos(\mu_1-\phi)$.

Table 3. The vertical variations of the expression $\overline{O_2}+\frac{\gamma O'}{2}\cos(\mu_1-\phi)$ at Sts. "T" and "X".

(a) St. "T" ($\phi=60°$)

Depth (m)	$O_2+\frac{\gamma O'}{2}\cos(\mu_1-\phi)$ (ml/L)
0	5.34
10	5.34
25	5.35
50	5.36
75	5.33
100	5.28
150	5.11
200	4.98

(b) St. "X" ($\phi=75°$)

Depth (m)	$\overline{O'}+\frac{\gamma O'}{2}\cos(\mu_1-\phi)$ (ml/L)
0	6.06
10	6.06
25	6.07
50	6.01
75	5.92
100	5.83
150	5.73
200	5.51

estimating the depth of compensation.

By inspecting the curvature in the figure, the average annual depth of compensation is estimated to be about 40 m and 20 m in the case of Sts. "T" and "X", respectively.

4. Discussion

Owing to the situation where the experimental determination of the compensation depth is too difficult or troublesome to be pursued throughout the year in a limited area of the open sea, the present method will be sure to make a somewhat contribution to the estimation of the average annual depth of compensation. Nevertheless, it is still required that our results should be justified by comparing

with those of other estimation. For this purpose we shall introduce OKAMI's estimation which was quoted by UYENO (UYENO, 1958). Based on an accurate measurement of light intensities in various wave lengths (SASAKI, OKAMI, OSHIBA and WATANABE, 1958), he computed the compensation depth at noon at the middle of November at two stations which were located in the Kuroshio to the north of St. "*T*", by use of the principles proposed by JENKIN (1937), HOGETSU and ICHIMURA (1954), and PETTERSON (1934), respectively.

Thus, at station 1 in 33°40′N and 136°50′E the depth of compensation was estimated to exist at a depth of 42.5 m, 41 m and between 51.5 m and 61 m, respectively, and at station 3 in 33°20′N and 135°40′E it was 67 m, 77 m and between 61.5 m and 71.5 m, respectively. These depths are found to be much deeper than that of our estimation for St. "*T*". It seems, however, to be a reasonable value on account of the reason that the average annual depth of compensation should be less than the compensation depth determined at noon in autumn with a clear sky.

In addition to OKAMI's estimation, we shall also make reference to an empirical method which was proposed by YOSHIMURA (1937). From a study of the relationship between the summerly compensation depth, Z_{sc}, and the transparency, D, in the lake water, he derived an empirical formula expressing approximately by $Z_{sc}=1.5D$, where Z_{sc} and D are given in meters. Application of this relation to our cases yields the results that the average annual depths of compensation are estimated to be about 47 m and 33 m at Sts. "*T*" and "*X*", respectively. Although these depths are found to be slightly deeper than those of our estimation, ours seem to be also reasonable values on account of the same reason as before.

Table 4. Summary of the results of computation of the compensation depth by means of the various methods.

	St. "*T*"	St. "*X*"
Location	29°N, 135°E	39°N, 153°E
Average annual transparency ($\overline{D}$)	31.2 m	21.9 m
Author's method	40 m	20 m
Empirical method (Yoshimura)	47 m	33 m
Okami's estimation	33°40′N, 136°50′E (Nov. 18, 1958) D=18 m	33°20′N, 135°40′E (Nov. 20, 1958) D=36 m
J-method	42.5 m	67 m
H-method	41 m	77 m
P-method	51.5~61 m	61.5~71.5 m
Depth of just saturation	80 m	40 m
	St. "*T*"	St. "*X*"

In Table 4 we summarize the results of computation of the compensation depth by means of the various method, together with other data which serve as a reference.

Finally relationship between the depth of compensation and that of being just saturated with oxygen (referred to a normal atmosphere) should be mentioned. Fig. 2 shows the vertical variations of the average annual values of dissolved oxygen and its saturation content in the upper layers at Sts. "*T*" and "*X*". As is

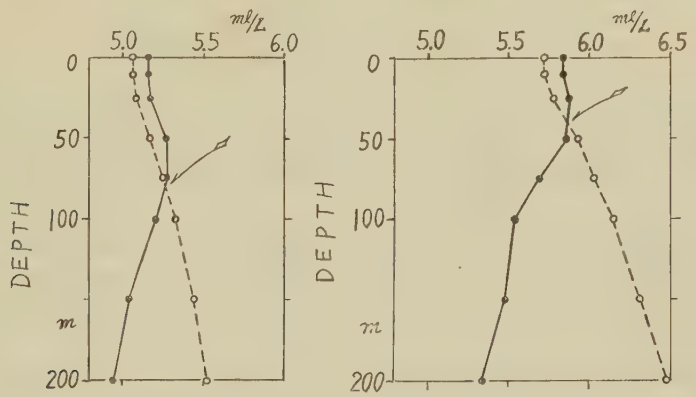

(a) St. "*T*" (b) St. "*X*"

Fig. 2. The vertical variations of the average annual values of dissolved oxygen (—●—) and its saturation content (- -○- -).

evidently seen in the figure, the waters being just saturated with oxygen are found at about 80 m at St. "*T*" and at about 40 m at St. "*X*", the depths of which do lie at 20~40 m below those of compensation contrary to a simple expectation that the compensation depth might approximately correspond to the depth of being just saturated with oxygen. The reason for this discrepancy may be interpreted as follows:

First we introduce to the biological term R in the basic equation (1) the expression mentioned below (Okubo, loc. cit.).

$$R(t,\ z)=C_1(t)e^{-mz}-C_2(t)e^{-nz}\ . \tag{9}$$

Then, it is obtained that

$$\frac{\partial O_2}{\partial t}=K\{1+\gamma\cos(\alpha t-\phi)\}\frac{\partial^2 O_2}{\partial z^2}+C_1(t)e^{-mz}-C_2(t)e^{-nz}\ . \tag{10}$$

As to the saturation value of oxygen O_2', it may be assumed to express as a function of water temperature only, if one considers the surface waters where the annual range of chlorinity is relatively small. Hence, one can write

$$O_2'=f(T)=\lambda-\sigma T \text{ (as the first approximation).} \tag{11}$$

While, a distribution of water temperature in the surface layers will be discussed by the following equation in which includes an effect of absorption of radiation

$$\frac{\partial T}{\partial t}=K\{1+\gamma\cos(\alpha t-\phi)\}\frac{\partial^2 T}{\partial z^2}+Q(t)e^{-qz}. \tag{12}$$

From the equations (11) and (12) the diffusion equation for O_2' is obtained as follows:

$$\frac{\partial O_2'}{\partial t}=K\{1+\gamma\cos(\alpha t-\phi)\}\frac{\partial^2 O_2'}{\partial z^2}-\sigma Qe^{-qz}\,. \tag{13}$$

Subtracting the equation (10) from (13), we have

$$\frac{\partial \Delta O_2}{\partial t}=K\{1+\gamma\cos(\alpha t-\phi)\}\frac{\partial^2 \Delta O_2}{\partial z^2}-\sigma Qe^{-qz}-C_1e^{-mz}+C_2e^{-nz}\,, \tag{14}$$

where ΔO_2 is defined by the difference between the saturation value and the observed content of oxygen. Taking mean values over a period of the year, the equation becomes

$$\frac{\partial \overline{\Delta O_2}}{\partial t}=K\frac{\partial^2}{\partial z^2}\overline{[\{1+\gamma\cos(\alpha t-\phi)\}\Delta O_2]}-\sigma\overline{Q}e^{-qz}-\overline{C}_1e^{-mz}+\overline{C}_2e^{-nz}\,. \tag{15}$$

At the depth of just saturation $z=z_s$, $\overline{\Delta O_2}$ must be zero. Then, again making use of the assumption that the term in the left-hand side of the above equation should be negligible, the following relation will be fulfilled under the appropriate boundary conditions.

$$\frac{\sigma\overline{Q}}{q^2}(1-e^{-qz_s})+\frac{\overline{C}_1}{m^2}(1-e^{-mz_s})-\frac{\overline{C}_2}{n^2}(1-e^{-nz_s})\simeq 0\,. \tag{16}$$

While, the average annual depth of compensation $z=z_c$ may be regarded as the depth at which the biological term proposed by the expression (9) must vanish when one takes the annual means, and hence

$$\overline{C}_1e^{-mz_c}-\overline{C}_2e^{-nz_c}=0\,. \tag{17}$$

From the equations (16) and (17) the depth of just saturation can be easily calculated for the proper numerical values of $\overline{Q}$, $\overline{C}_1$, q, m, n and z_c. For example, putting $\overline{Q}=28°$/month (SVERDRUP, et al., 1942 and MASUZAWA, 1952), $\overline{C}_1=3/4\times10^{-3}$ ml/L/month, $q=1/m$ (SVERDRUP et al, loc. cit.), $\sigma=0.09$ ml O_2/L/°C, $m=(1/25)$/m and $n=(1/200)$/m (OKUBO, loc. cit.) and $z_c=40$ m in the case of St. "T", we obtain $z_s=78$ m, which agrees very well with the observed depth of about 80 m.

Though the author has confined himself to an estimation of average annual depth of compensation, the present method or principle will be applied to compu-

tations of the average monthly depth of compensation and so on, in the case where the sufficient data for the vertical distribution of dissolved oxygen are available.

Acknowledgement

The author wishes to express his sincere thanks to Prof. Y. Matsue of Tokyo University for his helpful suggestions as regards the average compensation depth, and also to Dr. R. Marumo of Japan Meteorological Agency for his valuable informations about the biological environment at the ocean weather stations.

References

Hogetsu, K. and S. Ichimura 1954. Studies on the biological production of Lake Suwa. IV The ecological studies on the production of phytoplankton. Japan J. Bot., 14 (2).

Jenkin, P. M. 1937. Oxygen production by the diatom *Cosinodiscus excentricus* Ehr. in relation to submarine illumination in the English Channel. J. Mar. Biol. Assoc., 22 (1).

Masuzawa, J. 1952. The heat exchange between sea and atmosphere in the southern sea of Japan. J. Oceanogr. Soc. Japan, 7 (3~4).

Okubo, A. 1959. Discussions on the annual variation of dissolved oxygen in the ocean. J. Oceanogr. Soc. Japan, 15 (to be published).

Petterson, H. H. and S. Landberg 1934. Submarine daylight and the photosynthesis of phytoplankton. Göteborg Vetensk. Samh. Handl., 5, B-4-5.

Sasaki, T., N. Okami, G. Oshiba and S. Watanabe 1958. Spectral energy distribution of submarine daylight off Kii Peninsula—In relation to the investigation of oceanic productivity. Rec. Oceanogr. Works in Japan, special No. 2.

Sverdrup, H. U., M. W. Johnson and R. H. Fleming 1942. The Oceans. Chap. IV.

Uyeno, F. 1958. Water movements and distributions of diatoms in a vertical section of the cold water region off Enshu-nada, Japan. Memoirs Kobe Mar. Obs. XII (1).

Yoshimura, S. 1937. Limnology (in Japanese). p. 195.

Records of Oceanographic Works
in Japan Vol. 5, No. 1,
February, 1959

Preliminary Report on the Shelf Sediments off Kamo, Yamagata, Japan

By
Hideo Kagami
(Geological Institute, Faculty of Science, University of Tokyo)

1. Introduction

Only the chart No. 145 (Niigata Harber to Oga Peninsula) has been utilized along the Japan Sea side of the northeastern part of the main-land of Japan since 1926, with a correction in 1934. Hydrographic Department of Japan started re-examination of the chart by means of an echosounding system several years ago, and has continued up to the present. Surveying ships Tenkai and Torii of Hydrographic Department, Maritime Safety Board, Japan collected forty-one bottom samples during July 11 to 15, 1957, as a part of this survey.

This part of the investigation was planned by the Sedimentological Subcommittee, Science Council of Japan, and the following studies were alloted.

1) Mollusca
2) Foraminifera
3) Organic substance
4) Sedimentary petrography

The main purpose of this paper is to grasp the general character of the grain size distribution and heavy mineral associations in the shelf sediments of the surveyed area as a preliminary report.

The writer is sincerely indebted to Professor Takao Sakamoto of the University of Tokyo for his kind instruction and encouragement. He wishes also to express his thanks to Assistant Professor Noriyuki Nasu for his valuable advice. Appreciations are also expressed to Dr. Azuma Iijima of the University of Tokyo and to Dr. Ryohei Komukai, Mr. Michihei Hoshino and Mr. Keisaku Kudo of the Hydrographic Department of Japan for their assistance during the survey. This investigation has been partly supported by a Grant in Aid for Fundamental Scientific Research from the Department of Education of Japan.

2. General Environment

The continental shelf off Kamo measures about 18 kilometers in width and its gradient is about 6×10^{-3}. There are mainly three flat areas on the shelf; namely, those in between 20 to 30, 50 to 60 and 80 to 100 in meters, occasionaly, another flat plain in between 140 to 150 meters is also observed. The flat plain in between 80 to 100 meters develops most extensively in this area and its gradient is about

3.4×10^{-3}.

The gradient of the shelf along the Kamo-uplifted land is larger than that along Shonai plain, which occupies the northern half of the background of the surveyed area. At the eastern end of the Shonai Plain there lies mountains consisted of Miocene to Pliocene rocks, above which Mogami River cuts through. Mt. Chokai covers the northern and partly eastern ends of the Shonai Plain. Kamo-uplifted land occupies southern half of the surveyed area and consists of lower and middle Miocene sedimentary rocks which bears coal seams in small amount.

3. Particle Size Distributions

The sampling locations are shown in the Figure 1. The results obtained from grain size analysis are expressed by INMAN's equations (1952), and Mdϕ, Mϕ, $\sigma\phi$, $\alpha\phi$ and $\beta\phi$ values for each locations are calculated.

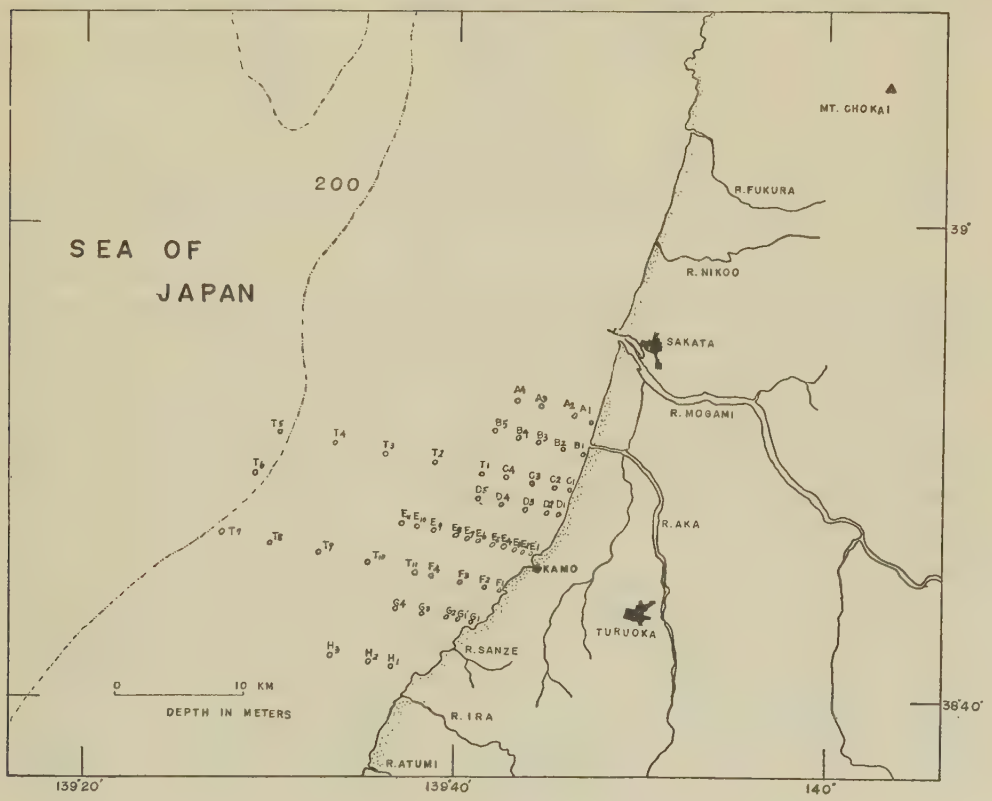

Fig. 1. Index Map (Sample Locations).

A representative particle size distribution pattern is figured by the phi median diameter (Figure 2). The obtained results suggest that the shelf sediments of this area are generally divided into three zones.

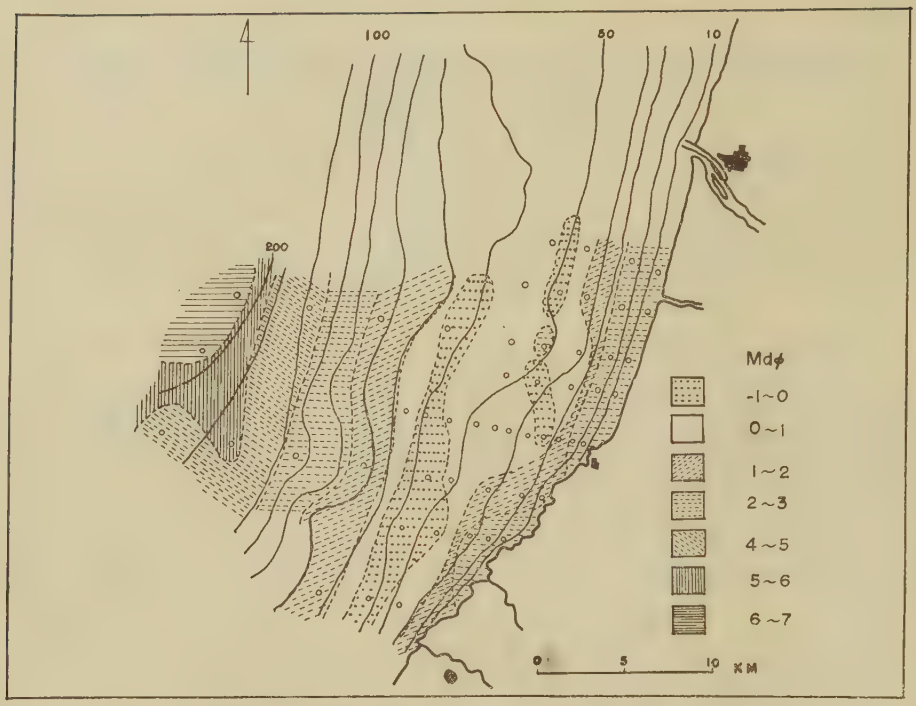

Fig. 2. Phi Median Diameter Distribution Map (Depth in Meters).

1) Near-shore sediments, to the depth of nearly 40 meters, are constituted by well sorted fine sand ($\sigma\phi<0.5$). The skewness shows negative values in general, except a few point where the finest sediment in this zone indicates intermediate skewness value ($\alpha\phi=0$). Mdϕ values increase as the depth increases.

2) Off-shore sediments, 40 to 70 meters in depth, are characterized by very coarse sand. The sorting values range from 0.6 to 1.8; the skewness values range from negative to positive. There are intermediate skewness values among the sediments having Mdϕ values close to zero. The very coarse sands are distributed into two zones, namely in the area shallower than 50 meters deep and in the deeper area. These two zones always have gravels and each sample is reddish brown in dry condition. The meaning of the spreads of gravels and very coarse sand in these sediments are interpreted as the lag deposits produced by winnowing of the inundated coastal plain sand or blanket sand during the periods of lower sea level that have not yet been covered by the younger sediments. (GOULD and STEWART, 1955).

3) Silt and clay below 100 meters in depth are poorly sorted; the skewness values of this sediments are positive. This sample shows bluish gray or gray in wet condition owing to the presence of Fe_2S_3.

There are, of course, transitional zones between these three zones, one of them

lies about 40 meters deep and the other about 90 to 120 meters deep. The latter is characterized by the medium sand of mutual mixing of the two types of sediments. The former is fine to very fine sand rich in tiny gravels; consequently the sediments show worse sorting. This zone seams to indicate another evidence of the old sea level, but this is not sure because of the inadequate number of samples.

By the relation diagram between phi median diameters and phi deviation measures, these grain size zones are easily recognized. Those from 2ϕ to 3ϕ in Mdϕ show the best sorting. Theoretical considerations of this sorting action were made by many authors. Variations of the skewness value from near-shore fine sand to silt and clay are usually seen in small delta deposits (Nasu, 1956).

Sediment coarser than 2ϕ in Mdϕ shows positive to negative phi skewness values. The coarsest sediment (-1ϕ to 0ϕ) in this surveyed area shows positive skewness value. Thus, it is deduced that phi skewness value changes from positive in very coarse sand, then through negative values in coarse to fine sand and to positive in silt and clay again.

4. Heavy Minerals of the Shelf Sediments

The sediments of twenty-three stations were examined to identify the heavy minerals included. The separation of heavy minerals was made here in Thoulet's Solution (specific gravity 2.9).

The variations of titanaugite, augite, common hornblende, hypersthene and iron ores are discussed as follows (Fig. 3). The variation of percentage of titanaugite indicates a rapid decrease at about 40 meters in depth, while the percentage of hypersthene and iron ores increase till to about 90 meters in depth. Hypersthene is stained by ferric iron and has well rounded shape. Some of them show hacksaw structure and individual point of hacksaw structure is usually truncated. In an area deeper than 90 meters there are abundant augite grains. Thus, the mineral assemblage can be divided into three zones, which roughly coincide with those of grain size distributions. The diameter of titanaugite is about 0.3–0.4 millimeters and it shows irregular shape. The hypersthene is generally about 0.5–0.7 millimeters in length, and the diameter of augite is about 0.1–0.2 millimeters.

The lateral diminution of titanaugite in percentage appears evidently from the Atsumi shore to the Yunohama beach. The lateral variation in percentage of hypersthene, on the contrary, is not always recognized.

Four major effects are considered on the diameter and distribution of the heavy minerals: (1) the effect produced by abrasion and chemical weathering during transportation (2) those resulted from the sorting action during transportation (3) those resulted from the derivation from the different source rocks (4) those resulted from the errosion of the bed-rocks.

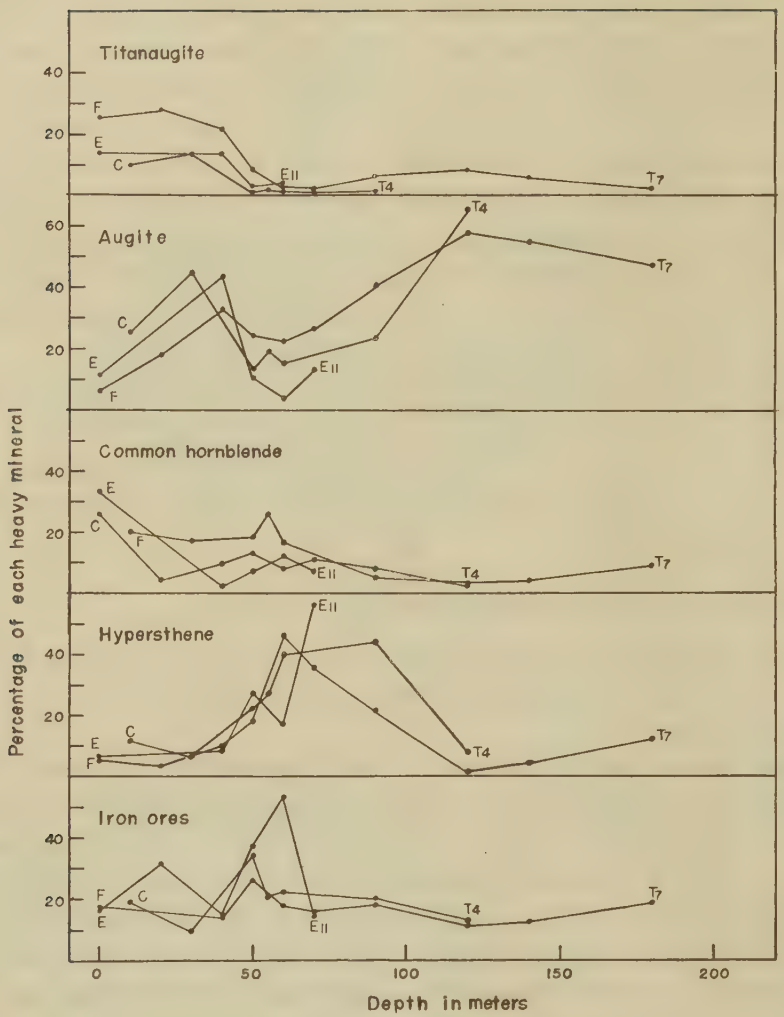

Fig. 3. Variation of the Heavey Minerals.

The evidence of abrasion and chemical weathering in marine sediments has not been known in detail and it is certain that marine sediments are more stable mechanically and chemically than the river sand. Considering from the grain size, very coarse sand bearing dominantly hypersthene were not sorted selectively from the near-shore fine sand. These sediments are thought to be derived from the different source rocks. It is possible that augite contained in fine sand and mud is also derived from the different source rocks, because these sediments contain relatively rich gravels. But, in this case it had better been interpreted that augite was derived from pre-existing sediment by sorting action during the stages of lower sea level.

It is difficult to define accurate provenance of the heavy minerals at this stage

of the research. Titanaugite might be derived from the alkaline rocks of the Kamo-uplifted land where the large outcrops of the Atsumi dolerite are distributed along the coast from Irakawa to Nezugasaki and further south. Origin of the hypersthene is guessed to be the secondary deposits derived from the hypersthenic rocks of Chokai Volcano (2240 M). It is known that Chokai Volcano was built up during Pleistocene. Southern margin of it is covered by the terrace deposits standing 50 meters above the sea level. Terrace deposits near Kannonji contains hypersthene characterized with hacksaw structure which resemble very closely to the hypersthene collected in the shelf sediments. Origin of augite is not yet known in detail.

5. Gravels of the Shelf Sediment

Since the distribution pattern of the gravels coincides with that of very coarse sand, the gravels are also differentiated in two zones. Upper gravel zone is characterized by heavy minerals of titanaugite and hypersthene, while lower gravel zone is only by hypersthene. Gravels of the upper gravel zone chiefly consist of rhyolite, andesite, tuff breccia and tuffaceous sandstone. Tuff breccia and tuffaceous sandstone are distributed along the coast of Kamo-uplifted land. Those of the lower gravel zone consist of rhyorite, andesite, hard shale and siliceous sandstone. Hard shale and siliceous sandstone are distributed along the upper course of the Mogami River. The facts suggest a great supply of detritus by the ancient rivers during the low stand of the sea and also during the upheaval stages of the level.

The provenance of the gravels well coincide with those of heavy minerals.

6. Application to Locating Ancient Shore Lines

Although many attempts have been made to define the ancient shore lines, the method to locate it has not yet been settled.

Indistinct features of the terrigenous material in the outer shelf sediments off Kamo do not serve to distinguish the coastal environment from that of the off-shore area.

The sediment of the near-shore zone consist of well sorted fine sand and are distributed in areas shallower than 40 meters. Distribution of titanaugite is confined almost to this zone. The titanaugite might have been eroded out from the outcrop of the background dolerite and transported since the sea level came nearly up to the present level, because wave erosion is appreciable only down to about 20 meters below sea level in general (Dietz and Menard 1951).

Whereas, the sediment from 50 to 70 meters deep consists almost of very coarse sand, and ferric iron staining on these sand suggests that they were subjected to the intense subaerial weathering before being covered by the subsequent rise in sea level.

The sediments from 70 to 90 meters in depth consist almost of medium sand. The percentage of the gravels included in this zone is less than those of the surroundings. It is characterized also by hypersthene, and those deeper than about 100 meters is characterized by augite. These distributions of each heavy mineral suggest that medium sand characterized by hypersthene might be near-shore sand when the old sea level was lower than the present level, so the old shore line may be identified at about 40 to 70 meters of the present depth. The flat plain between 80 to 100 meters deep, being widely developed in this area, may reflct this ancient wave-cut near-shore zone.

7. Summary and Conclusions

Bottom samples of forty-one stations are collected on the continental shelf off Kamo, Yamagata.

The grain size distributions of the bottom sediments show three major zones in this area, as follows.

1) Near-shore fine sand is the recent deposits characterized by the well sorting and the negative skewness value. This zone spreads over the wide area in front of the river mouths.

2) Off-shore sand and gravels are deposited as lag sediments produced by winnowing of the inundated coastal plain sand or blanket sand during the lower sea level that have not been covered by the younger sediment. The skewness value of this sediment ranges from negative to positive.

3) Silt and clay below 100 meters in depth is poorly sorted. The skewness value of this sediment is positive.

These three major zones are also characterized by the results of the heavy mineral analysis. The near-shore fine sand is characterized by titanaugite which might be derived from the alkaline rocks of the Kamo-uplifted land. Off-shore sand and gravels are characterized dominantly by hypersthene which is guessed to be due to the secondary deposits derived from the hypersthenic rocks of Chokai Volcano. Silt and clay contain augite dominantly, of which provenance is not yet known in detail.

Distribution manner of gravels roughly coincide with those of heavy minerals.

The consideration of the percentage of the gravels and distribution of heavy minerals indicates that medium sand at points 70 to 90 meters deep seams to be the ancient near-shore sediment. The old sea level, when the off-shore sediment was deposited, might be at about 40 to 70 meters of the present depth.

References cited

DIETZ, R. S. and H. W. MENARD, 1951, Origin of abrupt change in slope at continental shelf margin: Bull. Amer. Pet. Geo., V. 35, pp. 1994–2016.

GOULD, H. R. and R. H. STEWART, 1955, Continental terrace sediment in the northeastern Gulf of Mexico: Soc. Eco. Pal. Min., Spe. Publ. n. 3, pp. 2–20.

INMAN, D. L., 1952, Measures for describing the size distribution of sediment: J. Sed. Pet., V. 22, n. 3, pp. 125–145.

NASU, N., 1956, Particle size distribution in the vicinity of Sagami River mouth: J. Fac. Sci. Univ. Tokyo, Sec. 2, V. 10, pp. 65–108.

Records of Oceanographic Works
in Japan Vol. 5, No. 1
February, 1959

Morphometric Comparison of the Albacore from the Indian and the Pacific Ocean

By
Kenji Kurogane and Yoshio Hiyama
(Fisheries Department, Faculty of Agriculture,
University of Tokyo)

Introduction

The tuna fishing grounds in the Indian Ocean were first commercially exploited during the close of 1952. From then onwards many large sized boats have operated in these excellent grounds with high catches. However, we have scarcely had sufficient informations about the biological properties of the Indian albacore as well as other tunas. Mimura (1957)[1] reported on the fishing conditions and size composition of the albacore, basing on the materials by the tuna fishing operations. Examing the ovaries of two albacore, Ueyanagi (1954)[2] discussed the spawning possibility in the eastern area of the Indian Ocean. Several other papers are there referring to the fishing cruises in the Indian Ocean.

According to the records of operation of tuna fishing boats, two fishing grounds for albacore appear separately in the Indian Ocean. One is formed in the waters along the Equator during the season between April and September, and the other in the waters under the South Equatorial Current, all the year round, which lies southwards of 8°S. As has been shown in the Pacific Ocean, it seems that the formation of the tuna fishing ground in the Indian Ocean is also at the mercy of the sea current.

We have reported earlier, basing on the study of the morphometry of the Western Pacific albacore, that they could be separated into two populations, the Northwest Pacific population and the Southwest Pacific population, and these may widely migrate eastward and westward.[3,4] In the present study, we have examined the local differences in the Indian albacore, basing our study upon the morphometric data of 125 specimens collected since 1955, and then we have also compared the Indian albacore with the Pacific one.

We gratefully acknowledge and sincerely extend our gratitude to the director and staff of the Nankai Regional Fisheries Research Laboratory, who have given us all facilities for the collection of the samples.

Materials and Methods

Four samples, each consisting of 25 to 41 individuals, were taken from the following waters: two from the southern waters of the Sunda Islands in 1955 and 1956, which is under the South Equatorial Current; one from the western waters of Sumatra Island and one from the central waters of the Indian Ocean.

All specimens in the samples were caught by long line fishing boats and were all landed at the Tokyo Central Fish Market. These samples are tabulated in table 1, showing the fishing ground, fishing date, number of specimens, range and average of body length. These albacore are large in size, over 90 cm. in body length, and are considered to be of the spawning group.

Table 1. Fishing ground, date taken, number of fish, range and average of body length for each sample from the Indian Ocean.

Fishing ground		Date taken	No. of fish	Range of body length (mm.)	Average of body length (mm.)
9°S–11°S	113°E–118°E	Aug., 1955	41	901–1130	1013
13°S–14°S	110°E–112°E	Apr.-May, 1956	32	938–1133	1016
2°N- 4°S	84°E- 97°E	Mar.-Apr., 1956	27	951–1146	1021
1°S- 4°S	65°E- 71°E	Apr.-May, 1956	25	939–1127	1037

As regards the albacore from the Pacific Ocean, those caught by the long line fishery were mainly used in the present study. The fishing stations of these samples are shown in figure 1.

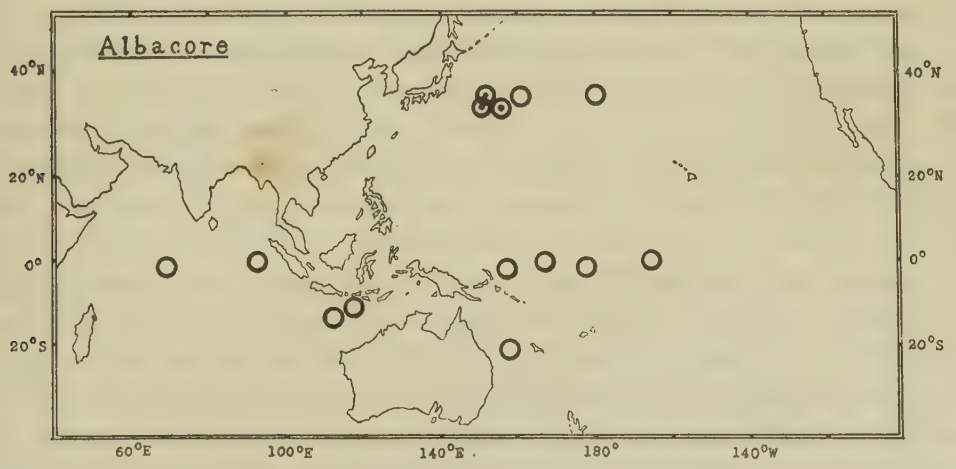

Fig. 1. Sampling stations of the albacore.
⊙: Sample taken by the pole-and-line fishery
○: Sample taken by the long line fishery

Methods of measurement and analysis of data of the non-meristic characters are identical with that employed in our previous reports on the albacore. Eighteen body characters were measured in millimeters with slide calipers and a pair of dividers according to the procedures employed by American tuna researchers and the covariance analysis was applied to test the group differences. Generally, the albacore were in full, with their gills and viscera intact when they were landed on to the fishing boats from the sea. This enabled us to collect data on the count of the gill rakers as well as the number of the first dorsal spines. We counted the number of anterior rakers on the upper and lower limbs of the most anterior gill arch on the left side of the albacore separately. By holding the first dorsal erect, we counted the discernable first dorsal spines. The most posterior spine may be completely subcutaneous and is then not counted. On these two denumerable characters, the between-area differences were tested in their variance and means.

Results

Prior to the comparison between the Indian and the Pacific albacore, we examined the problem whether or not the albacore taken from the different areas in the Indian Ocean are the component of the same population.

I) Comparison of the albacore from the three waters of the Indian Ocean

The covariance test for the homogeneity of relative growth lines of each body character over all areas studied resulted in an "F" value shown in table 2. We found that for the regression line of maxillary length on head length, a test for the homogeneity of the regressions yields a value that is significant at the 1% level. In snout to pectoral fin insertion and anal length, the differences of regression lines are significant at the 5% level, and in the remaining 14 characters no significant differences are noted. Excepting in maxillary length, recognizing the difference in the regression coefficient, we estimated the adjusted mean with its 99% confidence interval of each body character, basing on the regression coefficient estimated from the four samples. These values are tabulated in table 3.

As shown in figure 2A, for snout to pectoral fin insertion, the measurement is the greatest in the 1955 sample from the southern waters of the Sunda Islands and the least in the sample from the same area for 1956 and the difference is about 3 mm.. Other two samples from the waters around the Equator show moderate size. If we consider the two samples from the same area in the different years as samples from a common population, we may say that these albacore taken from the different areas in the Indian Ocean belong to the common population as far as this character is concerned.

Table 2. Comparison of body proportion of albacore by covariance analysis for four samples taken from the Indian Ocean. Data show variance ratio and its significance. F_r is the variance ratio to test the significance of the regression line difference, F_b to test the regression coefficient difference and F_a to test the adjusted mean difference.

Body character	F_r	F_b	F_a
Head length	1.34	2.06	<1
Snout to 1st dorsal	1.11	<1	1.22
Snout to 2nd dorsal	1.15	<1	1.94
Snout to anal	1.38	<1	2.28
Snout to ventral	<1	<1	1.05
Snout to pectoral	2.78*	2.43	3.01*
1st dorsal base	<1	<1	1.43
2nd dorsal to caudal	1.50	1.71	1.27
Anal to caudal	1.50	<1	1.96
1st dorsal spine length	2.17	2.09	1.88
2nd dorsal length	1.41	1.11	1.71
Anal length	2.18*	1.53	2.79*
Pectoral length	1.27	<1	1.65
Body depth	1.76	<1	2.78*
Spread caudal	<1	<1	<1
Maxillary length	3.05**	3.20*	(2.78*)
Diameter of iris	<1	<1	<1

N.B.: In the case where the regression coefficient difference is significant, the test of the adjusted mean difference becomes inappropriate, i.e. those figures within brackets under F_a.

*: Significant at the 5% level.

**: Significant at the 1% level.

For anal length (figure 2B), fish from the areas around the Equator have a shorter fin than the one from the southern area of the Sunda Islands, and the difference is about 3 mm..

Comparisons of regression coefficients indicate no significant differences between fish of any area in growth of body depth relative to size, but in the adjusted mean body depth (figure 2C) there is a 5% significant difference between areas. The adjusted mean body depth of albacore from the western area of Sumatra Island is significantly lower than that of the other three samples. In maxillary length, the regression coefficient of sample from the southern area of the Sunda Islands in 1955 is smaller than that of the other three samples. As we pointed out earlier in our reports on the albacore from the Pacific Ocean, the body depth and the maxillary length show great variability within areas, and it is necessary to take such results into consideration when using them as racial characters.

Generally, the significant differences are recongnized only in a few characters

Table 3. Adjusted mean of each body part with its 99% confidence interval, mean standard length in millimeters and estimated regression coefficient.

Body character \ Sample	Southern area of the Sunda in 1955	Southern area of the Sunda in 1956	Western area of Sumatra in 1956	Central Indian Ocean in 1956	Mean standard length (mm.)	Estimated regression coefficient
Head length	297.2±1.87	296.4±2.11	295.8±2.29	296.6±2.41	1020.4	0.3024
Snout to 1st dorsal	332.9±2.28	332.0±2.56	330.3±2.78	331.4±2.93	1020.4	0.3071
Snout to 2nd dorsal	591.4±2.43	589.8±2.74	588.9±2.97	588.5±3.13	1020.4	0.5691
Snout to anal	645.5±2.52	642.6±2.84	644.7±3.08	642.1±3.24	1020.4	0.6136
Snout to ventral	336.4±2.58	334.2±2.91	334.0±3.15	333.5±3.32	1020.4	0.3372
Snout to pectoral	304.2±1.91	301.3±2.15	301.6±2.33	303.1±2.45	1020.4	0.2992
1st dorsal base	266.4±2.31	266.1±2.61	266.1±2.83	263.6±2.98	1020.4	0.2599
2nd dorsal to caudal	456.7±3.73	460.4±4.20	456.8±4.56	459.1±4.79	1020.4	0.4611
Anal to caudal	401.6±3.57	400.9±4.02	397.3±4.36	402.6±4.59	1020.4	0.3971
1st dorsal spine length	123.1±2.45	124.2±2.67	122.6±2.85	120.6±3.14	1018.5	0.1516
2nd dorsal length	131.5±2.43	132.3±2.67	131.0±2.89	130.1±3.04	1020.2	0.1471
Anal length	128.7±2.32	129.0±2.61	126.8±2.83	125.2±2.98	1020.4	0.1401
Pectoral length	447.2±7.20	443.7±8.12	453.8±8.81	449.1±9.26	3.0083*	715.59
Body depth	261.6±3.13	259.1±3.44	256.2±3.81	260.3±3.93	1019.6	0.2770
Spread caudal	347.0±6.90	350.2±7.91	344.8±8.44	350.7±9.05	1020.4	0.5258
Diameter of iris	44.9±1.05	44.9±1.13	44.5±1.23	44.7±1.30	297.4	0.1418

*: The logarithmic transformation is applied to the raw data.

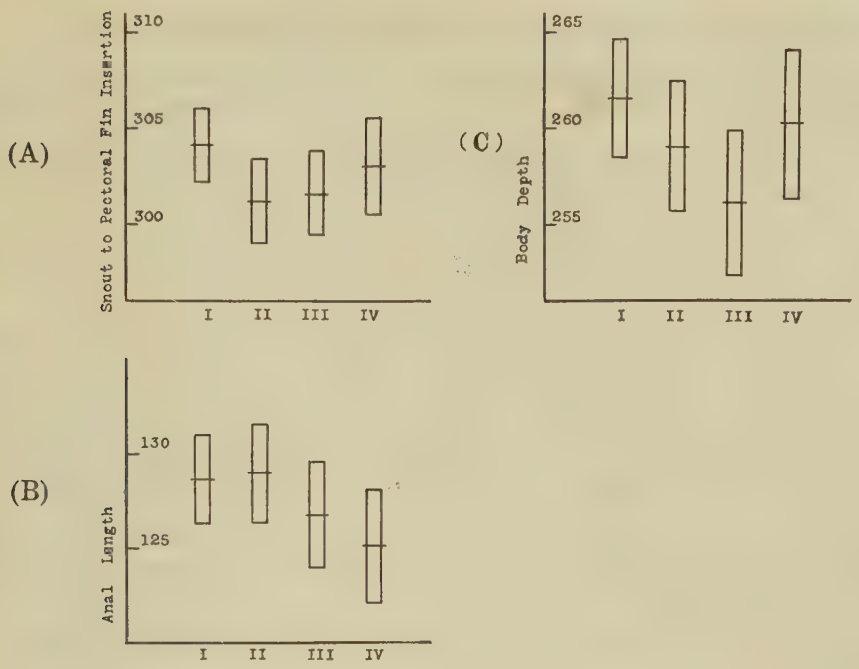

Fig. 2. Adjusted mean of body part and its 99% confidence interval.

(A): Snout to pectoral fin insertion at 1020.4 mm. body length
(B): Anal length at 1020.4 mm. body length
(C): Body depth at 1019.6 mm. body length
I: Albacore from the southern waters of the Sunda Islands in 1955
II: Albacore from the southern waters of the Sunda Islands in 1956
III: Albacore from the western waters of Sumatra Island in 1956
IV: Albacore from the central waters of the Indian Ocean in 1956

in the four samples from the Indian Ocean, but their morphometrical variations are slight and we did easily see such degrees of differences in the comparison of the samples from the same area in the Pacific Ocean. Accordingly, these samples may be considered to have been drawn from the common Indian albacore population.

At present, the Indian albacore caught by Japanese tuna long line boats is large in size and its body range is rather confined. So, great variances in the sample regression coefficients are observed. From the standpoint of the power of test to find the between-area difference, it is necessary to collect more samples with a wide body range and to analyse more accurately the variation between areas in the Indian Ocean. However, with the present data available, we may say with certainty, that the albacore from the southern areas of the Sunda Islands belongs to a common population to which the ones from the areas around the Equator also belong.

II) Comparison of the albacore from the Indian and the Pacific Ocean

We previously analysed the relationship of the albacore from three areas of the Western Pacific; the Northwest Pacific ones taken by the long line and the pole-and-line fishery boats, and the Equatorial and the Southwest Pacific ones taken by the long line fishery boats. The Equatorial Pacific albacore are very similar in morphometrical features with those from the Southwest Pacific and they seem to belong to a common population. We called it the Southwest Pacific albacore population.

By morphological study on the North Pacific albacore, GODSIL etc. (1944, 1948)[5,6] pointed out that these albacore from the Japanese, Hawaiian and the American west coast are similar and individually indistinguishable, but morphometrically the differences are recognizable. He concluded that the American and Japanese populations of albacore are probably distinct and nonintermingling. We have no morphometrical data on the albacore from the west coasts of America, but tagging experiments on the North Pacific albacore revealed that the albacore from the North Pacific migrate transversing the Ocean. At any rate, the albacore taken from the adjacent sea of Japan are called in this paper the Northwest Pacific population.

The Northwest Pacific albacore are characterized from the Southwest Pacific one in the following morphometrical features; smaller head, anteriorly positioned fins, shorter spine length, etc..

Basing upon their distribution, deduced from the operational data of tuna fishing boats, we may consider that the Indian albacore do not intermingle with the Northwest Pacific ones but probably with the Southwest Pacific albacore. As these problems are not analysed up to date, we may try to analyse them through morphometrical methods.

i) *Non-meristic characters*

a) *Comparison of the albacore from the Indian Ocean and the Northwest Pacific*

In order to compare statistically the albacore from the Indian and the Pacific Ocean, the four samples from the Indian Ocean and the two samples from the Northwest Pacific caught by long line fishery boats were treated as a single unit sample from each area respectively. The results tabulated in table 4 are based on the analysis, identical in method with that previously described. We may see the regression line differences in head length, snout to first dorsal and pectoral fin insertions, first dorsal base, second dorsal, anal and pectoral fin lengths, first dorsal spine length, spread caudal, diameter of iris at the 0.1% significant level and in snout to anal, ventral fin insertions at the 1% level.

In regression coefficients, the differences are recognized for the head length, snout to pectoral fin insertion, spread caudal and diameter of iris at the 0.1% level and four other characters at the 1 or 5% level.

Table 4. Comparison of body proportion of albacore by covariance analysis, for the samples from the Indian Ocean and the Northwest Pacific.

Body character	F_r	F_b	F_a
Head length	54.63***	30.84***	(69.20***)
Snout to 1st dorsal	7.67***	1.95	13.33***
Snout to 2nd dorsal	2.58	5.07*	(< 1)
Snout to anal	5.99**	< 1	11.07**
Snout to ventral	6.30**	4.99*	(7.49**)
Snout to pectoral	39.08***	19.05***	(59.36***)
1st dorsal base	8.11***	< 1	15.94***
2nd dorsal to caudal	3.26*	< 1	6.35*
Anal to caudal	< 1	< 1	< 1
1st dorsal spine length	29.87***	7.05**	(51.18***)
2nd dorsal length	10.37***	< 1	19.91***
Anal length	17.81***	< 1	35.74***
Pectoral length	17.94***	1.36	34.47***
Body depth	3.16*	6.03*	(< 1)
Spread caudal	59.00***	23.33***	(85.98***)
Maxillary length	1.41	2.63	< 1
Diameter of iris	< 1	< 1	< 1

*: Significant at the 5% level.
**: Significant at the 1% level.
***: Significant at the 0.1% level.

In adjusted means, these two samples indicate significant differences in many characters as shown in table 4. In the previous report on the relative growth of the Northwest Pacific albacore, we pointed out that the body size composition of samples affect greatly the values of the regression coefficient. Relatively high differences between these samples in the regression coefficient of many body characters may be resulted on the differences in the body size composition of the two samples.

We took 54 specimens over 90 cm. in body length from the Northwest Pacific sample, in order to be similar to the Indian sample in body size composition. These were compared by covariance analysis in the relative growth of head length, snout to pectoral fin insertion and spread caudal. Though these two samples are almost identical in their size composition, we can see again their regression coefficients are significantly different at the 1 or 5% level. We estimated the regression coefficient (b) with its 95% confidence interval and y intercept (a) on these three

Table 5. Estimates of the parameters of the regression line for the albacore from the Indian, the Northwest and the Southwest Pacific Ocean.

Body character \ Parameter \ Sample	Indian Ocean		Northwest Pacific total sample		Northwest Pacific sample over 90 cm.		Southwest Pacific	
	b	a	b	a	b	a	b	a
Head length	0.3018±0.0167	−11.4	0.2502±0.0079	34.6	0.2651±0.0183	18.8	0.2584±0.0097	33.2
Snout to pectoral	0.2987±0.0176	−2.1	0.2522±0.0091	38.8	0.2662±0.0209	23.9	0.2582±0.0113	38.3
Spread caudal	0.5293±0.0631	−192.1	0.3763±0.0219	−59.9	0.3890±0.0568	−73.1	0.4367±0.0306	−90.9

characters for each sample. It is readily seen from table 5 that the sample over 90 cm. body size from the Northwest Pacific has somewhat larger regression coefficient than that of the total sample from the same area. But its difference is rather small comparing with that between the Northwest Pacific and the Indian albacore. From these results, it appears that such degree of difference in body size composition is not so effective on the regression slope and that the Indian albacore have a rather large

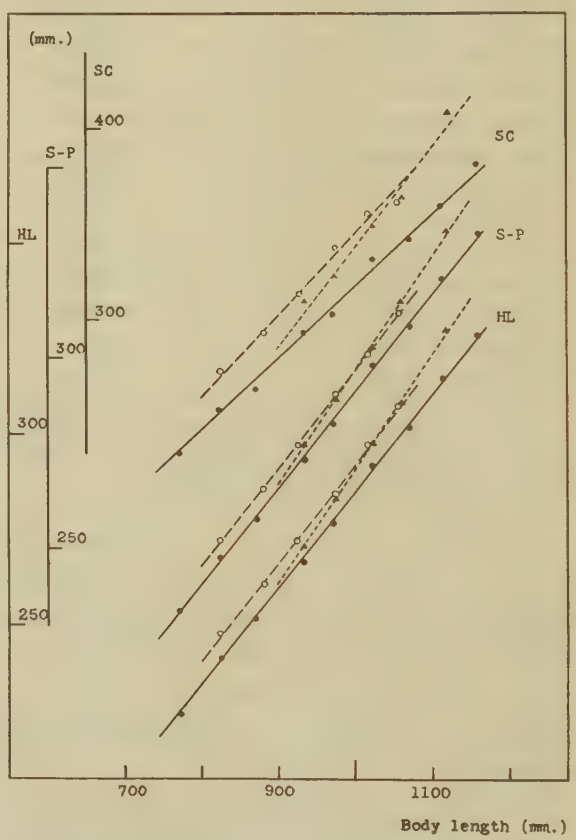

Fig. 3. The regressions of head length (HL), snout to pectoral fin insertion (S–P), and spread caudal (SC) upon body length. Solid circles and lines represent the Northwest Pacific data; open circles and broken lines represent the Southwest Pacific data; solid triangles and dotted lines represent the Indian data.

regression coefficient in these characters than that from the Northwest Pacific. The between-area difference is more apparent in the comparison of their relative size, as illustrated graphically in figure 3. Indian albacore have a relatively large head, more posteriorly positioned pectoral fin and high spread caudal than the Northwest Pacific albacore.

For diameter of iris, the regression coefficient is not homogeneous between these two samples. The Indian albacore have a relatively fast growing diameter of iris. But as pointed out earlier, this character shows a great variability within areas.

For snout to ventral fin insertion, the regression coefficient shows significant difference at the 1% level and from the value of the regression coefficient and y intercept, it may be seen that the ventral fin of the Indian albacore positions rather posteriorly and faster in relative growth than the Northwest Pacific one, as far as the large size albacore are concerned.

In the first dorsal spine length and body depth, we found differences in their regression coefficients.

In other 9 characters that do not show the significant difference in their regression coefficients, we estimated the adjusted mean with its 99% confidence interval. The result is shown in table 6.

Table 6. Adjusted mean of each body part with its 99% confidence interval, mean standard length in millimeters and estimated regression coefficient.

Body character \ Sample	Northwest Pacific	Indian Ocean	Mean standard length (mm.)	Estimated regression coefficient
Snout to 1st dorsal	318.5±1.51	321.5±1.35	985.2	0.2925
Snout to anal	626.3±1.94	622.8±1.73	985.2	0.5988
1st dorsal base	260.1±1.70	256.4±1.52	985.2	0.2635
2nd dorsal to caudal	444.9±2.36	441.6±2.10	985.2	0.4692
Anal to caudal	387.7±2.36	386.6±2.10	985.2	0.4018
2nd dorsal length	123.0±1.58	126.8±1.41	984.7	0.1353
Anal length	118.0±1.54	122.9±1.37	985.2	0.1333
Pectoral length	420.1±4.57	434.8±4.09	2.9916*	801.15
Maxillary length	101.8±0.65	102.1±0.58	284.8	0.3549

*: The logarithmic transformation is applied to the raw data.

We see from these adjusted mean values, that the Indian albacore have longer second dorsal, anal and pectoral fins than the Northwest Pacific one. It may be impossible to determine individually from these morphometrical features to which population this fish should belong. However, we may say that the Indian albacore have rather large head, more posteriorly positioned fins, and longer fins than the Northwest Pacific albacore. Furthermore, it will be noted that the relative growth

rates of head length and of characters showing the position of fins, are rather different, in contrast with the results obtained by the comparison of the Northwest and the Southwest Pacific albacore.

b) *Comparison of the albacore from the Indian Ocean and the Southwest Pacific*

The albacore taken from the Equatorial and the Southwest Pacific were treated as one and compared with the Indian albacore by covariance analysis. As shown in table 7, the two sample regression lines differ significantly in head length, snout

Table 7. Comparison of body proportion of albacore by covariance analysis, for the samples from the Indian Ocean and the Southwest Pacific.

Body character	F_r	F_b	F_u
Head length	12.73***	21.20***	(4.00*)
Snout to 1st dorsal	< 1	1.66	< 1
Snout to 2nd dorsal	1.83	1.81	1.84
Snout to anal	3.64*	2.85	4.40*
Snout to ventral	5.00**	8.38**	(1.58)
Snout to pectoral	7.40***	14.80***	(< 1)
1st dorsal base	< 1	< 1	< 1
2nd dorsal to caudal	1.05	< 1	1.97
Anal to caudal	< 1	< 1	< 1
1st dorsal spine length	2.00	3.11	< 1
2nd dorsal length	6.65**	1.75	11.53***
Anal length	8.64***	< 1	17.34***
Pectoral length	20.49***	1.73	39.15***
Body depth	7.25***	< 1	14.17***
Spread caudal	12.80***	7.06**	(18.13***)
Maxillary length	7.37***	< 1	14.58***
Diameter of iris	36.84***	< 1	73.92***

N.B.: Specimens from the Equatorial Pacific area are included in the Southwest Pacific sample.

to pectoral fin insertion, anal and pectoral fin lengths, body depth, spread caudal, maxillary length and diameter of iris at the 0.1% level, and in snout to ventral fin insertion and second dorsal fin length at the 1% level. The regression coefficients of head length, snout to pectoral and ventral fin insertions and spread caudal are not homogeneous. The regression coefficients of these characters, except the snout to ventral fin insertion, with their 95% confidence interval and y intercept for the Southwest Pacific albacore are shown in table 6, together with that for the Northwest Pacific and the Indian albacore. The regression coefficients of these characters for the Indian sample are larger than the Southwest Pacific one, but as seen in figure 3 in the level of the relative growth line these two samples are almost the

same. The same is true of the ventral fin insertion. In these characters, it is desirable to compare the samples with the same size composition. Indian albacore are somewhat larger than the Southwest samples in size composition, but the difference is slight. As we saw in the previous section, it seems such degree of body size difference does not affect so greately the regression coefficient. Of the characters which do not show the significant differences in their regression coefficients, we estimated the adjusted mean with its 99% confidence interval. These values are tabulated in table 8. The Indian albacore have a little longer second dorsal, anal

Table 8. Adjusted mean of each body part with its 99% confidence interval, mean standard length in millimeters and estimated regression coefficient.

Body character \ Sample	Southwest Pacific	Indian Ocean	Mean standard length (mm.)	Estimated regression coefficient
Snout to 1st dorsal	318.3±1.18	318.8±1.48	976.1	0.2937
Snout to 2nd dorsal	549.8±1.26	548.9±1.58	976.1	0.5528
Snout to anal	619.4±1.32	617.6±1.65	976.1	0.5935
1st dorsal base	254.8±1.17	254.2±1.46	976.1	0.2590
2nd dorsal to caudal	436.2±1.72	437.8±2.15	975.1	0.4580
Anal to caudal	383.9±1.76	383.4±2.20	975.1	0.3916
1st dorsal spine length	117.8±1.10	117.1±1.27	975.1	0.1321
2nd dorsal length	123.3±1.09	125.7±1.35	976.2	0.1336
Anal length	118.7±1.02	121.6±1.32	976.3	0.1350
Pectoral length	420.6±3.56	435.5±4.46	2.9885*	641.46
Body depth	251.8±1.57	247.9±1.96	976.3	0.2690
Maxillary length	103.5±0.46	102.4±0.55	285.2	0.3409
Diameter of iris	45.1±0.43	43.2±0.41	285.8	0.1383

*: The logarithmic transformation is applied to the raw data.

and pectoral fins and shorter maxillary length and diameter of iris than the albacore from the Southwest Pacific. But the difference is not so great as that seen in the comparison with the Northwest Pacific albacore. We did not have relatively small size albacore from these areas, and so whether or not the albacore from these two areas partially intermingle in the young ages with each other are questionable. The morphometrical features of the spawning groups of albacore from these two areas may have shown that the Indian albacore have a somewhat closer relation with the Southwest Pacific albacore than with the Northwest Pacific albacore. They also show a rather similar distributional status. However, the small but significant differences of these albacore suggest that even if these partially intermingle with each other, these are not homogeneously intermingling but form rather independent populations with slight mixing.

ii) *Meristic characters*

The meristic characters are used well to advantage in the racial investigations

on many fishes, since they will avoid the difficulties in comparisons which plagued us in regression analysis. But in tuna research, they are not always useful, because of their little variation and the difficulty to get such materials. We examined whether the gill-raker count and the first dorsal spine count are suitable for this study or not. In these denumerable characters, we need not take into consideration the difference in the body size of samples. So, the specimens taken by the pole-and-line fishery in the Northwest Pacific are included in the sample.

Table 9 shows distributions of gill-raker counts on upper and lower limbs, separately and combined. At the beginning, we tested the homogeneity of variance by the BARTLETT method. We could not find any significant difference between areas in the variance of each character. Next step in the analysis is to examine whether or not these three areas' albacore have the same mean of gill-raker counts, using the analysis of variance. Any between-area differences are not found in the mean gill-raker count of each character, too. In the gill-raker counts, three samples from the Pacific and Indian Ocean seem to have the same unspecified mean and unspecified variance.

Table 9. Frequency distributions of gill-raker counts by geographic samples on upper and lower limbs, separately and combined.

Character / Gill-raker / Sample	Upper limb				Lower limb					Upper and lower limbs combined							
	7	8	9	10	18	19	20	21	22	25	26	27	28	29	30	31	32
Indian Ocean	1	12	25			7	20	10	1			5	9	15	8	1	
Northwest Pacific	2	38	58	4	4	14	59	24	1	1	1	8	32	44	12	3	1
Southwest Pacific	5	52	66	4	1	23	71	29	3		2	14	41	45	23	2	

The distributions of first dorsal spine counts are shown in table 10. No significant differences in variance and in mean are found between samples. Accordingly any between-area difference is not found in the denumerable characters.

Table 10. Frequency distributions of first dorsal spine counts by geographic samples.

First dorsal spine / Sample	8	9	10	11	12	13	14	15
Indian Ocean						39	84	
Northwest Pacific				1*	3	74	206	1
Southwest Pacific	1*					53	127	

N.B.: These specimens are omitted from this analysis, because the posterior parts of their first dorsal spine were damaged.

Although Godsil and Byers (1944)[6] and Schaefer (1952)[7] showed on the yellowfin tuna that the gill-raker counts seemed to offer good possibilities for racial analysis, as far as our albacore samples are concerned, we failed to establish that these characters could be useful to indicate racial characters.

Discussion

It is generally considered that the albacore caught by the Japanese tuna long line fishery boats in the Indian Ocean are of the spawning group and in farther southward areas of the present fishing grounds, the feeding group of albacore, relatively small in body size, may be richly distributed. Two fishing grounds for the spawning group of albacore, are separately formed during the season between April and September but these albacore are almost similar in morphometrical features. We reported on the yellowfin tuna from the Indian Ocean[8] that they could be considered to be separated into three independent or semi-independent populations. On the contrary to the yellowfin tuna, we found it feasible to consider the existence of a single albacore population in the Indian Ocean, basing upon the morphometrical results as well as the seasonal change of the size composition of catches and of the fishing conditions reported by Mimura (1957). But this conclusion have to be more exactly reexamined, when we further collect the samples from the western area and from the feeding groups.

This study also indicates that there are marked differences in the morphometrical features of the albacore from the Indian and from the Pacific Ocean. In head length and position of some fins, the relative growth rate for the albacore from the Indian Ocean is larger than that for the Pacific fish. Furthermore, the Indian albacore have larger head and much posteriorly positioned fins than the Northwest Pacific albacore.

There is the question whether the Indian and Pacific forms should be classed as different species or races of the same species. Albacore have been found not only in the Pacific and the Indian Ocean but also in the Atlantic and the Mediterranean. Two species of albacore have been described up to date, *alalunga* from the Atlantic and *germo* from the Pacific. This problem cannot be finally settled until the degree of variation encounted among populations within each ocean, especially the Atlantic Ocean have been carefully studied, and the informations on the more detailed external and internal characters are obtained. However, this study is to compare the albacore from the Indian Ocean with the form from the Western Pacific in order to settle the question whether they are racially distinct, question of taxonomy will be passed over at this time.

We can see that the Indian albacore is distinct from the Northwest Pacific one from not only their morphometry but also their separated distributions. As

regards the Indian and the Southwest Pacific albacore, however, their distribution does not seem to be distinct. In the southeast and the southern areas of Australia, small sized albacore is distributed.[9] In the Indian Ocean it is probable that in the farther southward areas from the Japanese fishing grounds, small sized albacore is distributed. On the other hand, the large albacore is distributed in the low latitudes and the spawning is occurred at almost the same season in the Eastern Indian Ocean and the adjacent waters of the Coral Sea.[2,10] Accordingly, the Indian and the Southwest Pacific albacore have possibilities to intercause through the southern and the northern waters of Australia. From the morphometrical study showing the rather great difference between them, we could not consider that these form a homogeneous population. But that difference is not so great as we see in the comparison between the Indian and the Northwest Pacific albacore. Accordingly, they may have intercause each other to a slight degree. This will be more clear when we compare the small sized albacore from the two oceans.

We have still numerous problems on the racial study of albacore and this study will be further continued, keeping in mind the following matters. Comparison of the repeated samples from the same area yields more frequently the significant difference than that expected in the comparison of the random samples from a population. But the significant differences at the 0.1 or 1% level are observed only in few characters, for example, in the body depth, maxillary length and diameter of iris etc.. Though we do not have any precise data to determine the factors which produce such differences, we see in many fishes that body depth shows the great variability connecting with season, age and sex etc.. In maxillary length and diameter of iris, however, the great variation occurred without any connection with such promising factors to produce variation. It is probable that in these two characters their measurability is the main factor to produce such heterogeneity within an area. Measures of these characters being short, slight bias of the measurement on each sample may greatly confound with the between-group differences.

In some characters, there appears rather great differences in size composition of samples producing such heterogeneity. However, in many characters, the comparison of several samples from the same area yields a slight difference and we may consider that they are useful as a racial character, because of their rather high reproducibility in morphometry and of their between-area differences.

As regards the denumerable characters, it appears that the gill-raker counts and the first dorsal spine counts do not show the between-area difference, and are not useful as a racial character as far as these areas' albacore are concerned. In practical, we can not find easily other appropriate denumerable characters of the tunas in field work.

We have no assurance that the samples are indeed representative of the popu-

lations from which they were drawn. GODSIL (1948) pointed out that such differences within area are due to incomplete mixing of fish from different spawning grounds. Such incomplete mixing may indeed be true in the schooling fish as tunas. SETTE (1949)[11] emphasized that a suitable sampling technique is the most important for racial study of pelagic fishes and proposed that samples are drawn widely from many different schools within the region to be studied. At any rate, it is necessary to test the variation between areas basing on the variation within an area.

On the yellowfin tuna, racial study basing on the morphometry showed that the fish seems to grow and spawn and at last die in rather confined area. On the contrary, by morphometrical analysis and tagging experiments, the albacore seem to migrate very widely, transversing the ocean. We have to further examine whether or not the albacore distributed in the eastern and the western waters of the ocean, are throughly intermingling and whether they form a homogeneous population. This problem is very important and remains for further analysis. It is also necessary to know the relationships between albacore of different oceans and between albacore of the northern and southern hemispheres. These relationships will be well disclosed by informations about their biological properties together with tagging, morphometrical and serological studies.[12]

References

1) MIMURA, K. (1957): Studies on the albacore –IV Fishing condition in the Indian Ocean, especially the size composition in the eastern seas of the Ocean.
Report. Nankai Regional Fish. Research Lab., No. 5.

2) UEYANAGI, S. (1954): On the ripe ovary of the albacore, *Germo germo* (*Lacépède*), taken from the Indian Ocean.
Bull. Jap. Soc. Sci. Fish., 20 (12).

3) KUROGANE, K. and Y. HIYAMA (1957): Morphometric characteristics of the albacore, *Germo germo*, from the Northwest Pacific.
Records. Oceano. Works. Japan, 4 (1).

4) KUROGANE, K. and Y. HIYAMA (1958): Morphometric comparison of the albacore from the Northwest, the Equatorial and the Southwest Pacific.
Records. Oceano. Works. Japan, 4 (2).

5) GODSIL, H. C. and R. D. BYERS (1944): A systematic study of the Pacific tunas.
Calif. Div. Fish and Game, Fish Bull., 60.

6) GODSIL, H. C. (1948): A preliminary population study of the yellowfin tuna and the albacore.
Calif. Div. Fish and Game, Fish Bull., 70.

7) SCHAEFER, M. B. (1952): Comparison of yellowfin tuna of Hawaiian waters and of the American west coast.
U. S. Fish and Wildlife Service, Fish. Bull. 72.

8) KUROGANE, K. and Y. HIYAMA (1958): Morphometric comparison of the yellowfin tuna from six grounds in the Indian Ocean. Bull. Jap. Soc. Sci. Fish., 24 (6 & 7).

9) SERVENTY, D. L. (1941): The Australian tunas.
Council for Scientific and Industrial Research. Pam., 104.
10) ISHII, K. and M. INOUE (1956): Some notes on the ovary of albacore, *Germo germo*, taken from the Coral Sea.
Bull. Jap. Soc. Sci. Fish., 22 (2).
11) SETTE, O. E. (1949): Method of biological research on pelagic fisheries resources.
I.P.F.C. 1st Meeting.
12) SUZUKI, A., Y. SHIMIZU and T. MORIO (1958): Serological studies of the races of tuna –I The fundamental investigations and the blood groups of albacore.
Report. Nankai Regional Fish. Research Lab., No. 8.

Records of Oceanographic Works
in Japan Vol. 5 No. 1
February, 1959

A Measure of Role of Utilization of Plankton-feeders by Carnivorous Fishes in a Certain Area[1)]

By
Fujio Yasuda[2)] and Yoshio Hiyama[3)]

1. Introduction

In the preceeding reports[(1)(2)] the authors roughly enumerated the relative abundance of plankton-feeders in relation with their predators in the off-shore area of Japan, as an over-all figures based upon the landing statistics available for this purpose. In discussions on the productivity of plankton-feeders, if we want to know further detail, it is important to know upon the relation between the two ranks in food order about each species.

Really, it is entirely difficult to know all the quantitative values neccessary to know the abundance of all the livings in a certain area. And the composition of fauna there differs according to the season of a year, as some species comes in and some goes out when the season comes.

However, if we could find out some fishing method, the catch by which could represent the faunal composition in some degree, by some method of analysis of the data of caught fish, we would be able to know about the role of each species in a certain area in a certain season.

Here, Yasuda, by his own idea, tried to analyse the data of experimental fishings done in the coastal area near the Misaki Marine Biological Laboratory of the University of Tokyo, hoping this idea might do something for the consideration of relation between plankton-feeders and carnivorous fishes, especially of degree of obstractive role of a certain carnivorous fish against production of a certain plankton-feeders in a certain area.

Our experimental fishings were carried out at three seasons, May 1958, July and October 1957, in Moroiso and Koajiro Bay near the Misaki Marine Biological Laboratory of the University of Tokyo. In each season, several experimental fishings by beach seine and small set net were operated during a few days.

2. Materials

The catches of these operations were shown in Table 1.

1) Work by financial support of the Japanese National Commission for UNESCO.

2) Post-graduate student in fisheries course. A part of thesis work for Dr. degree at the author.

3) Professor of the University of Tokyo.

Table 1.

Season	Fishing ground	Fishing gear	Number of species (fish)*	Number of species other than fish	Total number of fish	Total weight of fish (kg)	Interval of experiment (day)
May 1958	Moroiso Koajiro	Beach seine	32	3	1881	21.6	2
July 1957	Moroiso	Beach seine Set net	47	3	2262	13.4	2
October 1957	Moroiso Koajiro	Beach seine	29	2	2015	5.2	3

* Silasu stage (younger fishes) consider as one species.

Moreover the stomach contents of almost every individual fish were examined. (if number of the fishes were too numerous we examined sveral fishes of each different sizes as the representatives.)

3. Method of analysis

a) Index of relative abundance.

Premising the catch of these non-selective fishing gear can represent the faunal composition in that small area in that short period in a season, we though that the size of the proportion of a certain species in the total catch could be an index to denote the relative abundance of that species in that area at that time. Thus, the index of relative abundance of species *a* (*Aa*) can be obtained as follows,

$$Aa=\frac{T'a}{T} \qquad (1)$$

where, $T'a$ is the total weight of given species *a* in the catch by these fishing operations, and T is the total weight of all species caught by these fishing operations.

b) Index of degree of consumption of plankton-feeders by carnivorous fishes.

By the data on the stomach contents of the caught fishes, we could define which is carnivorous species. Here, we thought that frequency of occurrence of plankton-feeders in the stomach of carnivorous fishes could be an index to denote the degree of consumption of plankton-feeders by a certain carnivorous fish *a* (*Ba*), premising the chance to meet the prey was equal to all the fishes. Thus,

$$\frac{Pa}{Na}=Ba \qquad (2)$$

where, *Pa* is the number of plankton-feeders found in the stomach of examined species *a*, and *Na* is the number of individual of species *a* examined.

Here, *Ba* was obtained not by weight, but by number of fish. Because so often

digestion reduces the real weight in stomach contents. However, we thought no serious difference could be found between these two methods.

By these two, *Aa* and *Ba*, the author thought that *Ca* obtained by the following formula can represent the intensity of power of reducing the plankton-feeder by a certain carnivorous fish among that community or fauna.

$$Aa \times Ba = Ca \qquad (3)$$

For example, if *Ca* is bigger than *Cb*, it could mean that carnivorous species *a* is doing bigger role than species *b* in consumption and reduction of plankton-feeders in that community or fauna, if we are right expressing the phenomena in these index.

Beside these indexes, one more index was considered for the reference in the interpretation of the results of experimental fishing. Though, *A* already includes the idea of relative abundance of a certain species in that community, the abundance of a certain carnivorous fish in ratio to the amount of plankton-feeders, which is a prey that this species feeds upon, is the matter of consideration to know which species is powerful in competition to take prey.

For that purpose the relative abundance of a carnivorous species *a* to total amount of plankton-feeders, (*Da*) was obtained as follows,

$$Da = \frac{Va}{P} \qquad (4)$$

where, *Va* is total weight of a species of carnivorous fish *a* in the catches, and *P* is total weight of all plankton-feeders to be preys for this fish in the catches.

4. The results of analysis of data by experimental fishing

We analysed these data obtained by the examination of catches of the experimental fishing. The results are shown in Table 2–7, separated according to the season and locality.

Table 2. July 1957, Set net, Moroiso Bay

No.	Species	(*A*)	(*B*)	Index (*C*)	(*D*)	Range of body length (cm)
1	*Fugu niphobles* (JORDAN et SNYDER)	0.49	0.65	0.32	2.7	4～11
2	*Stenoteuthis bartrami* (LESUEUR)	0.065	0.80	0.052	0.35	2～21
3	*Sphyraena pinguis* GÜNTHER	0.065	0.55	0.036	0.35	11～15
4	*Sepioteuthis lessoniana* FÉRUSSAC	0.042	0.80	0.034	0.23	9～12
5	*Scombrops boops* (HOUTTUYN)	0.028	0.56	0.016	0.15	7～12
6	*Cociella crocodila* (TILESIUS)	0.026	0.30	0.0078	0.14	17～33
7	*Stephanolepis cirrhifer* (T & S)	0.0064	1.00	0.0064	0.031	13
8	*Apogon semilineatus* T & S	0.042	0.061	0.0027	0.23	6～9

Table 3. July 1957, Beach seine, Moroiso Bay

No.	Species	(A)	(B)	Index (C)	(D)	Range of body length (cm)
1	*Sepioteuthis lessoniana* FÉRUSSAC	0.20	1.00	0.20	1.18	6～16
2	*Sphyraena pinguis* GÜNTHER	0.11	0.80	0.088	0.64	7～14
3	*Trachurus japonica* (T & S)	0.067	0.40	0.027	0.39	4～9
4	*Pseudoblennius percoides* GÜNTHER	0.0084	1.00	0.0084	0.050	7～9

Table 4. October 1957, Beach seine, Moroiso Bay

No.	Species	(A)	(B)	Index (C)	(D)	Range of body length (cm)
1	*Sepia esculenta* HOYLE	0.035	1.00	0.035	5.1	4～12
2	*Zeus japonicus* C & V	0.035	1.00	0.035	5.1	18
3	*Chelidonichthys kumu* (LESSON et GARNOT)	0.024	1.00	0.024	3.5	13～14
4	*Sepioteuthis lessoniana* FÉRUSSAC	0.028	0.78	0.022	4.0	4～12
5	*Pseudoblennius cottoides* (RICHARDSON)	0.011	0.75	0.0083	1.54	8～10
6	*Sebastes inermis* C & V	0.0081	1.00	0.0081	1.21	8～9
7	*Polypus vulgaris* (LAMARCK)	0.0063	1.00	0.0063	0.85	4
8	*Fistularia villosa* KLUNZINGER	0.0080	0.50	0.0040	1.15	12～29
9	*Stephanolepis cirrhifer* (T & S)	0.031	0.02	0.0062	4.5	3～9

Table 5. October 1957, Beach seine, Koajiro Bay

No.	Species	(A)	(B)	Index (C)	(D)	Range of body length (cm)
1	*Sepioteuthis lessoniana* FÉRUSSAC	0.135	1.00	0.135	—	12
2	*Fistularia villosa* KLUNZINGER	0.012	0.50	0.0060	—	13～44

Table 6. May 1958, Beach seine, Moroiso Bay

No.	Species	(A)	(B)	Index (C)	(D)	Range of body length (cm)
1	*Plotosus anguillaris* (LACÉPÈDE)	0.036	0.50	0.018	0.33	18
2	*Pseudoblennius percoides* GÜNTHER	0.0071	0.17	0.0014	0.080	16
3	*Sebastes inermis* C & V	0.100	0.0040	0.00040	0.91	11～12
4	*Sphyraena pinguis* GÜNTHER	0.0032	0.11	0.00035	0.030	7

Table 7. May 1958, Beach seine, Koajiro Bay

No.	Species	(A)	(B)	Index (C)	(D)	Range of body length (cm)
1	*Lateolabrax japonicus* (CUVIER)	0.17	0.67	0.11	2.3	13～25
2	*Sebastes inermis* C & V	0.027	1.00	0.027	0.37	11

5. Interpretation

These two localities, located not far from each other, abundantly have thrives of *Zostera* on the bottom, and are shallow (3~5 meter deep) productive area, and commercially intensive fishing were going on about two kinds of fishes, the one is squids (carnivorous) by beach seine, and an other is anchovy (plankton-feeders) by purse seine.

Beside these, among carnivorous fishes, barracuda (*Sphyraena* spp.), sea bass (*Lateolabrax japonicus*), *Scombrops boops* has commercial value but less abundant than squids (*Sepia esculenta*, *Sepioteuthis lessoniana*, and *Sepioteuthis bartrami*.).

In the school of anchovy (*Engraulis japonica*) some other plankton-feeders, such as sardine (*Sardinops melanosticta*), big-eye-sardine (*Etrumeus microps*), younger mackerel (*Scomber japonicus*) are mixed and caught, however, these are quite minor in the amount.

From the data of the first experiments (Table 2 & 3), we found that the index C is highest in squids (*Sepioteuthis* spp. and *sepia* sp.) and lowest in *Cociela crocodila*, *Stephanolepis cirrhifer* and *Apogon semilineatus*. Puffer (*Fugu niphobles*) here was eliminated from the consideration of the present discussing since they only consume the dead or damaged fishes.

From the data of the second experiments (Tables 4 & 5), we found that the index C are generally lower than that in first experiment, however, here also squids only shown the high value. Here, some carnivorous fishes were found to consume small goby but not plankton-feeders.

From the data of the third experiment (Tables 6 & 7), we found that the index C are generally lower than those mentioned above except in case of *Lateorabrax japonicus*.

Generally the size of fish was smaller in spring than in summer and autumn.

Among the carnivorous species any of three species of squids were dominant in relative abundance ($A=0.03\sim0.2$), and were powerful predators ($B=0.8\sim1.0$). Consequently they are playing a biggest role in consumption of plankton-feeders (mainly anchovy) in this area ($C=0.03\sim0.2$). And, their relative abundance to that of their prey (anchovy) is very high ($D=0.4\sim0.5$) compared with other species.

Here, as frequency of experimental operations was not large enough to make the ratio of total carnivorous fishes to that of plankton-feeders to be constant for that locality.

So, the sum of A for each experiment varies somewhat, and then accordingly that variation makes the value of C rather relative value available only for comparison of species within one experiment than to be an absolute value available to comparison with other experiment. However, A has rather big variation among the species of each experiment, mostly caused by the abundance or scarceness (or

presence or absence) of that species in that area at that time. While, B denote the ecological charactor of species, e.g. frequency of food taking and others, and remains rather constant than case of A. And consequently, the variation of C in an experiment is caused more by the variation of A than by that of B.

Here, the frequency of the experiments are not enough to get accurate figures of these index, especially that to see relation with squids and sardine considering the co-existence of other minor species, however, if we can get more over-all-figure than this we might be able to know more clearly on this phenomena.

As density of these predominant species in a area is high, it is natural to be the object of commercial fishing. However, it may be a matter of some interest that the predominant powerful carnivorous fish, squids, is object of commercial fishing in this area.

Literatures

(1) Y. HIYAMA and F. YASUDA, 1958. Productivity of Plankton-feeders in the Off-shore Area of Japan. (Records of Oceanographic Works in Japan 4–2).

(2) F. YASUDA and Y. HIYAMA, 1957. Mechanism of Utilization of Plankton by Some Fishes. (Records of Oceanographic Works in Japan 3–1).

(3) H. YAMASHITA, 1957. Relation of Foods of Sardine, Jack mackerel, Mackerel, and so on, in the Waters Adjacent to West Kyushu. (Bulletin of Seikai Regional Fisheries Research Laboratory No. 11.).

Records of Oceanographic Works
in Japan Vol. 5 No. 1,
February, 1959

Measurements of Submarine Light Polarization

By
Tadayoshi Sasaki*, Noboru Okami**, Seiichi Watanabe**
and Gohachirō Ōshiba**

Introduction

The polarized light on horizontal lines of sight in the sea was measured by a photoelectric polarimeter placed in the underwater chamber "Kuroshio" and the interference analizer attached to the underwater camera. Our results are very similar to those obtained by T. H. Waterman[1)2)3)] and A. Ivanoff[4)5)]. It is recognized that with the increase of the depth in respect of the change of polarization patterns both the tilt of polarization plane and the degree of polarization in all the bearings have a tendency to approach the same values.

Results of Measurements and Discussion

1. Degree of Polarization

The degree of polarization on horizontal lines of sight was measured from the underwater observation chamber "Kuroshio" in Mutsu Bay, Aomori Prefecture in November, 1956.

The outline of the light receiver of the photoelectric polarimeter used is shown in Fig. 1. A rotary cylinder, on the bottom of which a polarizing plate of polaroid is fixed, is attached to the front of the light receiving window of the shield-case containing a multiplier phototube (R. C. A. 931-A). The angular aperture of the field of view of the light receiver is about 10°. The light receiver is fixed horizontally to the inner surface of the observation window and the change of the photoelectric current corresponding to the rotation of the cylinder is measured. If the maximum and minimum values of the photoelectric current be I max and I min respectively, the degree of polarization P will be expressed in the equation shown below.

$$P=\frac{I\ \max-I\ \min}{I\ \max+I\ \min}$$

The degree of polarization in each bearing measured at the depths of 10, 15, 20 and 25 m are shown in Fig. 2. In the figure the sun's bearing is 0° and the antisun's bearing is 180°. The measurements at a depth of 10 m are performed

* Tokyo University of Fisheries and RIKAGAKU KENKYUSHO.
** RIKAGAKU KENKYUSHO (The Institute of Physical and Chemical Research), Tokyo.

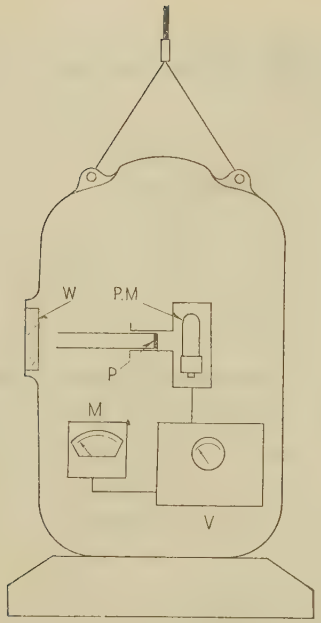

Fig. 1. Schematic diagram of the photoelectric polarimeter in the underwater observation chamber "Kuroshio",
W: Observation window.
P: Polarizing plate of polaroid with hood.
P.M: Multiplier phototube.
V: High-voltage stabilizer.
M: Microammeter.

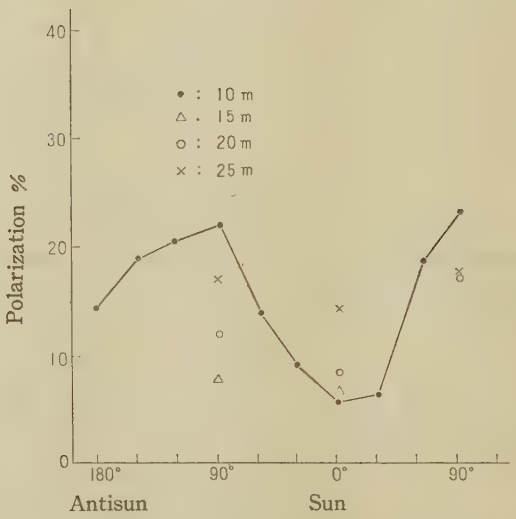

Fig. 2. The degree of polarization on horizontal lines of sight in each bearing measured at various depths.
Measurements were done in Mutsu Bay, Aomori Prefecture in November, 1956.

in every 30° of azimuth and those at the other depths are performed at the sun's bearing and azimuths 90° to its bearing. It is found that the degree of polarization at each depth reaches its maximum at azimuths 90° to the sun's bearing. These are quite the same as those of WATERMAN[3] and of IVANOFF[4][5]. From the figure it is understood that the difference between the degree of polarization at azimuths 90° to the sun's bearing and that at the sun's bearing has a tendency to decrease with the increase of depth, where measurements are performed.

2. Plane of Polarization

WATERMAN used the method of photographing interference patterns formed by convergent beams of polarized light falling on a interference analizer consisting of a plate of a uniaxial crystal cut perpendicularly to its axis, a quarter wave plate and a disk of polaroid film. This method seems suitable for measuring submarine polarization, because presence or absence of polarized light, type of polarization and

in the case of linear polarization orientation of e vector can directly be determined from the interference patterns. Therefore we have constructed an analyzer similar to that of WATERMAN for the purpose of measuring tilt of the plane of submarine polarization. The uniaxila crystal used is artificially crystallized ammonium di-

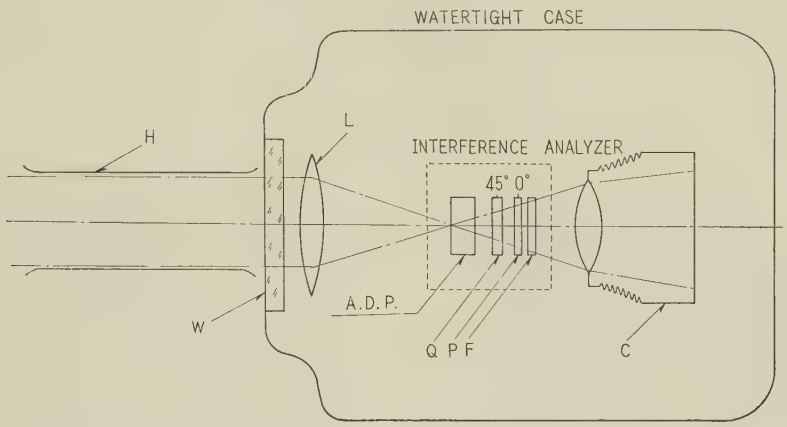

Fig. 3. Schematic diagram of the underwater camera "KAKEN" equipped with the interference analyzer.
H: Hood, W: Glass window, L: Lens, A.D.P.: Ammonium dihydrogen phosphate, Q: $1/4\lambda$ phase plate, P: Polaroid F: Color filter (green), C: Camera.

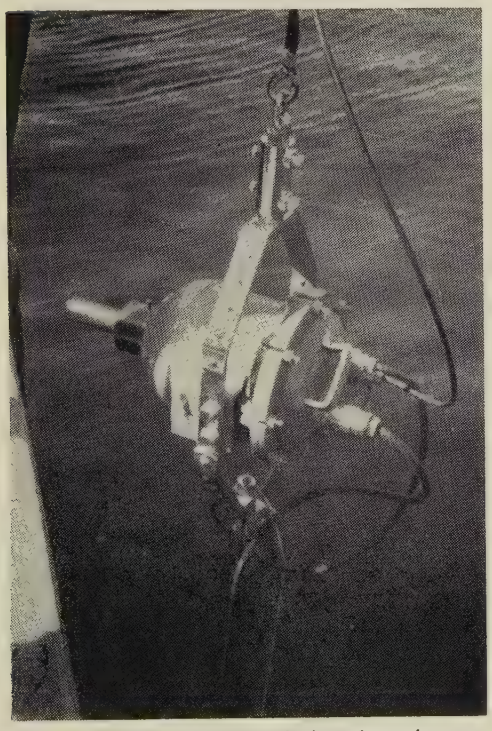

Fig. 4. The apparatus before lowering.

Fig. 5. Magnetic compass and the plumb attached to the bottom of the apparatus.

hydrogen phosphate (A. D. P.).[6] The outline of an apparatus combining the interference analyzer with the underwater camera "KAKEN"[7] is shown in Fig. 3. The angular aperture of the apparatus is about 8°. For the purpose of determining the orientation of *e* vector of linear polarization from the interference patterns the upper and lower edges of the aperture of the camera are assumed to be the fiducial lines. When *e* vector of the falling linearly polarized light is parallel to the fiducial lines, the analyzer is fixed to the camera so as to let the straight line passing the center of the break of the concentric rings spreading the left side of the tow black fan-shaped areas placed in center of the interference pattern be parallel to the

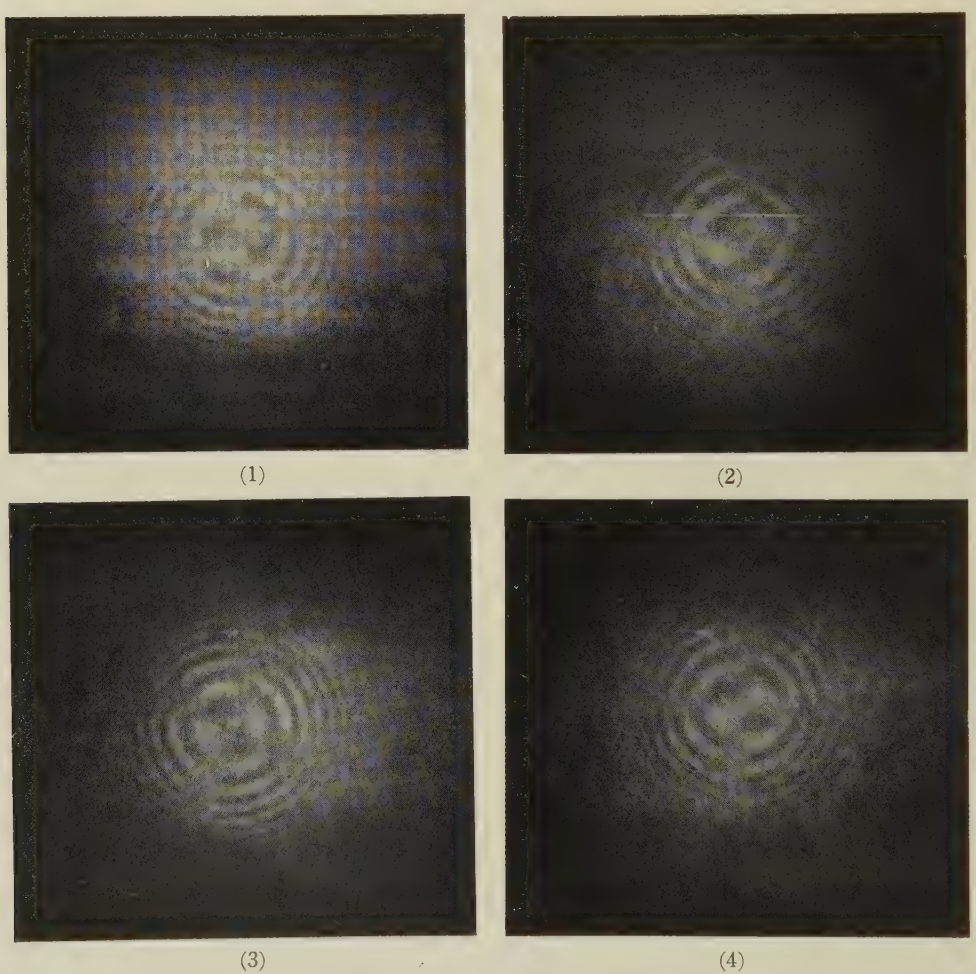

Fig. 6. Interference patterns formed by natural light at a depth of 3 m on a fine day in October, 1957.
(1) West, 17° tilt toward the left, (2) Southwest, 3° right, (3) Southeast, 29° right, (4) East, 9° right.
Sun's altitude: 27°10′.
Transparency: 9 m.

fiducial lines. Using the apparatus described above and shown in Fig. 4, polarized light on horizontal lines of sight was measured in 1957–8. The bearing and the level of the photoaxis of the apparatus suspended in the sea are determined by the diviver observing the magnetic compass and the plumb (Fig. 5) attached to the bottom of the apparatus. Photographing can be performed by the underwater camera "KAKEN" suspended in the sea and controlled from on board and the procedures are performed from on board after the diver has reported by telephone that the bearing and the level of the apparatus have determined. The interference pattern obtained from measuring degree of polarization in every 45° of bearing at a depth of 3 m on a fine day in October, 1957 is shown in Fig. 6. The interference pattern shows that the polarized light on the horizontal lines of sight is linear polarization. The angle between *e* vector found from the interference pattern and the horizon is plotted and shown in Fig. 7. From the figure it is found that the tilt of polarization plane in the sun's bearing and in the antisun's bearing is horizontal and those in azimuths 90° to the sun's bearing reach the maximum. Our results are quite similar to those of WATERMAN[1)2)3)]. The interference pattern obtained from measuring degree of polarization in every 30° of bearing at a depth of 5 m on a cloudy day in December, 1957 shows that the polarized light on the horizontal lines of sight is linear polarization. The tendency of changing tilt of polarization plane shown in Fig. 8 is quite the same as that measured on a fine day. The sun's bearing and the antisun's bearing shown in the figure are determined from tables using the date, latitude and longitude, when and where measurements were performed. The results obtained from the measurements at the depths of 7, 10 and 25 m on a slightly rainy day in March, 1958 shows that

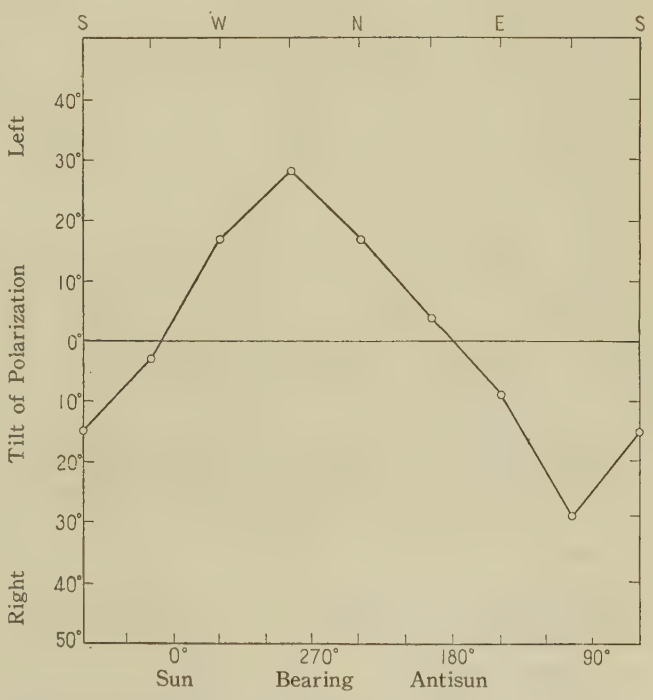

Fig. 7. Effect of sun's bearing on plane of submarine light polarization on horizontal lines of sight.
Measurement were done in Manazuru Bay, in Kanagawa Prefecture, on a fine day in October, 1957.
Depth: 3 m.

the tilt of polarization plane at a depth of 7 m is the maximum of 5° and those at 10 and 25 m are almost horizontal.

From the results of measurements on a cloudy day it is found that in the neighborhood of the sea surface *e* vector of the linear polarization in all the bearings except the sun's and antisun's bearings has small angle to the horizon, but with the increase of depth becomes parallel to the horizon at last.

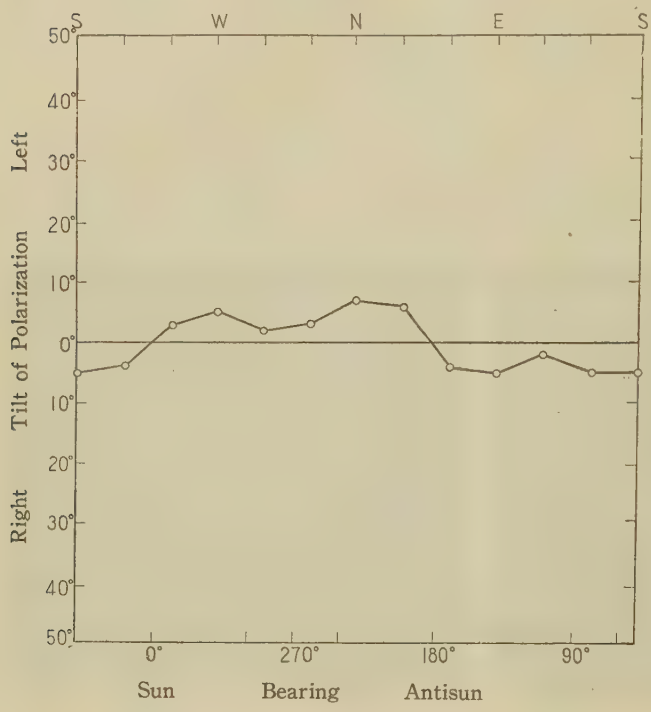

Fig. 8. Effect of sun's bearing on plane of submarine light polarization on horizontal lines of sight. Measurement were done in Sagami Bay, Shizuoka Prefecture, on a cloudy day in December, 1957. Depth: 5 m.

From the results of measuring angular distribution of submarine daylight intensity[8] on a cloudy day it is deduced that the depth, at which the tilt of the *e* vector becomes parallel to the horizon, is identified with the depth, at which the angular distribution becomes symmetrical with the vertical axis and horizontal plane. The tendency that the angular distribution of submarine daylight approaches the symmetrical patterns described above is very similar to that of reducing tilt of polarization plane with the increase of depth.

The depth, where the angular distribution of submarine daylight on a fine day becomes the symmetrical, is much deeper than that of a cloudy day[8] and therefore on a fine day the depth, where the tilt of polarization plane becomes parallel to the horizon must be deeper than that of a cloudy day. This tendency is also shown in the results of measurements performed by WATERMAN[2] at depths down to 200 m.

Summary

It is obvious that the polarized light on the horizontal lines of sight on each layer in the sea is owing to the scattering of directional light penetrating each layer, and therefore the directionality of penetrating light is one of essential factors

governing the polarization patterns.

The directionality of penetrating light is governed by several conditions such as weather, sun's altitude, turbidity, depth and so forth. Therefore the polarization pattern must change according to the change of angular distribution pattern. But if there be some difference between the depth, where the stationary condition lies on a fine day, and that of a cloudy day, the direction of penetrating light will tend to become vertical with the increase of depth. It is easily deduced that with the increase of depth the state of polarization tends to approach the same value in all directions. The tendency appearing in the results shown above is quite similar to this tendency.

It is necessary to let the polarized light at depths down to the layer, where the state of polarization reaches the same value in all directions, correspond to the directionality determined from the measurement of angular distribution of vertical plane at the same depths. We will measure the polarized light and the angular distribution of submarine daylight at the same time and intend to develop our studies.

The authors wish to express their hearty thanks to Messrs. S. Nanba and T. Ogawa of RIKAGAKU KENKYUSHO (The Institute of Physical and Chemical Research) and members of Marutake Laboratory, Kobayashi Institue of Physical Research for their kind suggestions and collaborations in constructing the interference analyzer. The authors also wish to express their thanks to members of Faculty of Fisheries, Hokkaidō University and those of Itō-Branch of Fisheries Experimental Station in Shizuoka Prefecture for their kind helps in experiments at sea.

This work was supported by the Ministry of Education.

References

1) T. H. Waterman (1954): Science, 120, 927–932.
2) T. H. Waterman (1955): Deep-Sea Res., 3 (Suppl.) 426–434.
3) T. H. Waterman (1956): J. Marine Res., 15, 149–168.
4) A. Ivanoff (1956): J. Opt. Soc. Amer., 46, 362.
5) A. Ivanoff (1957): Bull. du C. O. E. C. IX, 9, 491–499.
6) B. H. Billings (1949): J. Opt. Soc. Amer., 39, 797–808.
7) T. Sasaki et al (1955): J. Sci. Res. Inst., 49, 107–116.
8) T. Sasaki et al (1958): Ibid, 52, 71–77.

BUREAU OF COMMERCIAL FISHERIES
SEP 30 11 49 AM '59
HAWAII AREA
HONOLULU